(2)

U. S. Army Communications-Electronics Command

Night Vision & Electronic Sensors Directorate

Title: Nanosecond and Subnanosecond Investigations of Intrinsic Optical Limiting Mechanisms in Photorefractive and Semiconducting Materials

Author(s): A. L. Smirl and T. F. Boggess

Address: University of Iowa, Center for Laser Science and Engineering, 144 IATL, Iowa City, IA 52242-1000

Type of Report (Final, Interim, etc.):

Interim Final

Date: June 28, 1993

Contract Number

DAAB07-89-C-F412

Report Number

NV-93-C08

CONQUEST OF DARKNESS

Fort Belvoir, Virginia 22060-5677

URITY CLASSIFICATION OF THIS PAGE

REPORT DOCUMENTATION PAGE

Form Approved
OMB No. 0704-0188

REPORT SECURITY CLASSIFICATION Unclassified	1b. RESTRICTIVE MARKINGS none
2a. SECURITY CLASSIFICATION AUTHORITY N/A	3. DISTRIBUTION/AVAILABILITY OF REPORT Approved for Public Release Distribution Unlimited
2b. DECLASSIFICATION/DOWNGRADING SCHEDULE N/A	
4. PERFORMING ORGANIZATION REPORT NUMBER(S)	5. MONITORING ORGANIZATION REPORT NUMBER(S) NV-93-C08
6a. NAME OF PERFORMING ORGANIZATION University of Iowa 6b. OFFICE SYMBOL (If applicable)	7a. NAME OF MONITORING ORGANIZATION U.S. Army CECOM NVESD
6c. ADDRESS (City, State, and ZIP Code) Center for Laser Science & Engineering 144 IATL Iowa City, IA 52242-1000	7b. ADDRESS (City, State, and ZIP Code) Ft. Belvoir, VA 22060-5677
8a. NAME OF FUNDING/SPONSORING ORGANIZATION ARPA 8b. OFFICE SYMBOL (If applicable)	9. PROCUREMENT INSTRUMENT IDENTIFICATION NUMBER DAAB07-89-C-F412
8c. ADDRESS (City, State, and ZIP Code) 3701 N. Fairfax Dr. Arlington, VA 22203-1714	10. SOURCE OF FUNDING NUMBERS PROGRAM ELEMENT NO.: 62 301 E PROJECT NO.: TASK NO.: DO WORK UNIT ACCESSION NO.:

11. TITLE (Include Security Classification)
Nanosecond and subnanosecond Investigations of Intrinsic Optical Limiting Mechanisms in Photorefractive and Semiconducting Materials (U)

12. PERSONAL AUTHOR(S)
Smirl, A. L., Boggess, T. F.

13a. TYPE OF REPORT	13b. TIME COVERED	14. DATE OF REPORT (Year, Month, Day)	15. PAGE COUNT
Interim Final	FROM 3/31/89 TO 6/28/93	6/28/93	105

16. SUPPLEMENTARY NOTATION

17. COSATI CODES			18. SUBJECT TERMS (Continue on reverse if necessary and identify by block number)
FIELD	GROUP	SUB-GROUP	
20	5		
20	6		

19. ABSTRACT (Continue on reverse if necessary and identify by block number)

This program has been directed at exploring the fundamental physics underlying optical nonlinearities in a variety of materials, including semiconductors, organometallics, and photorefractive ferroelectrics, that have potential applications to eye and sensor protection. In addition, simple "proof-of-principle" optical limiting devices have been demonstrated and analyzed. Specific materials have included GaAs and Si at 1.06μm, and at 532 nm the semiconductor GaP, the organometallic compound known as King's complex, and the ferroelectric oxide $BaTiO_3$. This document summarizes progress on the program, delineates conclusions drawn from the research, provides recommendations for future research, and briefly describes research that will continue (until September 1995) on this contract under AASERT funding.

20. DISTRIBUTION/AVAILABILITY OF ABSTRACT	21. ABSTRACT SECURITY CLASSIFICATION	
☒ UNCLASSIFIED/UNLIMITED ☐ SAME AS RPT ☐ DTIC USERS	U	
22a. NAME OF RESPONSIBLE INDIVIDUAL Byong H. Ahn	22b. TELEPHONE (Include Area Code) (703) 704-2031	22c. OFFICE SYMBOL AMSEL-RD-NV-LPD

DD Form 1473, JUN 86 *Previous editions are obsolete.* SECURITY CLASSIFICATION OF THIS PAGE

Interim Final Report

NANOSECOND and SUB-NANOSECOND INVESTIGATIONS of INTRINSIC OPTICAL-LIMITING MECHANISMS in PHOTOREFRACTIVE and SEMICONDUCTING MATERIALS

DAAB07-89-C-F412

June 28, 1993

DARPA/NVEOD

Center for Laser Science and Engineering
University of Iowa
100 IATL
Iowa City, Iowa 52242

(319) 335-3520
FAX (319) 335-3462

Arthur L. Smirl, Professor and Endowed Chair
and
Thomas F. Boggess, Associate Professor

The Contractor, Center for Laser Science and Engineering, University of Iowa, hereby certifies that, to the best of its knowledge and belief, the technical data delivered herewith under Contract No. DAAB07-89-C-F412 is complete, accurate, and complies with all requirements of the contract.

Thomas F. Boggess

June 28, 1993
Thomas F. Boggess
Associate Professor
Center for Laser Science & Engineering
Department of Physics and Astronomy and
Department of Electrical & Computer Engineering
University of Iowa

Table of Contents

Executive Summary

The objective of our project has been to explore the fundamental physics underlying optical nonlinearities in a variety of materials that have potential application to eye and sensor protection and to demonstrate simple proof of principle devices based on these materials. Initially, we studied optical nonlinearities in well-understood near infrared materials, GaAs and Si, that had been used previously for optical limiting at 1064 nm. These studies allowed us to develop an understanding of the magnitude of nonlinearities required for eye protection, the trade offs between fluence dependent and intensity dependent nonlinearities, and allowed us to recognize the potential for broad band limiting based on deep level transitions. Our studies subsequently focused on materials more appropriate to limiting in the visible, specifically organometallic compounds and the indirect, visible band gap material GaP.

Picosecond spectroscopy of the organometallic compound known as King's complex allowed us to measure the excited state properties of this compound and to identify an anomalous behavior for ns excitation of solutions of this compound that was subsequently identified as optically induced scattering. The implication of these results was that this compound was not suitable for incorporation into solid hosts for eye protection goggles.

Measurements in GaP indicated that this material could provide eye-safe optical limiting levels in low f/# configurations for ps pulses over a narrow bandwidth near 532 nm. Specifically, in an f/5 configuration, the GaP limiter, which had a linear transmission of ~ 30%, displayed a limiting threshold of ~ 10 nJ. Once threshold was reached, the output level remained below 0.1 $\mu J/cm^2$ over a range well in excess of 45 dB increase in input energy. Time-resolved spectroscopy demonstrated that the dominant nonlinearities were fluence dependent, indicating that the device should function well for much longer pulses, provided that recombination and diffusion of carriers out of the illuminated spot do not become important. This conclusion was verified by measurements of the optical nonlinearities using ns pulses at NVESD. The primary liability of the device is its narrow operating bandwidth (estmated to be ~ 20 nm) due to the frequency dependence of the linear absorption coefficient. We have proposed the use of absorption through deep levels in this and/or other semiconductors to address this issue.

Our key conclusions from this research are as follows. Given the program requirements and the nature of available nonlinear optical materials, it is likely that the most reasonable choice of device is one employing a nonlinearity associated with resonant excitation (single photon absorption) and an intermediate focal plane. While nonresonant nonlinearities provide broadband responses, they are generally too weak to provide eye-safe limiting levels. Hence, we should seek broad band linear absorbers that subsequently exhibit strong excitation-related nonlinearities, e.g., reverse saturable absorption in organics or organometallics or carrier related nonlinearities in semiconductors. The key to the successful implementation of such a device resides in finding materials that exhibit broad, slowly varying linear absorption in the visible and large excited state coefficients. While the organics and organometallics seem to have an edge in this regard, we should not overlook heavily doped or even amorphous semiconductors, which generally have very broad bandtail absorption features.

Finally, we note that this contract continues until September 1995 at a greatly reduced level of effort under AASERT funding.

NANOSECOND and SUB-NANOSECOND INVESTIGATIONS of INTRINSIC OPTICAL-LIMITING MECHANISMS in PHOTOREFRACTIVE and SEMICONDUCTING MATERIALS
DAAB07-89-C-F412

1. Contract Information

This contract, which had an original total cost of $775,560, began 31 March 1989 and was scheduled to end 30 March 1993. In March of 1992, a proposal for a Department of Defense Augmentation Award for Science and Engineering Research Training (AASERT) was selected for funding. The purpose of this award was to provide funding for one additional Ph. D. student on the current parent contract. Funding for the AASERT award, which had a 15 September 1992 start date, totaled $84,132, and the award was for a three year period. The AASERT award extended the performance period of the parent contract from 31 March 1993 to 14 September 1995. It must be emphasized, however, that during this extended period, the level of effort on the contract will be greatly reduced; while the parent contract provided support for two students, one post doc, and significant faculty time, the AASERT award provides funding for only one student. Since as of 30 March 1993 the bulk of the research on this contract has been completed, it is appropriate to summarize our results and conclusions in this Preliminary Final Report. This document is also intended to serve as the first Quarterly Report for 1993.

2. Project Description and Summary

The objective of our project has been to explore the fundamental physics underlying optical nonlinearities in a variety of materials that have potential application to eye and sensor protection and to demonstrate simple proof of principle devices based on these materials. The direction of these studies was determined by the overall program goal, which was to implement optical limiting devices capable of providing limiting levels of 0.1 $\mu J/cm^2$, high linear throughput

(> 70%), and a large dynamic range (> 60 dB) for 10 ns pulses throughout the spectral range of 400-700 nm. In addition, to preserve field of view, the devices must be based on low f/# configurations. While these criteria may be easily satisfied individually in various materials, the requirement that they be simultaneously satisfied in a given device places extreme performance demands on the nonlinear element in the device. To our knowledge, no single material or combination of materials in any device has yet completely satisfied all of the program goals. Nevertheless, progress has been made on many fronts leading to an improved understanding of material properties that govern optical limiting devices and to the demonstration of optical limiters that satisfy many (though not all) of the program requirements.

Specifically on this project, we began by studying optical nonlinearities in well characterized and well understood near infrared materials, GaAs and Si, that had been used previously for optical limiting at 1064 nm. While not directly applicable to eye protection, these studies allowed us to develop an understanding of the magnitude of nonlinearities required for eye protection, the trade offs between fluence dependent and intensity dependent nonlinearities, and allowed us to recognize the potential for broad band limiting based on deep level transitions. These studies demonstrated to us that, given the magnitude of two-photon absorption coefficients in existing materials, in order to provide limiting at eye safe levels for nanosecond and longer pulses, fluence dependent nonlinearities are required. In addition, photorefractive measurements in GaAs and comparison with the effect in high-gain materials such as $BaTiO_3$, made it clear to us that the program goals could not be met using photorefractive beam fanning or coupling, unless improvements were made in photorefractive materials. Specifically, a material was needed with the high sensitivity of a photorefractive semiconductor, such as GaAs, but with the high gain of, e.g., $BaTiO_3$. Since such a material was not available, we subsequently focused our attention on two processes, reverse saturable absorption in organometallics and free carrier nonlinearities associated with linear absorption in semiconductors. Both of these processes can be fluence dependent over broad time scales. These studies were all conducted at visible wavelengths. We note that all of our measurements have been conducted with picosecond pulses to ensure that

measurements of material parameters are accurate. This accurate determination of the nonlinear constants of the material were then incorporated into computer models that allowed us to simulate device response under other excitation conditions. In some instances, nanosecond measurements have been performed at Hughes Research Laboratories (HRL) and at the U. S. Army Night Vision and Electro-Optics Directorate (NVEOD) to corroborate and supplement our findings.

The organometallic studies focused on solutions of the specific cluster compound known as King's complex, $[(C_5H_5)Fe(CO)]_4$, which was shown at HRL to exhibit strong optical limiting of ns pulses at 532 nm. These ns measurements were sufficiently promising to warrant the consideration of this compound for incorporation into solid hosts suitable for microlens arrays to be implemented in eye-protection goggles. These preliminary results led us, in collaboration with colleagues at HRL, to a detailed study of the nonlinear optical properties of King's complex. Picosecond measurements of the optical response of this compound allowed us to determine the system dynamics responsible for reverse saturable absorption (RSA), including excited state lifetimes and cross sections and bounds on the lifetime of the second excited state and intersystem crossing rate, which were then used to model the ns response. Such measurements, in conjunction with molecular engineering, specifically ligand substitution, allowed us to identify the excited state transition as a d-d transition involving the metal core of the molecule. Serious deviations were found between the predicted nanosecond limiter response, based on the results of these ps measurements, and the measured ns response. Subsequent ps investigations revealed an apparent induced scattering in this compound occurring on ns time scales after optical excitation. Indeed, by repeating the ns measurements and detecting the off-axis scatter, a significant nonlinear scatter was observed. Nanosecond measurements on samples of King's complex embedded into a solid host (PMMA) revealed little optical limiting indicating that this scatter actually dominated the ns limiter response for solutions. Following this sequence of measurements, HRL focused on alternate compounds for protective eye ware. This is a perfect example of the importance of developing a complete understanding of the physics of a device prior to attempting to extrapolate

its performance to new environments. The HRL-University of Iowa collaboration succeeded quite well in this endeavor.

The measurements of carrier related optical nonlinearities centered on the indirect band gap semiconductor GaP. Because of the details of the band structures and the nature of the optically-coupled states, this material was expected to behave at 532 nm much like Si at 1064 nm. Our initial measurements of optical limiting in Si indicated that such a correlation would allow eye-safe limiting levels to be achieved in GaP at 532 nm. Indeed, we straightforwardly demonstrated that limiting levels of less than 0.2 $\mu J/cm^2$ were readily attainable using thin layers of this material in large f/# configurations. This initial success led us to a detailed investigation of the nonlinear optical properties of this material. In addition to the expected free carrier absorption and refraction processes, we observed two-photon absorption (TPA) in this material for ps excitation, in spite of the fact that the wavelength used (532 nm) provided photon energies above the indirect band edge. Numerical modeling, however, demonstrated that the limiter response was not significantly influenced by this TPA, but was in fact dominated by free carrier refraction associated with linearly generated carriers, a fluence dependent process. This conclusion was experimentally verified by repeating our measurements with longer pulses - these measurements gave essentially the same results, indicating that the fluence of the pulses and not the intensity drove the dominant nonlinearity. The fluence dependence was also corroborated by ns z-scan measurements at NVESD, which demonstrated the same magnitude refractive nonlinearity as determined with ps excitation.

Having demonstrated the fluence dependence of the optical nonlinearities in GaP, we next turned our attention to the practical aspects of optical limiters based on GaP. To this end, we constructed low f/# devices based on this compound and characterized their performance for 532 nm excitation. These devices have demonstrated ~30% linear throughput at 532 nm and effective dynamic ranges for eye safe limiting (defined as the ratio of the input energy at which the output exceeds 0.2 μJ to the switching energy of ~10 nJ) of > 45 dB. While these are very promising results, this limiter has two significant drawbacks: 1) much of the dynamic range is achieved by

operating the device at fluences above the single shot damage threshold of the GaP. Nevertheless, in this mode the device fails safe and the low f/# ensures that the damage does not significantly degrade the linear imaging through the device. 2) A more severe shortcoming is that the device in its present form is expected to operated only over a narrow bandwidth of perhaps 20-30 nm. This limitation is not easily reconciled but may be reduced by using thinner GaP samples or by utilizing deep level impurities for the optical transitions.

2.1 Primary Conclusions

While we have made significant progress in developing an understanding of a wide variety of optical nonlinearities in numerous materials potentially suitable for optical limiting and have explored several optical limiting configurations, we can summarize some of our key findings as follows.

- For eye protection devices, an intermediate focal plane must be available or provided in any practical device due to the limited magnitude of optical nonlinearities in existing materials.

- The most promising device configuration for eye protection is the simplest, i.e., one that utilizes a single beam and single intermediate focal plane at which the nonlinear medium is placed.

- It is likely that the devices that most closely meet the program goals will involve multiple nonlinear elements in self-protecting configurations.

- Two-photon related nonlinearities in semiconductors can provide broad-band, eye-safe optical limiting, but only for subnanosecond pulses.

- Nonlinearities associated with linearly generated carriers in semiconductors such as GaP can provide eye-safe limiting levels for a wide range of pulse durations, but only over a limited bandwidth. We have identified two potential approaches for improving the bandwidth: 1) reducing the GaP thickness, in effect trading off dynamic range for bandwidth and 2) incorporating deep levels into the GaP and utilizing impurity to conduction band and valence band to impurity transitions for broad band absorption. Another potential problem that must be addressed in such a material is the issue of diffusion of carriers out of the focused spot for low f/# configurations. This would lead to a decrease in the "effective" nonlinearity.

- In the low f/# limiters that are required for practical applications, damage to the nonlinear element itself should not necessarily be used to determine the dynamic range of the device. For example, the GaP limiter continues to limit far above the GaP damage threshold, and the small spot size associated with the low f/# configuration ensures that the damaged spot does not significantly degrade the imaging performance of the optical system. In addition, the damage to the GaP is a consequence of melting. The molten region quickly recrystallizes, providing protection against subsequent threat pulses.

- We have demonstrated an improved limiter response in an f4/f5 input/output configuration. Such a geometry takes advantage of the fact that in the nonlinear medium, light is preferentially blocked in the center of the focused spot, resulting in a ring-like far field pattern. The larger output f/# can be used to block much of this ring, thereby reducing the limiter throughput.

- While the particular organometallic compound that we focused on (King's complex) may not be appropriate for eye protection applications, we believe that organics and organometallics may provide the best route to approaching the program goals, in part because these materials

can often provide broadband responses and can be engineered for specific applications. We caution, however, that if these compounds rely solely on reverse saturable absorption, they will necessarily have a limited dynamic range, since the best that can be done in such a system is to achieve a new and lower steady-state transmission (see Appendix A).

- Finally, we believe that it is unlikely that any nonlinear material or combination of materials will ever meet all of the program goals in a single device configuration. The best approach may be to utilize devices optimized for most likely threats but with broader and compromised coverage for less likely threats.

A large body of detailed additional information regarding progress on this contract has been communicated in the regular quarterly reports and in manuscripts included in those reports as Appendices. Further information and details may be found in the Appendices attached to this report. Appendix A contains a review paper on optical limiting to be published in Progress in Quantum Electronics. This review, which resulted in part from work on this contract, contains an overview of optical limiting using a variety of materials, including organics, organometallics, fullerenes, semiconductors, and liquid crystals. Appendix B contains an internal report describing preliminary f/15 limiting results and measurements of optical nonlinearities in GaP.

2.2 Recommendations

By considering both our own experience on this program and by incorporating our knowledge of the successes and failures of others involved in the eye and sensor protection program, we conclude the following regarding directions for future research in this area.

- We believe that the material systems with the most potential for success for eye and sensor protection are the organics and organometallics. This is primarily because of the extreme flexibility inherent in these materials, i.e., their amenability to molecular engineering. This property allows the molecules to in principle be tailored to a given application and, more importantly, offers hope for engineering improved optical nonlinearities. We believe that the most promising approach to utilizing such molecules is to explore systems that exhibit RSA. Attempts should be made to identify compounds with weak, broad-band linear absorption (perhaps metal-metal transitions in an organometallic) in the visible but that have strong excited state absorption (characteristic of, e.g., a charge-transfer transition). Ideally, the system should exhibit rapid intersystem crossing, e.g., from a singlet excited state to a triplet state, and the lifetime of the triplet should be long compared to the potential threat pulse duration. The ratio of the excited-state cross section to ground-state cross section should be as large as possible (a ratio of 1000:1 is not inconceivable and should be sought). Since at best RSA acting alone can only result in a new and lower transmission, such a system is doomed to have an output that exceeds the MPE for some input level. Hence, careful consideration should be given to supplementing the RSA with, e.g., refractive nonlinearities associated with either excitation of the molecule itself or with heating, electrostriction, or $\chi^{(3)}$ in the solvent or host. We note that even if a suitable molecular system is found, many systems issues must still be addressed before it could be implemented into a practical configuration for eye protection. For example, a sufficient number of molecules must be placed within the focal volume of a low f/# system to provide adequate dynamic attenuation for eye protection. The associated molar concentrations may be limited by solubility in a molecular system. As a specific example of a molecular system that remains promising, we cite the metallated phthalocyanines, naphthalocyanines, and related compounds. Steady progress has been made in engineering such compounds for optical limiting applications, and continued research should be encouraged. Also, the fullerenes remain interesting due to the novel nature of these

molecules, their optical properties, and the potential for engineering enhanced nonlinear optical properties.

- While photorefractives continue to appear promising for eye and sensor protection from long pulses or CW radiation, adequate protection from ns pulses requires that photorefractive materials with both high gain and high sensitivity be developed. This and other applications have led to the study of controlled doping and post growth processing to increase the sensitivity of materials such as $BaTiO_3$. Such an increase in sensitivity can be obtained by increasing the carrier lifetime, carrier mobility, or both. Continued research into high-speed, high-sensitivity photorefractives, such as Co-doped and chemically reduced $BaTiO_3$, should be encouraged, and this research should include studies to develop a thorough understanding of the cause and effect associated with materials engineering by growth and post-growth processing.

- Optically-induced damage in transmission mode configurations should continue to be examined for optical limiting. In low f/# configurations, damage can be used as an effective means for limiting without rendering an optical system inactive. This is a consequence of the small spot sizes and, hence, small damage spots that occur in the focal plane of a low f/# lens. We have demonstrated that damage in GaP can be used to provide optical limiting below the MPE over many decades of input fluence for an f/5 configuration. While the damage results in some ablation of material, no "punch through" has been observed. Once a spot has been severely damaged, it remains essentially opaque, thereby protecting the sensor from subsequent illumination on that same spot (note that it is extremely unlikely that this same spot would be illuminated if the threat laser is a low repetition rate {e.g., ~ 10 Hz} system). Again, the imaging quality of the optical system is not severely degraded by this single spot because of its small size, i.e., thousands of damaged spots could be sustained before significant image degradation occurred.

Transmission configurations such as used with GaP have the advantage over reflection configurations in that they are not limited by the residual reflection from the undercoating in a thin film reflective device. While the GaP results are intriguing, we recognize that the GaP limiter, even operating via the damage mode, is constrained by its bandwidth limitation (we have demonstrated that optical damage at 1.06 μm in GaP does not provide adequate limiting levels for eye protection). An ideal material for limiting by damage would be a broad band linear absorber with a low damage threshold (~ 100 mJ/cm^2) that was either pulse width independent or depended only weakly on pulse width. The absorption coefficient should be such that the material can be made thick enough to avoid "punch through" by ablation while still providing adequate luminous transmission. Still another issue is that of diffusion, which could tend to increase the damaged spot size for a given fluence; the material should have a low diffusion coefficient. We have considered broad band absorbers in the visible such as amorphous silicon (Si on sapphire) for this application. Such Si films must be made quite thin (~ 100 nm) to provide reasonable luminous transmission in the visible, and they may not be adequate to avoid catastrophic ablation. It may be possible to use a hard transparent overcoat, such as diamond, to reduce this problem. Amorphous Si (or some other semiconductor) embedded into a glass (or other hard, transparent host) may also be a route to consider for this application.

- We recommend that systems issues related to optical limiting continue to be studied theoretically. Parametric studies of a limiter response should be conducted for a given system configuration as a function of nonlinear material parameters and for a given material as a function of system configuration. Finally, the influence of aberrations on the limiter response should be carefully considered. The limiter response should be modeled for off-axis illumination to determine the effects of coma on its response, an aberration that could significantly reduce the effectiveness of limiting in low f/# systems. We have found that, in a limiter dominated by defocusing and optically-induced damage (GaP

limiter), the limiter response was dramatically improved when the plano-convex singlet focusing lens was replaced by a doublet of the same focal length and f/#, thereby reducing spherical aberration. This indicates a significant potential pitfall of blindly following the Gleason protocol, which calls for use of a simple plano-convex f/5 lens in all limiter configurations.

3. Goals for the Remainder of the Contract

As mentioned, the level of effort for the remainder of the contract will be greatly reduced, essentially consisting of the effort of the single AASERT student with guidance from the principal investigators. It must be emphasized that the program at this point is student oriented, since the goal of the AASERT program is to increase the number of high-quality U.S. scientists and engineers trained in areas relevant to the D.O.D. As a continuation of our program, we will complete our experimental and theoretical studies of the GaP optical limiter. These studies will include the incorporation of diffusion into our theoretical model for the GaP limiter. Our concern is that in the low f/# systems that are of the most practical importance, carrier diffusion out of the focused spot could severely degrade the GaP (or any other semiconductor) limiter response for nanosecond excitation. We will also numerically analyze the unmatched input/output f/# systems to quantify the limiter improvement in this configuration. We also intend to perform some of the parametric systems studies mentioned above. In addition, we plan to conduct picosecond measurements of the optical response of high-speed $BaTiO_3$. The material, which will be provided by Sandoz Huningue of France, is state-of-the-art, Co-doped and chemically reduced $BaTiO_3$, that is being grown as part of a major program for improving the reproducibility of growth and speed of response of this photorefractive material. The measurements are expected to allow for the separation of the carrier mobility from the carrier lifetime in sensitivity measurements. This information will be correlated to growth conditions and used for improving

material properties. Measurements will also be conducted with a tunable infrared optical parametric oscillator to explore the deep levels in these $BaTiO_3$ samples to aid in quantifying the nature of the levels and their role in the photorefractive response.

Appendix A

A Review of Optical Limiting Mechanisms and Devices Using Organics, Fullerenes, Semiconductors and Other Materials

An Invited Review Paper

To be Published

Progress in Quantum Electronics

A Review of Optical Limiting Mechanisms and Devices using Organics, Fullerenes, Semiconductors and Other Materials

Lee W. Tutt
Eastman Kodak Co.
Rochester, NY 14650

and

Thomas F. Boggess
Center for Laser Science & Engineering and Department of Physics and Astronomy
University of Iowa
Iowa City, IA

Abstract

We review nonlinear optical processes in various materials which can be utilized in passive optical limiting devices. Specifically, the mechanisms of reverse saturable absorption, two-photon and free-carrier absorption, nonlinear refraction, and induced scattering are examined, and the implementation of these processes in optical limiting devices is discussed. The effectiveness of each approach depends on the specific application for the optical limiting device, and the advantages and limitations of each are addressed. Different materials, such as fullerenes, organometallics, carbon black suspensions, semiconductors, and liquid crystals, all of which have been used in optical limiting devices, are discussed.

1. Introduction

The continuing integration of all-optical, electro-optical, acousto-optical and opto-mechanical devices into modern technology has led to the development of an ever increasing number of novel schemes for efficiently manipulating the amplitude, phase, polarization, or direction of optical beams. The ability to control the intensity of light in a predetermined and predictable manner is one of the most fundamental and important of manipulations, with applications ranging from optical communications to optical computing. Although there are numerous methods that can be used to switch, limit, amplify, or modulate the amplitude of an optical signal, all of these may be broadly categorized into two groups: dynamic and passive methods.

Dynamic control is accomplished by a device that uses some form of active feedback. A photosensor which controls an iris that restricts the intensity of light incident on an optical system is an example of dynamic control. There are virtually an infinite number of schemes and devices that can be constructed to control light in such a manner. These dynamic devices suffer a number of disadvantages, such as a tendency to high complexity and slower speeds than passive devices. The higher complexity results from the need for multiple components that must communicate with one another. A device designed for dynamic intensity control generally requires a sensor, a processor, and an actuation module to accomplish this task. The tendency to slower speeds is due to the sense, process, and actuate functions being separate. Individual modules require time to operate in a serial manner and time for communication between the modules.

By contrast, passive control is typically accomplished using a nonlinear optical material in which the sensing, processing and actuating functions are inherent. This type of material has been referred to as an intelligent or smart material. Since the optical control function is part of the physical characteristics of the material, the speed is not limited by communication between individual modules and the device can potentially be very simple and fast. Such devices are crucial for controlling short optical pulses.

Two important and distinctly different types of passive devices used to control the amplitude of an optical signal are all-optical switches and limiters. While both have many realized and potential applications, of particular interest in this review is their application to sensor protection. An ideal passive optical switch is a nonlinear optical device that is activated at a set intensity or fluence threshold, whereupon the device becomes completely

opaque. By contrast, an ideal optical limiter exhibits a linear transmission below threshold, but above threshold its output intensity is constant. The response of an optical limiter and an optical switch are shown in figures 1a and b. We emphasize that these responses are those of ideal devices to ideal optical pulses that are uniform in both space and time. Pulses with realistic temporal and spatial profiles modify these responses. Under more realistic conditions, the limiter activation threshold is less well defined, and the output fluence will not be perfectly clamped at a constant value. For any realistic switch, the leading edge of a fast optical pulse will pass through the device before activation, yielding a response intermediate between a limiter and an ideal switch (Fig. 1c). Although optical limiters and optical switches are both important nonlinear optical devices that can often be used interchangeably for certain applications, in this review we restrict our discussions to passive optical limiters.

Optical limiters have been utilized in a variety of circumstances where a decreasing transmission with increasing excitation is desirable. For example, these devices have been used for various laser pulse shaping applications. While saturable absorbers had long been used for pulse compression, Q switching and mode locking, in 1984 Harter and Band[1] demonstrated that an optical limiter consisting of a reverse saturable absorber could be used for passive mode locking. Harter, et al.[2], have also shown that amplitude modulated pulses can be smoothed by an optical limiter, provided the duration of the amplitude substructure is long compared to the activation time of the limiter. In this application, a long optical pulse with short intensity spikes incident on the limiter will have the spikes preferentially attenuated with respect to the average pulse shape. The net result is a pulse with a more temporally uniform shape. In 1986 Band, et al.[3], demonstrated that an optical limiter could be combined with a saturable absorber for improved pulse compression. In this configuration, the leading edge of the pulse is preferentially attenuated by the saturable absorber, and the trailing edge of the pulse is preferentially attenuated by the optical limiter. The latter is activated by the energy absorbed from the leading portion of the pulse. The net result is a more temporally compressed and symmetric pulse than would be obtained for either mechanism acting alone.

Yet another application of optical limiters has been proposed and demonstrated by Bialkowski[4]. In this case, a slow optical limiter was used to reduce the background in pulsed, infrared-laser-excited, photothermal spectroscopy. This application makes use of the slow response of a $BaTiO_3$ photorefractive beam fanning optical limiter to reduce a large background signal, thereby relatively enhancing the fast transient signals of interest.

This particular application is unusual because it requires an optical limiter with a very slow response. The method of using slow optical limiters for rejection of constant background is likely to be applicable to other areas of spectroscopy.

One of the most important application for optical limiters, however, is eye and sensor protection in optical systems, such as direct viewing devices (telescopes, gunsights, etc.), focal plane arrays, night vision systems, etc. All photonic sensors, including the eye, have an intensity level above which damage occurs. Using an appropriate optical limiter in the system prior to the sensor extends the dynamic range of the sensor and allows the sensor to continue to operate under harsher conditions than otherwise possible.

In this review we attempt to provide a broad overview of passive optical limiters, with an emphasis on devices intended for eye and sensor protection. All of these devices necessarily rely on optical nonlinearities and use a variety of nonlinear mechanisms. Their application to optical limiting is discussed. We address the advantages and liabilities of various nonlinear media which may serve as the active material for these devices. There exists a rather extensive literature on optical limiters for sensor protection, and many of the key references are included herein. However, the scope of the review, and hence the reference list, is not intended to be all inclusive, and undoubtedly some devices, applications, materials, and references have been omitted. There have been several recent overviews[5,6,7,8] of various aspects of this topic, and the reader is referred to these papers, as well as the other references herein, for supplementary and complementary information to the present review.

The review is organized in the following manner. In the next section, we discuss a variety of nonlinear optical phenomena that can be used to construct an optical limiter. These include absorptive processes such as reverse saturable absorption, two-photon absorption, and free-carrier absorption, nonlinear refractive processes such as self focusing, self defocusing, and photorefraction, and optically induced scattering. Various optical limiter design considerations are discussed in Section 3. In Section 4, we consider specific material examples, such as carbon black suspensions, organometallics, fullerenes, semiconductors, and liquid crystals, and our conclusions are presented in Section 5.

2. Mechanisms for Passive Optical Limiting

The optical limiting devices that have been reported in the literature are many and varied, but they all rely on a material (or materials) that exhibits at least one nonlinear optical mechanism. Such mechanisms include, e.g., nonlinear absorption, nonlinear refraction, induced scattering, and even phase transitions. The origins of such nonlinearities vary widely. For example, nonlinear absorption may be associated with two-photon absorption, excited-state absorption, or free-carrier absorption. Nonlinear refraction may arise from, e.g., molecular reorientation, the electronic Kerr effect, excitation of free carriers, photorefraction, or optically-induced heating of the material. Induced scattering is typically a consequence of optically-induced heating or plasma generation in the medium. Optically-induced phase transitions are also usually of thermal origin. Often, more than one of these processes is operative in any given device, but in this section each process is addressed individually. The section on specific material examples illustrates how multiple nonlinearities are often combined in a single device.

All optical nonlinearities can be broadly classified into two groups: instantaneous and accumulative nonlinearities. For the former, the polarization density resulting from an applied electric field occurs essentially instantaneously. For such interactions, the polarization density amplitude is usually expanded in a Taylor series[9] in the electric field amplitude, E, or :

$$P=\varepsilon_0[\chi^{(1)}E+\chi^{(2)}EE+\chi^{(3)}EEE+\ldots], \qquad (1)$$

where $\chi^{(n)}$ is the complex susceptibility tensor of order n. The first term, $\chi^{(1)}$, is responsible for linear absorption and refraction, while the remaining terms are associated with light-induced nonlinear effects. The $\chi^{(2)}$ term is present only in noncentrosymmetric materials, and it gives rise to sum and difference frequency mixing, optical rectification, and the electro-optic effect. The term most widely applied to optical limiting is that involving $\chi^{(3)}$. The most important $\chi^{(3)}$ processes for optical limiting are two photon absorption, which is associated with the imaginary part of $\chi^{(3)}$, and the electronic Kerr effect, which is associated with the real part of $\chi^{(3)}$.

In contrast with the instantaneous nonlinearities, accumulative nonlinearities arise from interactions with memory, i.e., the polarization density generated by an applied field either develops or decays on a time scale comparable to or longer than the excitation duration. Such interactions are generally dissipative, i.e., they require energy transfer from the field to the medium, and the nonlinearity itself is initiated by this energy transfer. Hence, in

contrast with the instantaneous nonlinearities that depend on the instantaneous intensity within the medium, the accumulative nonlinearities typically depend on the energy density deposited in the medium. Examples of such accumulative nonlinearities include nonlinear absorptive processes, such as excited-state absorption and free-carrier absorption, and nonlinear refractive processes associated with free-carrier generation or optically-induced heating. These nonlinearities can also be nonlocal, i.e., the polarization density induced at position $\mathbf{r}$ may depend on the optical intensity at position $\mathbf{r}'$. An important example of such a process with applications to optical limiting is the photorefractive effect.

Accumulative nonlinearities can in principle depend only on the fluence (as opposed to the intensity) in the incident pulse and, therefore, can be used to construct optical limiters with responses that are insensitive to the incident pulse duration. The resonant nature of the accumulative nonlinearities, however, frequently results in a narrow bandwidth of operation for devices utilizing these mechanisms. By contrast, optical limiters that rely on instantaneous (nonresonant) nonlinearities can be very broad band. These nonlinearities, however, require high intensities and typically effectively operate only for very short optical pulses.

All of the nonlinear phenomena discussed above can be used for optical limiting, and Fig. 2 schematically illustrates the application of some of these processes in several of the optical limiting configurations reported in the literature and subsequently discussed below. Fig. 2a depicts the use of induced absorption, such as reverse saturable absorption, two-photon absorption, and free-carrier absorption. Fig. 2b-d represent, respectively, a self defocusing limiter, self focusing limiter, and an induced scattering limiter. Finally, Fig. 2e and 2f illustrate a photorefractive beam fanning limiter and a photorefractive excisor device. While it is often the case that any given material will exhibit multiple nonlinear properties, for simplicity the effects of each individual process have been separately depicted in Fig. 2 and will be separately discussed in some detail below. Specific material examples where multiple nonlinearities are important will be discussed in a subsequent section.

A. Reverse Saturable Absorption

In the mid 1960's, shortly after the invention of the laser, many researchers were investigating dyes for potential application to Q-switching of the laser cavity. For this application, dyes were sought that would bleach to transparency under intense illumination (saturable absorbers). Guiliano and Hess[10] in 1967 were investigating vat dyes and their

modified cousins and noted some examples that not only did not bleach to transparency but instead darkened at high intensities. This was the first recognition of the property of reverse saturable absorption (RSA).

Reverse saturable absorption generally arises in a molecular system when the excited state absorption cross section is larger than the ground state cross section. The process can be understood by considering a system that is modeled using three vibronically broadened electronic energy levels, as shown in Fig. 3a. The cross section for absorption from the ground state N_1 is σ_1, and σ_2 is the cross section for absorption from the first excited state N_2 to the second excited state N_3. The lifetime of the first excited state is τ_2. As light is absorbed by the material, the first excited state begins to become populated and contributes to the total absorption cross section. If σ_2 is smaller than σ_1, then the material becomes more transparent or "bleaches"; i.e., it is a saturable absorber. If σ_2 is larger than σ_1, then the total absorption increases, and the material is known as a reverse saturable absorber. This behavior is shown in Fig. 4. The change in intensity of a beam as it propagates through the material is :

$$dI/dz = - [N_t\sigma_1+N_2(\sigma_2-\sigma_1)]I \,, \qquad (2)$$

where z is the direction traversed, and N_t is the total number of active molecules per area in the slice dz, and the population of level 3 has been neglected. Initially, the material obeys Beer's law when N_2 is unpopulated, and the transmission is constant as the incident fluence is increased. The slope is given by $T=-\log(\sigma_1 N_t L)$. At a sufficiently high fluence, however, the first excited state N_2 becomes substantially populated and in the limit of complete ground state depletion the slope again becomes constant at the new value of $-\log(\sigma_2 N_t L)$. The optical limiting action is not truly limiting, as the fluence which is transmitted is still increasing with increasing incident fluence, but it does so more slowly. If the ratio σ_2/σ_1 is sufficiently large, however, the new transmission will be small and in a properly designed system the dynamic range of the sensor will be greatly extended.

The three level diagram describes the simplest case for RSA materials but can generally only be applied for subnanosecond pulses and under circumstances such that transitions from the second excited state are negligible. The energy states involved in three level materials usually consists of singlet states and the transitions are all allowed. The transition cross sections are therefore large, but a disadvantage is that de-excitation is rapid (τ_2 small). This necessitates larger intensities for long pulses to activate the nonlinearity

through populating the excited electronic state. Fortunately, on longer timescales in some systems, significant intersystem crossing to other states can occur from the first excited state. In this case the five level diagram shown in Fig. 3b is applicable. The excited state N_4 is usually a triplet or other long lived state, and for long pulses it can act as a metastable state that accumulates population during the pulse. The lifetime of N_4 gives an indication of the maximum pulse width for which the material is efficient to act as an optical limiter. Pulses with duration longer than the metastable state allow some of the metastable molecules generated by the leading edge of the pulse to decay to the ground state before the trailing edge has passed, thereby reducing the RSA.

In most systems, τ_3 and τ_5 are very small and significant population of N_3 and N_5 do not accumulate. Therefore, N_3 and N_5 can be set to zero, considerably simplifying the dynamical equations describing Fig. 3b. The equations representing the full five level model are given by:

$$\partial N_1/\partial t = -\sigma_1(N_T-N_2-N_3-N_4-N_5)I/h\nu+N_2/\tau_2+N_4/\tau_4 \quad (4)$$

$$\partial N_2/\partial t = \sigma_1(N_T-N_2-N_3-N_4-N_5)I/h\nu-\sigma_2N_2I/h\nu-N_2/\tau_2-N_2/\tau_{24} \quad (5)$$

$$\partial N_3/\partial t = \sigma_2N_2I/h\nu-N_3/\tau_3 \quad (6)$$

$$\partial N_4/\partial t = -\sigma_4N_4I/h\nu-N_4/\tau_4+N_2/\tau_{24}+N_5/\tau_5 \quad (7)$$

$$\partial N_5/\partial t = \sigma_4N_4I/h\nu-N_5/\tau_5 \quad (8)$$

$$N_T = N_1+N_2+N_3+N_4+N_5 \quad (9)$$

and

$$\partial I/\partial z = -\sigma_1(N_T-N_2-N_3-N_4-N_5)I-\sigma_2N_2I-\sigma_4N_4I\,, \quad (10)$$

where $h\nu$ is the energy per photon, I is the intensity of the pulse, and stimulated emission has been neglected. The latter assumes that optical coupling to the excited states is well above the bottom of the vibronic manifolds and that relaxation from the optically-coupled states to the bottom of the manifolds occurs on a time scale that is much shorter than the pulse duration. To completely understand the response of an RSA device, these equations

must be solved as the pulse propagates through the material. The material parameters necessary to solve the equations are σ_1, σ_2, σ_4, τ_2, τ_4, and τ_{24}. For optimum optical limiting performance, certain parameters need to be maximized. The ratio of the excited state absorption to the ground state, σ_2/σ_1, σ_4/σ_1 should be large to minimize the transmission of the limiter at high incident intensity. For maximum efficiency, the lifetime of the triplet state (τ_2) and the intersystem crossing rate $1/\tau_{24}$ should be large to populate the triplet state and maintain the population throughout the pulse.

B. Two-Photon Absorption

Two photon absorption (TPA) can also be used in a manner similar to RSA to construct optical limiters. In contrast with reverse saturable absorption, TPA is an instantaneous nonlinearity that involves the absorption of a photon from the field to promote an electron from its initial state to a virtual intermediate state, followed by the absorption of a second photon that takes the electron to its final state. Since the intermediate state for such transitions is virtual, energy need not be conserved in the intermediate state but only in the final state. The mechanism of TPA can be thought of in terms of the three level RSA model for the case where the lifetime of the intermediate state approaches zero and the ground state absorption is extremely low (highly transparent). The intensity of the beam as it traverses the material is :

$$\partial I/\partial z = -(\alpha + \beta I)\, I\,, \tag{11}$$

where α is the linear absorption coefficient and β is the TPA coefficient which is related to the imaginary part of $\chi^{(3)}$ by the equation:

$$\beta = \frac{3\omega}{2\varepsilon_0 c^2 n_0^2}\, \mathrm{Im}\left[\chi^{(3)}\right] \qquad \text{(SI)} \tag{12}$$

Here, ω is the circular frequency of the optical field, n_0 is the linear index of refraction, and c is the speed of light in vacuum. The solution to the propagation equation for $\alpha=0$ (transparent material at low intensities) is given by

$$I(L) = \frac{I_0}{(1+I_0\beta L)}\,, \tag{13}$$

where L is the length of the sample. This clearly demonstrates that the output intensity decreases as the input intensity increases, exactly the behavior that is desired for an optical limiter. The strength of this reduction is explicitly dependent on the TPA coefficient, the incident intensity, and the sample thickness.

For TPA, the material response is on the order of an optical cycle and is, therefore, independent of the optical pulse length for a fixed intensity. The device will respond virtually instantaneously to the pulse. On the other hand, because of the limited magnitude of β in existing materials, high intensities are required to realize significant TPA. Since the intensity is essentially the energy density divided by the pulse duration, short pulses are required to achieve limiting with TPA for energy densities that may be high enough to damage an optical sensor.

To illustrate this, consider a pulse of duration τ that is incident upon an optical limiter that is constructed by placing a TPA material at the focal plane of a unity magnification inverting telescope. The fluence at the focal plane is 10^5 times that at the input, i.e., the limiter incorporates an optical gain of 10^5. The 1-mm-thick active material has a TPA coefficient of $\beta = 10$ cm/GW. For eye protection, as later discussed, the output of this device must be clamped below ~ 1 $\mu J/cm^2$, which corresponds to a fluence of 0.1 J/cm^2 transmitted through the sample. For a pulse that is rectangular in time and cylindrical in space, Eq. (13) indicates that the transmitted fluence, F, for high intensities ($I_0 >> 1/\beta L$) approaches

$$F = \tau/\beta L \, . \tag{14}$$

Hence, to achieve a transmitted fluence below 0.1 J/cm^2 (and, therefore, a device output of less than 1 $\mu J/cm^2$) requires a pulse duration of $\tau = 100$ ps or less. This approximation assumes a uniform beam profile at the sample, which of course is not typically the case in an optical system with gain; for an Airy pattern or a Gaussian profile at the sample, an even shorter pulse would be required. For a pulse that is again rectangular in time but Gaussian in space, it can be shown[11] that the transmission of the sample is

$$T = \frac{1}{\beta I_0 L} \ell n(1 + \beta I_0 L) \, . \tag{15}$$

The Gaussian spatial profile results in a less effective clamping of the output as is illustrated in Fig. 5, which shows the fluence transmitted through the nonlinear medium versus input

fluence measured at the surface of the medium for three pulse durations (1 ns, 100 ps, and 10 ps) and for the parameters mentioned above. Clearly, even for a 100 ps pulse, the output fluence of the device will not be adequate for eye protection. In principle, improved performance could be obtained using a thicker sample. Realistic systems, however, are likely to possess a low f-number, and focused spots in the sample may only be a few microns in radius. The Rayleigh range associated with such spots may be less than 100 μm. This effectively restricts the useful length of the nonlinear medium to comparable dimensions. Of course, an improved response could also be realized if a larger value of β is used. Unfortunately, at visible wavelengths the value of 10 cm/GW used in this example is not atypical. Thus, TPA acting alone is not a practical approach to eye protection for nanosecond and longer threat pulses.

Examination of Fig. 5 also demonstrates a phenomenon that is common to limiters in which the spatial beam profile within the nonlinear medium is nonuniform, e.g., a Gaussian or Airy pattern. That is, the limiter does not exhibit a perfectly clamped output at high input levels, but the output continues to gradually increase (albeit quite slowly). This is simply a consequence of the low intensity or fluence associated with the wings of the pulse passing through the medium unaffected.

Semiconductors are by far the most widely studied TPA materials for optical limiting applications. While narrow band gap semiconductors can exhibit large TPA coefficients and may be of interest for infrared sensor protection[12,13], wider gap (transparent at visible wavelengths) materials, which one might consider for eye protection, have rather small TPA coefficients, on the order of 10 cm/GW or less[14]. Again, this makes these materials suitable for eye protection against only very short threat pulses. The scaling of β with band gap energy was theoretically predicted by Wherrett[15], who used a two-band **k•p** model to show that

$$\beta(\omega) = K \frac{\sqrt{E_p}}{n_0^2 E_g^3} F\left(\frac{2\hbar\omega}{E_g}\right), \tag{16}$$

where

$$F(2x) = \frac{(2x-1)^{3/2}}{(2x)^5} \tag{17}$$

and where K is a material-independent constant, Eg is the bandgap of the material, and Ep~21eV, which is approximately material independent for direct bandgap materials. Subsequently, Van Stryland and co-workers[14] experimentally verified this relationship for a wide range of materials with band gaps from the near UV to the near IR, and Hutchings and Van Stryland[16] extended the theoretical model to include four bands and nondegenerate conditions to obtain excellent quantitative agreement with measured values of β. This sequence of results is extremely important from not only a fundamental perspective but from a practical point of view in that it provides a predictive capability, allowing one to estimate the performance of a TPA material in a limiter without necessarily measuring its response. Note that, as mentioned above, Eq (16) clearly shows that wider band gap materials have smaller TPA coefficients. Also for a given material, i.e., a fixed band gap, β is dependent on the incident frequency, and thus the limiting action will be frequency dependent. Nevertheless, this frequency dependence is weak compared to that associated with single photon resonant processes, which are discussed below.

It is interesting to note that, while TPA is an important process for optical limiting, most devices that have used TPA in semiconductors have responses which are dominated by self defocusing associated with the TPA generation of free carriers[17]. These processes will be discussed in detail below.

C. Free-Carrier Absorption

Once carriers are optically generated in a semiconductor, whether by single photon or two-photon absorption, these electrons (holes) can be promoted to states higher (lower) in the conduction (valence) band by absorbing additional photons This process is often phonon assisted, although depending on the details of the band structure and the frequency of the optical excitation, it may also be direct. The phonon assisted phenomenon is referred to as free-carrier absorption, and it is analogous to excited-state absorption in a molecular system. It is clearly an accumulative nonlinearity, since it depends on the build up of carrier population in the bands as the incident optical pulse energy is absorbed.

Free-carrier absorption can readily be incorporated into the intensity propagation equation in the following form:

$$\partial I/\partial z = - (\alpha + \sigma N) I , \qquad (18)$$

where we have assumed only linear and free-carrier absorption. Here, N is the number density of electron-hole pairs and σ is the total (electron + hole) free carrier absorption cross section. The free-carrier cross section for each charge species may be expressed as

$$\sigma = \frac{e^2}{n_0 \varepsilon_0 m^* \omega^2} \left\langle \frac{1}{\tau_m} \right\rangle \tag{19}$$

from a simple high-frequency optical conductivity model[18]. In Eq. (19), m^* is the carrier effective mass, ε_0 is the permittivity of free space, e is the fundamental electric charge, and τ_m is the carrier momentum relaxation time, which is dependent on the details of the various scattering mechanisms in the medium. Free-carrier absorption appears as a nonlinear absorption process through the intensity dependence of N. This can be rather complicated depending on the mechanisms responsible for carrier generation and on the importance of recombination and diffusion during the pulse. In the presence of only linear absorption and in the absence of recombination and diffusion (i.e. for pulse durations short compared to the characteristic times associated with these latter two processes), the electron-hole number density can be obtained from

$$\partial N/\partial t = \alpha I/\hbar\omega. \tag{20}$$

For temporally and spatially Gaussian pulses and for weak nonlinear absorption, Eqs. (18) and (20) can be solved to yield an analytical approximation to the transmission, T, of the medium[11]:

$$T = \frac{T_0}{1+(1-T_0)\left[\frac{F_0\sigma}{4h\nu}\right]}, \tag{21}$$

where surface reflections have been neglected, and $T_0=\exp(-\alpha L)$ is the linear transmission. Eq. (21) applies, e.g., for linear indirect absorption near the band edge of Si[19] or GaP[20]. In Eq. (21), it is readily apparent that the nonlinearity in the transmission depends on the incident fluence rather than the incident intensity. Again, such a nonlinearity is desirable because it results in a device response that is independent of the incident pulse duration.

The above analysis has been simplified to illustrate the nature of free-carrier absorption. One must keep in mind the limitations of this solution. Both diffusion and recombination

have been neglected. If the pulse duration is long enough for these processes to be significant during the pulse, numerical solutions are required, and the device response will be pulse width dependent. In general, multiple absorptive and refractive nonlinear processes are active, and again numerical solutions are required. Also, Eq. (21) was arrived at in the small signal limit, i.e., under conditions such that the nonlinear absorption is small compared to the linear absorption. This is clearly not a reasonable assumption for an optical limiter. In the strong signal limit, Eqs. (18) and (20) can be solved exactly for Gaussian pulses to yield[11]

$$T = T_0(F_c / F_0)\ell n(1 + F_0 / F_c), \tag{22}$$

where

$$F_c = 2\hbar\omega / \sigma(1 - T_0), \tag{23}$$

and again surface reflections are ignored. Using the same device configuration as was used for the TPA limiter discussed above (i.e., 10^5 optical gain), the transmitted fluence versus incident fluence for a free-carrier absorption limiter is shown in Fig. 6 for three different values of σ. This analysis assumes that the linear transmission is 70%, the wavelength is 532 nm, and the nonlinearity is due entirely to free carrier absorption. Notice that even for a free carrier cross section of 10^{-16} cm^2, the fluence transmitted through the nonlinear medium approaches 0.1 J/cm^2 for incident fluences exceeding 1 J/cm^2. Given that free carrier cross sections in semiconductors at visible wavelengths are typically on the order of 10^{-17} to 10^{-18} cm^2, these results indicate that free-carrier absorption acting alone is not likely to provide adequate limiting for eye protection.

Free-carrier absorption always plays some role in the operation of a semiconductor limiter, if the excitation process results in the generation of significant free carrier populations in the bands. While it certainly contributes to the limiter performance and its inclusion is important in the precise modeling of the response of such devices, just as in the case of TPA, its importance typically pales in comparison with nonlinear refractive effects, whether the carriers are generated by single photon or two photon transitions. In the next section we address the refractive nonlinearities that often dominate the response of optical limiters.

D. Nonlinear Refraction

Optical limiters based on self focusing and defocusing form another class of promising devices. The mechanism for these devices may arise from, e.g., the real portion of $\chi^{(3)}$ or from nonlinear refraction associated with carrier generation by either linear or two photon absorption in a semiconductor. Both self focusing and defocusing devices operate by refracting light away from the sensor as opposed to simply absorbing the incident radiation. Compared to strictly absorbing devices, these limiters can, therefore, potentially yield a larger dynamic range before damage to the limiter itself. As is evident from the discussions below, devices primarily based on nonlinear refraction have been examined by numerous researchers. Theoretical discussions of these devices may be found in the work of Hermann[21] and Hermann and Chapple[22]. While there is a large body of experimental work based on the application of nonlinear refraction to optical limiting, perhaps the first such demonstration was reported by Leite, et al.,[23] who used thermal lensing in a thick (compared to a confocal parameter) cell of nitrobenzene, in combination with spatial filtering, to achieve optical limiting. Many subsequent devices relied on thin nonlinear media, taking advantage of "external self-action" as described by Kaplan[24], and we now give a brief description of such devices based on this concept.

Fig. 7a shows the typical device configuration for a self defocusing limiter, while Fig. 7b shows a similar device based on self focusing. A converging lens is used to focus the incident radiation so it passes through the nonlinear medium. This lens provides optical gain to the system, allowing the device to activate at low incident intensities. The output passes through an aperture before impinging on the detector. At low input levels, the nonlinear medium has little effect on the incident beam, and the aperture blocks an insignificant portion of the beam, thus allowing for a low insertion loss for the device. When nonlinear refraction occurs, however, the nonuniform beam profile within the medium results in the generation of a spatially nonuniform refractive index. This acts as either a negative or positive lens, depending on the sign of the refractive nonlinearity, causing the incident beam to either defocus or focus. In a properly designed system, this self lensing results in significant energy blocked by the system aperture, thereby protecting the sensor.

This type of limiting action can be understood with the following simplified model. Although in many practical situations the beam inside the nonlinear medium will be an Airy pattern as a consequence of overfilling the input optic, for simplicity it is assumed here that the beam propagating through the nonlinear medium is Gaussian. In addition, in the simplest case, the change in index due to the incident beam is linearly dependent on the

incident excitation intensity or fluence. Hence, the radial dependence of the intensity gives rise to a radially dependent parabolic refractive index change near the beam axis. That is,

$$\Delta n=\Delta n_0 e^{-2r^2/w_0^2} \equiv \Delta n_0(1-2r^2/aw_0^2), \quad (24)$$

where Δn_0 is the on axis index change, r is the radial distance, w_0 is the electric field radius associated with the beam in the medium, and a is a correction term to the Taylor expansion for higher order terms. For the thin nonlinear medium of thickness L, the parabolic approximation yields a thin spherical lens with a focal length of

$$f = aw_0^2/4\Delta nL. \quad (25)$$

Eq. (25) clearly demonstrates that the effective focal length of the lens decreases as the strength of the nonlinearity (Δn) increases. If the nonlinearity of the medium is negative, then the resulting focal length is negative and self-defocusing occurs. On the other hand, if the nonlinearity is positive, the effective focal length of the induced lens is positive and self-focusing occurs. In either case, in a properly designed device, the optical generation of this lens causes a portion of the light transmitted through the sample to miss the exit aperture, thereby reducing the aperture transmission and protecting the sensor. Since self-focusing can lead to catastrophic damage to the nonlinear medium itself, self-defocusing media may have an advantage in practical devices, by providing a self-protecting mechanism for the limiter itself[25,26]. On the other hand, since self-focusing produces higher intensities inside the nonlinear medium, this process may allow the limiter to activate at a lower input intensity.

Again this discussion has been overly simplified in order to illustrate the application of this phenomenon in an optical limiter. In reality, the situation is often such that both $\chi^{(3)}$ and optical generation of carriers contribute to the nonlinear refraction (i.e., both instantaneous and accumulative refractive nonlinearities) and significant nonlinear absorption may also be present. Under these conditions, the index change is not simply proportional to the input intensity, and the precise nature of the energy deposition (linear and nonlinear absorption) and redistribution (recombination and diffusion) must be known to accurately model the total nonlinear refraction. Furthermore, the paraxial approximation of Eq. (24) is not strictly applicable, and the Gaussian nature of the induced lens must be considered.

As an example of a circumstance where both instantaneous and accumulative nonlinear refraction occur, consider a limiter constructed with a TPA material. In addition to limiting due to TPA, such a limiter can take advantage of the electronic Kerr nonlinearity and refraction due to carrier generation by TPA. The strength of the former refractive process is determined by the constant γ, where for an isotropic medium and for SI units

$$\gamma = \left(\frac{\mu_0}{\varepsilon_0}\right)^{1/2} \frac{3\mathrm{Re}\{\chi^{(3)}\}}{4n_0^2}, \tag{26}$$

with μ_0 being the permeability of free space. The constant γ is related to the more customary n_2 through

$$n_2[\mathrm{esu}] = (n_0 c/40\pi)\gamma[\mathrm{SI} \tag{27}$$

The change in index due to this electronic nonlinearity at a given peak intensity, I_0, is

$$\Delta n_{\mathrm{Kerr}} = \gamma I_0. \tag{28}$$

Sheik-Bahae, et al.,[27,28] have demonstrated that, for photon energies below approximately 0.8 times the bandgap energy E_g, γ can be accurately predicted from a nonlinear Kramers-Kronig transformation of the TPA dispersion. (An excellent review of the application of the Kramers-Kronig transformation to nonlinear optics has been recently presented by D. C. Hutchings, et al.[29]). Since the TPA dispersion is now well characterized both theoretically[15,16] and experimentally[14], this result has led to a powerful predictive capability for determining bound electronic nonlinear refraction in semiconductors and dielectrics. The dispersion, bandgap scaling, magnitude, and sign of γ have been predicted and experimentally verified in a wide range of materials with band gaps ranging from the UV to the IR and with magnitudes of γ ranging over four orders of magnitude. These results have demonstrated that in a given material γ peaks near the TPA absorption edge, changes sign from positive to negative as the photon energy exceeds approximately $0.7E_g$, and possesses a magnitude with an E_g^{-4} dependence. The discrepancy between the predicted and measured values of γ for photon energies near the single-photon absorption edge have largely been accounted for by including the quadratic Stark effect[30].

By contrast with and distinct from the bound electronic nonlinearity, which is directly proportional to the intensity of the incident beam, the nonlinear refraction associated with

carrier generation is dependent on the carrier density. In the simplest model, this index change is directly proportional to the carrier density with the proportionality constant n_{eh}. When TPA is the only significant absorption process, the carrier density is given by Eq. (11) with $\alpha=0$, i.e.,

$$\partial N/\partial t = \beta I^2/2\hbar\omega . \tag{29}$$

For a rectangular pulse of duration τ and peak intensity I_0, this yields

$$N = \beta\tau I_0^2/2\hbar\omega . \tag{30}$$

For linear carrier generation, the carrier density is determined by Eq. (20), leading to $N=\alpha F_0/\hbar\omega$. In either case, the peak on axis index change associated with the generation of these free carriers is

$$\Delta n_{FC} = n_{eh}\, N. \tag{31}$$

From a model that assumes two parabolic bands in a direct bandgap semiconductor, the index change per photogenerated carrier pair, n_{eh}, is[31]

$$n_{eh} = -\frac{e^2}{2n_0\varepsilon_0 m_{eh}}\left(\frac{1}{\omega^2} - \frac{1}{\omega^2-\omega_g^2}\right) \tag{32}$$

where ω_g is the bandgap frequency and m_{eh} is the reduced effective electron-hole mass. The first term in Eq. (32) is associated with the addition of a free electron-hole pair (intraband contribution), while the second term corresponds to the removal of a bound electron resonant at ω_g (interband contribution). When the optical frequency is less than the direct bandgap frequency, the interband contribution is negative and enhances the intraband effect. By contrast, if the optical frequency is above the direct bandgap, the interband contribution is positive and it competes with the intraband component. It is clear from this simple model that one should expect that n_{eh} is significantly enhanced by the resonance contribution as the laser frequency approaches the band edge from below.

For either the bound electronic or the carrier related nonlinear refraction and for a thin nonlinear medium, the phase distribution of the pulse after traversing the medium can be readily determined from the above equations without accounting for diffraction within the

medium itself. To determine the net effect of any induced phase distortion, the output field is then propagated through the optical system using Fresnel diffraction theory. The response of a thick medium can be modeled in terms of a complete four dimensional propagation theory or as propagation through a sequence of thin media, each of which acts as a thin lens[32,33].

It is interesting to compare the relative contributions of the accumulative and instantaneous nonlinearities to the overall nonlinear refraction. Examination of Eqs. (30) and (31) reveal that, for the case of TPA-generated carriers, the accumulative refractive nonlinearity is effectively fifth order, while the Kerr nonlinearity is third order. This clearly implies that the carrier related nonlinearity will dominate the Kerr nonlinearity above some excitation level. This level can be estimated by setting $\Delta n_{FC} = \Delta n_{Kerr}$, to obtain a critical fluence, F_c, above which TPA-generation of carriers dominates the nonlinear refraction:

$$F_c = \frac{\gamma \ 2\hbar\omega}{n_{eh} \ \beta}. \tag{33}$$

Using values of β, n_{eh}, and n_2 appropriate[17] for ZnSe at 532 nm, this critical fluence is found to be on the order of 0.1 mJ/cm^2, indicating that even at relatively low fluences the TPA generated carriers will dominate the response of a ZnSe limiter.

The location of the nonlinear medium is critical to the operation of the refractive limiting device. A self-focusing limiter works best if the nonlinear medium is placed approximately a Rayleigh range before the intermediate focus of the device. When the focusing lens is induced the effective focal length of the device is reduced, and hence a larger beam appears at the exit aperture. For a self-defocusing material, the optimum geometry is approximately one Rayleigh range after the focus. This geometry dependence can be exploited to determine not only the sign of the nonlinear refraction in a given medium, but the magnitude as well. This is the principle behind the so-called Z-scan technique, which has been pioneered by Van Stryland and coworkers[34,35]. The technique consists of moving the nonlinear medium through the focal region of a tightly focused beam while measuring the transmittance through an aperture placed in the far field of the focal plane. When the medium is far before the focal plane, no self-lensing occurs. As the medium approaches the focal plane, the high intensity begins to induce a lens in the medium. For a negative nonlinearity, this lens tends to collimate the beam, thereby increasing the transmittance through the aperture. Near the focal plane, even though the intensity is highest, the

influence of the induced lens is minimized, resulting in a transmittance comparable to the linear transmittance. This is similar to placing a thin lens at the focus of a beam; this results in minimal effect on the far field beam pattern. As the sample is moved beyond the focal plane, the negative lens tends to increase the beam divergence, resulting in a decrease in the aperture transmittance. As the medium is moved still farther from focus, the intensity again becomes weak enough that the induced lensing is negligible. This sequence results in a change in transmittance with a characteristic peak, followed by a null, followed by a valley as the sample is moved from the input lens, through focus, toward the output lens. For a positive nonlinearity, the pattern consists of a valley, a null, and then a peak. Thus, the sign of the nonlinearity is readily determined. A more complete analysis of the pattern allows the magnitude of the refractive nonlinearity to be determined. While nonlinear absorption has been neglected in this discussion, if present, it must also be accounted for. This is readily done by removing the aperture in the limiter and collecting all the light transmitted by the nonlinear material. This measurement is then insensitive to nonlinear refraction. The response in this case is a valley symmetrically located about the focal plane. It should be noted that nonlinear absorption and induced scattering cannot be distinguished by this technique. The general shape of the Z-scan for a positive index change, negative index change, and a nonlinear absorber or scatterer is shown in Fig. 8.

While we have concentrated the discussion in this section on nonlinear refraction associated with the electronic Kerr effect and with free carrier generation, it should be noted that many other processes, such as molecular reorientation, absorption saturation, and optically induced heating, can also lead to refractive nonlinearities that can be used for optical limiting. Another very important nonlinear refractive phenomenon is photorefraction. Since this process is quite distinct in that it is nonlocal, transport related, and highly anisotropic, we discuss this process separately (see Section 2F).

E. Induced Scattering

Scattering is a mechanism that has been extensively studied, as it occurs in many circumstances where reduced optical throughput is not acceptable, e.g., astronomical observations, optical communication under battle field conditions, etc. Scattering is caused by light interacting with small centers that can be physical particles or simply interfaces between groups of nonexcited and excited molecules. The scattering can be highly directional or fairly uniform depending on the size of the scattering centers. It is obvious that if an optical signal induces scattering centers in a given medium, the transmission of

the medium, measured in a given solid angle, will decrease. Hence, optically induced scattering can be used in optical limiters for sensor protection. Induced scattering limiters usually rely on liquid media, because the process in such media is often reversible. That is, if chemical or structural decomposition has not occurred, the excited liquid can readily return to equilibrium. Even when decomposition does occur, the illuminated volume can be refreshed by either diffusive processes or by circulation. In solids, when scattering centers are generated, they are usually due to irreversible decomposition processes that can lead to a degradation in the linear operation of the device.

When light impinges on a particle (an atom, molecule, or cluster) the electric field interacts with the particle causing the electric charges within to oscillate. The oscillation in turn leads to radiation. The analytic expression and theory of the elastic scattering of light from particles which are smaller than the wavelength of light was originally presented by Lord Rayleigh in 1899. The process now receives his name: Rayleigh scattering. Further development of the theory was presented by Sinclair and Lanier[36]. The angular distribution of the intensity of scattered unpolarized light from a single scattering center is given by:

$$I_t(t)= \frac{9\pi^2}{2r^2} \left|\frac{m^2-1}{m^2+1}\right|^2 \frac{V^2}{\lambda^4}(1+\cos^2(t)I_0), \qquad (34)$$

where t is the angle from the incident light, m is the refractive index difference between the particle and the surrounding medium, V is the volume of the particle, r is the distance to the observer, λ is the wavelength of the incident light, and I_0 is the incident intensity. An example plot of the scattered intensity versus angle is shown in Fig. 9a It is interesting to note that the scattered radiation is symmetric with respect to forward and back scattering. For polarized incident light the total scattered intensity is identical but is unequally proportioned between the two polarizations.

Rayleigh scattering can only be applied to particles much smaller than the wavelength of light or where the particle is non absorbing (refractive index which is real). For particles where the size is comparable to the wavelength of light or larger a more complete theory was developed by Mie[37] in 1908. A good discussion of the theory was presented by Van de Hulst[38] . The equations for the transmitted intensity are significantly more complex than for Rayleigh scattering. The essential point that can be obtained is that as the size of the scattering particles increases, a larger percentage of the scattered radiation is forward

scattered. Fig. 9b shows the Mie scattering from an example particle whose size is on the order of the wavelength of the incident light. The implication is that since more scattering occurs in the forward direction, limiting based on Mie scattering will be less effective than Rayleigh scattering. For a nonzero field of view, this type of device will be very inefficient.

A number of methods have been devised that can induce scattering centers. The simplest method of generating such centers is to utilize absorbing molecules in solution. The optical energy is initially absorbed and heats the liquid until the local boiling point has been exceeded. When this occurs, bubbles are generated. The vapor-liquid interface is very good at scattering since the refractive index discontinuity is large. Bubbles have the disadvantage in that the nucleation time is at least on the order of nanoseconds[39] and in some cases may be microseconds.[40] For short pulses this is not acceptable. The bubbling may be used as a secondary limiting process in liquids when long pulse protection is desired.

More efficient limiting using the scattering process in novel ways has been proposed by two groups. Both rely on inducing a periodic scattering structure. The first is a colloidal crystalline array and the second uses stimulated Rayleigh scattering.

Asher and coworkers have extended their research on crystalline colloidal filters [41] to induced crystalline gratings[42]. The colloidal crystalline array is made by placing index-matched spheres into a liquid. If the liquid is ionic (e.g., water) and the spheres are charged due to the ionization of acidic or basic functional groups, the spheres will interact through electrostatic interactions. These interactions can occur over relatively large distances (>1 micron). When the sphere concentration is sufficiently high, and if the charges on the spheres are of the same sign, the spheres will self assemble into a regular lattice. The lattice will be either a face centered cubic or body centered cubic lattice.

When low intensity light impinges on the device, no scattering occurs because there is no refractive index difference between the solvent and the spheres. As the incident intensity increases, the induced refractive index change in the spheres yields a periodic structure. This structure acts as a grating, diffracting the light which meets the Bragg condition away from the exit aperture. The diffraction efficiency increases with increasing intensity, thereby limiting the transmitted intensity.

The disadvantage of this type of limiter is that it is only effective for light which meets the Bragg condition. This occurs for only a narrow bandwidth and a narrow incident angle. The result is a device which is effective for limiting a specific wavelength. Also, since the Bragg condition is angle dependent the device will only have a limited field of view.

Another interesting method to increase the scattering efficiency has been proposed by Peterson [43]. He analyzed the use of stimulated Brillouin scattering, stimulated Raman scattering and stimulated Rayleigh scattering for optical limiting. When the incident wave traverses a medium with scattering centers, a backscattered wave occurs, as previously discussed. The backscattered wave beats against the forward traveling wave to generate a density wave. This density wave is essentially a phase grating that stimulates backscattering of the incident field. As the intensity of the incident field increases, the magnitude of the phase grating increases, leading to more scattering. When a cylindrical lens is used to focus the incident beam, the region of highest gain is along a line directed perpendicular to the incident beam. If mirrors are placed along this axis to form a cavity, then the stimulated radiation can achieve threshold in this cavity. In this case, significant optical energy can be coupled out of the incident beam and directed away from the beam propagation direction, thus, protecting the sensor. The time required to initiate this mechanism is stated to be on the order of nanoseconds. The disadvantage is that this mechanism requires coherent monochromatic light. Arc lights and other high intensity white light sources do not activate it.

F. Photorefraction

Two novel devices designed to limit coherent optical radiation are the coherent-beam excisor and the beam fanning limiter, both of which rely on the photorefractive effect. Photorefractive materials must possess a nonzero $\chi^{(2)}$. Hence, liquids and centrosymmetric[44] crystals, which both have by symmetry a zero $\chi^{(2)}$, cannot be photorefractive. As mentioned previously and described below in more detail, the photorefractive effect is a nonlocal, accumulative nonlinearity that requires charge transport. While the photorefractive effect has generated considerable interest in recent years as a mechanism for optical limiting, this nonlinearity is unique from the other processes discussed in this review, and we introduce it only briefly here.

The conventional photorefractive mechanism relies on the existence of deep levels in the photorefractive crystal that can be optically excited to produce free charge in the conduction

or valence band. When two coherent beams interfere in a photorefractive material, photoexcitation of the deep levels generates more mobile charge (negative or positive) at the peaks of the intensity pattern than at the valleys. The photoexcited charges at the peaks diffuse into the valleys resulting in a spatial variation of charge corresponding to the interference pattern in the material. The charges in turn give rise to an electrostatic space-charge field which, for a properly oriented crystal, leads to a refractive index change through the electrooptic effect. The unusual result is that a grating is produced which is 90 degrees phase shifted with respect to the intensity of the photon field. This allows energy coupling and energy exchange between the two beams.

When a single high intensity coherent beam is incident on a photorefractive crystal, the energy can be coupled into a multitude of low intensity scattered beams. Qualitatively, this arises from the following. Inside the crystal, the incident beam will scatter off of any crystal imperfections to produce fields with new wavevectors. The incident field then interferes with these scattered fields, and this interference can result in the generation of photorefractive gratings. Light can then be coupled from the incident beam into the scattered beams by diffracting from these gratings. Since for photorefractive gratings there is a preferred direction of energy transfer determined by the direction of the c-axis of the crystal and the sign of the charge carriers, this results in the light being scattered preferentially to one side of the crystal. This process, which is referred to as photorefractive beam fanning[45], can be quite efficient, significantly reducing the intensity of the transmitted beam. Cronin-Golomb and Yariv[46] have shown that this beam fanning process can be used to construct an optical limiter.

The photorefractive excisor[47,48,49] takes this one step farther by providing a weak seed beam to interfere with the incident beam. The device is constructed such that at high intensities the photorefractive grating associated with the interference of the primary beam with the seed beam couples energy from the strong incident beam into this weak seed beam, thereby protecting the sensor. This design not only increases the speed of the device but also the efficiency.

Aside from the nonlinearity itself, a number of other facets set photorefractive devices apart from most other limiters. Both the beam fanning limiter and the photorefractive excisor will only react to coherent radiation, e.g., laser light. High intensity incoherent radiation is unaffected by the crystal. This can be both an advantage and a disadvantage for limiting devices. A major advantage over other devices is that, upon activation, low intensity

incoherent radiation is not attenuated, thus allowing continued sensor operation. That is, these devices allow the sensor to continue to monitor incoherent optical signals in the presence of the threat laser. A disadvantage is that high intensity incoherent sources such as arc lamps and flash lamps are not affected and no protection can be afforded. Furthermore, since charge transport is required to generate the photorefractive effect, these devices exhibit a response time that may be inappropriate for protection against nanosecond and shorter pulses. Another difference which sets these devices apart from other passive devices arises from the fact that the conventional photorefractive index change is independent of the total intensity of the incident beams (above a dark intensity related to the dark conductivity). It is the time for formation of the space charge field, and therefore the index change, that is the intensity dependent parameter. Another potential problem with these devices is that at high incident intensities residual absorptions, which can lead to local heating, or high electric fields can depole the crystal. If depoling occurs, the photorefractive effect is reduced but the crystal is not damaged. This effect may reduce the dynamic operating range.

3. Device Designs

The optimal design of an optical limiting device requires some knowledge of the sensor and optical arrangement leading to the sensor, as well as the nature of the most likely threat. Information as to the damage level of the sensor is necessary to determine the required limiting level of the device and to ascertain whether an intermediate focal plane will be required for the optical limiter. A knowledge of the sensor bandwidth, dynamic range, sensitivity, and field of view is necessary so that the limiter can be designed to minimally degrade the sensor performance under normal operating conditions.

The most widely studied optical limiters rely on either liquid or solid nonlinear media. Liquid limiters are often very desirable because they are extremely resilient. The energy from high intensities typically is dissipated by solvent heating and bubbling which, for sufficiently long pulses, adds extra reversible protection through scattering. Solid hosts have the disadvantage that when the thermal heating becomes too large the composite becomes irreversibly damaged.

The simplest configuration for optical limiting is realized by simply placing a nonlinear absorber or scatterer in front of the sensor. In practice, however, typical sensor damage thresholds and the limited magnitude of existing nonlinearities in optical materials ensure

that most limiter configurations require an intermediate focal plane, i.e., a focal plane between the input of the device and the sensor, at or near which the nonlinear medium is placed. In a practical device, the f-number associated with this focusing arrangement should be equal to or less than the f-number of the original system, so as not to restrict the field of view of the sensor. If the optical system to be protected is a direct viewing device, such as a periscope, telescope, binocular, or gunsight, an existing focal plane may be suitable for this purpose. Most such systems are f/10 or less to provide a reasonable field of view. If the input optic of such a system is filled by the threat beam, the spot size in the focal plane is on the order of $\lambda f\#$ for diffraction limited optics. For visible wavelengths the Rayleigh range associated with such small spots is less than 200 μm, restricting the effective interaction length in the nonlinear medium to a comparable distance.

If the nonlinear medium exhibits either self-focusing or defocusing, limiting action can be achieved by taking advantage of an aperture located behind the medium but before the sensor. To avoid degradation of the system field of view, the aperture should not reduce the effective f-number of the system. At low input levels, light passes through the system unaffected, but at high input levels, self-lensing causes the beam to spread beyond the acceptance angle of the aperture, thereby reducing the device transmission and protecting the sensor. In many cases, both nonlinear absorption (or scatter) and nonlinear refraction are simultaneously present, and both can be used for limiting.

The most important sensor to man is unquestionably the human eye, which is also the most difficult sensor to protect (and repair). The human eye is an amazing sensor, exhibiting a broadband response, self-adjusting collection optics, a dynamic range in excess of 100 dB, and even some self-protection capabilities. To accomplish the wide dynamic range, the eye has a variable aperture, a collection and focusing lens, and very photosensitive chemical sensors. The aperture (iris) for the eye compensates for high intensity light by constricting, and for very high intensity, nature has instilled a blink reflex to completely block all incoming light. Unfortunately, both the blink reflex and the muscular iris closure are no faster than a tenth of a second and, therefore, these natural reponses offer essentially no protection at all against high intensity pulses of less than 0.1 seconds duration. While mechanical devices can be used for protection against slow pulses, they have difficulty responding to pulses shorter than 10 microseconds. Hence, this is the regime for which it is essential for passive optical limiters to provide protection.

The eye is most sensitive and most susceptible to optically-induced damage when the iris is fully opened. For this condition, the optical gain of the eye, defined as the ratio of the fluence at the retina to the fluence at the cornea, is typically greater than 10^5. It is this large optical gain that can lead to irreversible damage to the retina for even very low energy optical pulses incident on the cornea. Since it is not possible to place a protective material directly in front of the retina, any limiter designed for eye protection must be activated at an input intensity at least 10^5 times smaller than the level at which the retina is damaged. As a consequence of the limited magnitude of optical nonlinearities in existing materials, this fact dictates that an intermediate focal plane must be used in the limiting device at or near which the nonlinear medium is placed. Ideally, any such device should not reduce the detection band width (400-700 nm), the dynamic range (> 100 dB), nor the field of view (> 150°) of the eye, and it must activate at an energy density compatible with eye protection. These requirements place extremely difficult design parameters on devices intended for eye protection, and to date, no single device or combination of devices has adequately satisfied all of these criteria.

The limiting level for eye protection can be determined by using the ANSI standards with some safety margins. The ANSI standards are shown in Fig. 10 as a function of the optical pulse width and energy[50]. When the eye is fully open, the maximum permissible exposure to a short, visible wavelength pulse should not exceed 0.2 μJ, which for uniform exposure of the cornea corresponds to a fluence of ~ 0.5 $\mu J/cm^2$. It should be noted that the damage level for the eye is power dependent for pulse widths longer than approximately 10 μs but is energy density or fluence dependent for pulse widths below this value. The reason is that for short exposure times thermal diffusion is negligible and the maximum energy deposited contributes to damage. During longer optical pulses the power begins to heat the retina, and the limitation is the thermal diffusion rate away from the irradiated spot.

In contrast with the eye, solid-state sensors in optical systems are generally more readily protected. Such systems often naturally incorporate relay and/or magnification optics, which provide intermediate focal planes in the system prior to the final image or detection plane in which the sensor is located. By placing a nonlinear optical material in or near one of these intermediate focal planes, one can take advantage of the high intensities in such regions to activate the nonlinear medium in the limiter. In a properly designed high optical gain configuration, the optical limiter can readily provide the sensor with 50 dB of additional dynamic range.

The damage threshold for Si PIN sensors is approximately 1 J/cm^2 at a wavelength of 690 nm for pulses ranging from 100 μsec to less than 100 ns.[51] At a wavelength of 1060 nm the damage threshold for Si PIN photodiodes is reported to rise to about 15 J/cm^2. The damage level for other detectors vary somewhat, but most thresholds fall within a range of 0.1 to 100 J/cm^2, depending on the detector material, the incident wavelength, and the incident pulse duration. One notices that these levels are much higher than the level that can damage the eye. This is predominately due to the lens in the eye which provides optical gain at the retina. The damage threshold of the retina itself is actually comparable to that of the standard Si PIN photodiode.

For general personnel protection, a goggle-type optical limiting device is highly desirable. Goggle-type devices have proven extremely difficult to implement, primarily because of the limitation on the magnitude of known nonlinearities. For example, no RSA material to date has come close to providing a limiting level of half a microjoule/cm^2 necessary for a direct view goggle. It seems unlikely that there ever will be a material developed that can be used directly as a film. The most promising method for making protective goggles involves the use of lenslet arrays. In this approach, low f-number microlenses (as small as 100 microns diameter) create an intermediate focal plane and then further lenslets reimage the light to the eye. By sandwiching a thin nonlinear medium between a pair of lenslet arrays, an optical limiter can be realized. If the lenslets are sufficiently small they will act as pixels and no reinversion of the image is necessary. If an image is required from each individual lenslet then there will be a limited field of view. The challenge is to make the curvature of the goggle such that each lenslet adds to give a wider field of view. Among the many potential problems with these goggles is vignetting between lenslets. An off axis beam can cross talk between lenslets and may not be fully limited.

Since a liquid limiter for goggle protection is not desirable, we have concentrated on solid device designs, specifically those which use RSA active materials. One aspect of this work has involved the optimization of the distribution of absorbing molecules in a RSA device. For a RSA active material homogeneously distributed in a solid host and for a converging beam configuration, we modeled the best placement of the medium by using the nonlinear differential equations for the five level RSA model. Fig. 11 shows the peak fluence as a function of position for an 8 ns pulse propagating through a RSA active material in a system with an optical gain of 100. In this example the material has strong triplet state absorption but no singlet state absorption. Each curve represents a different incident intensity. The absorption is highest at the focus due to activation of the RSA material. The

material outside the focal region is not activated and acts as a normal absorber. For maximum efficient utilization of active material it is evident that one would desire the material to all be placed at the focus. Unfortunately the maximum density of the active material and the large thermal dissipation at high intensity limit this design. For a solid material, thermal dissipation limits the absorption level above which the material suffers irreversible degradation. This process is fail-safe for the sensor, but it is desirable to achieve the largest possible dynamic range between activation of the RSA material and host breakdown.

To reduce the problems of optically-induced damage, we have explored the use of nonhomogenous concentration profiles[52]. We place the highest concentration of nonlinear material at the focal plane and decrease the concentration prior to the focus. The concentration after the focus is zero. In this scheme, as the intensity increases, more molecules are activated prior to the focus and thus the focal region is protected. The thermal energy is spread out over a wider region, the host material is more fully protected, and the active molecules are more efficiently used. Fig. 12 shows the effect of 8 ns optical pulses of various intensities incident on a nonhomogeneous distributed active medium. The concentration profile was generated by using the equation $(1+Cd)^{-1.5}$, where d is the distance in the sample from the focus, a gain of 5000, and the example RSA parameters and transmittance used to generate Fig. 11. The figure clearly shows how the absorption becomes spread out from the focal region as the incident intensity increases and, thus, increasing the dynamic range. Using the higher gain of 5000, the fluence still does not exceed 10 J/cm^2 inside the sample. This method will yield more robust solid limiters but probably will not achieve the dynamic ranges possible with liquid limiters. Fabrication problems will also limit the utility of this class of limiters to specific sensor protection problems.

Other self-protecting optical limiter configurations have been proposed and demonstrated. Hagan, et al.[53], have discussed a device they call a SPROL (self protecting optical limiter), which is realized by tightly focusing a visible wavelength picosecond pulse into a slab of ZnSe that is thick compared to the Rayleigh range of the focused beam. An aperture is used prior to detection in the standard self defocusing arrangement. As discussed below, the nonlinearities in ZnSe that give rise to the limiting action are TPA and self defocusing. Since the linear absorption in ZnSe at wavelengths below the bandgap can be quite small, in principle, the thick material will not significantly influence the linear throughput of the device. On the other hand, as the intensity in the ZnSe increases, defocusing reduces the

intensity inside the sample at the focal plane, thereby preventing the material from damaging and providing a high dynamic range. These devices have been shown to work well for 30 ps pulses at 532 nm and are expected to be broadband. The dynamic range was greater than 10^4 and limiting was observed at 3 nJ. The disadvantages are the restriction on field of view previously discussed and, in this specific device, the low linear transmission (10%). Furthermore, the nonlinearities are intensity dependent and require short pulses for activation. This device concept was extended to the MONOPOL (monolithic optical power limiter)[23], which was fabricated from a single piece of ZnSe with spherically polished input and output faces to provide internal focusing and recollimation. This device demonstrated a limiting input energy of 10 nJ for 20 ps 532 nm pulses with a dynamic range > 10^4.

Another manner in which enhanced dynamic range can be achieved is through the use of multiple devices in series. Said, et al.,[54] have demonstrated high dynamic range and a low activation threshold for optical limiting with such devices. This "hybrid" limiter consisted of a liquid optical limiter, which exhibits RSA, placed in front of a solid two-photon /nonlinear refractive material. When chloroaluminum phthalocyanine was used as the RSA material and the solid material was ZnSe, the dynamic range was increased by about a factor of 5 and the limiting threshold was reduced by half over that obtained using ZnSe alone. When the RSA material was replaced by silicon naphthalocyanine the dynamic range was increased by 30 but the threshold was twice as large. The pulse length was 30 ps and the nominal low intensity transmission was 40% for these measurements. In this device the liquid is not activated until after the ZnSe has been activated. In this manner, the liquid limiter can take over the energy load as the intensity is increased, thereby, protecting the latter material and extending the dynamic range of the device.

The use of multiple elements in series is not limited to different types of limiters. Walker, et. al.[12], have shown that enhanced limiting of CO_2 laser pulses could be obtained by using cascaded InSb etalons. The optical arrangement used two intermediate focal regions each containing a piece of the nonlinear optical material. The limiting was significantly improved relative to that obtained with a single focal plane, smoothing the 1 microsecond pulse to virtually a square pulse after the second limiter. The dynamic range was increased, as expected, by distributing the power between the two materials.

Finally the highest dynamic range protection and most general purpose devices are probably a combination of passive and active devices. The purpose of the passive device is

to provide just enough protection for the sensor to allow active control over the intensity either through shutter, movable filter, or electrooptic filter.

4. Specific Material Examples

In this section we will discuss some of the major classes of materials that are useful for optical limiting applications. These materials generally exhibit multiple nonlinear optical interactions but usually have one mechanism which is dominant. Most research efforts related to device designs are usually geared toward specific classes of materials . In most cases, the goal of achieving major improvements in optical limiter performance centers on the identification of existing materials or the synthesis of new materials with improved nonlinear optical properties. Among the more widely studied materials for optical limiting applications are carbon black suspensions, organometallics, fullerenes, semiconductors, and liquid crystals, and we discuss each of these material systems below. Again, while photorefractive materials continue to attract interest for optical limiting applications, a detailed discussion of these materials is not within the scope of this review.

A. Carbon Black Suspensions (CBS)

Carbon black suspensions are a very promising material for optical limiting applications. These suspensions consist of very small carbon particles suspended in a liquid, usually an alcohol. Carbon is a very uniform absorber at wavelengths across the visible spectrum, and the suspensions therefore exhibit a very neutral optical density. It was discovered over 10 years ago[55] that when CBS is placed in a cell at an intermediate focal plane and the intensity is raised, limiting action occurs. Many investigators have studied CBS systems because of their apparent simplicity and potential[56,57] for device applications. Their studies indicate that the limiting action is the result of a number of mechanisms, although only one dominates. These mechanisms include nonlinear absorption, nonlinear scattering, and nonlinear refraction.

The typical CBS suspension is filtered to contain particles that are smaller than the wavelength of visible light (<0.5 microns). The small size serves two purposes. First, linear scattering from such particles is weak, and unacceptable degradation of the imaging properties of the device in which the CBS limiter is utilized is prevented. Also, particles

which are extremely small will not precipitate over time because Brownian motion is appreciable.

When CBS is subjected to visible radiation, the small particles absorb the radiation, and this energy is eventually transferred into breaking the particles apart and into heating the surrounding liquid. This process can lead to thermal lensing, which can be used for optical limiting. When the incident intensity is sufficiently large the suspension is observed to give a white flash. This white flash has a spectrum which corresponds to a blackbody radiation of ~4500K. The lifetime of the flash is on the order of 30 ns when the excitation pulse is short compared to this time scale. These observations are consistent with microplasma formation.

In his thesis, which the reader is directed to for a more in depth analysis, K. Mansour[58,59] investigated the fluence dependence of the optically induced scattering in CBS using nanosecond pulses of 532 nm radiation. In Fig. 13 we show one of Mansour's results, which clearly shows that, although induced absorption initially contributes, the dominant mechanism quickly becomes induced scattering. Investigation of the far field beam profile as a function of intensity revealed that nonlinear refraction was present but relatively weak. These results indicate the major mechanism for optical limiting on a nanosecond timescale is microplasma formation and subsequent scattering from these centers. For longer timescales, bubbles occur from the thermal energy dissipated, and these act as large scattering centers.

A major advantage for CBS is that the dynamic range appears to be quite large. This follows from the fact that the scattering results from the break up of the carbon particles, and in this liquid limiter reaggregation of the carbon and influx of new material can replenish the active volume. The liquid also can "self repair" the thermal disruption. A potential drawback for CBS is that under fast repetitive pulse limiting much of the active material leaves the interaction volume in the early pulses causing a reduction in limiting for later pulses. Another problem is that, after many pulses, some agglomeration and precipitation of the carbon is seen to occur. This could cause a slow degradation of the limiting performance. CBS solutions are extremely cheap and periodic replenishment may obviate the latter problem.

B. Organometallics

The first compounds in which RSA properties were recognized were organic compounds[10], and a number of organic compounds have since been shown to possess RSA properties.[60,61,62] Organometallics are compounds similar to organic compounds, but they contain at least one metal. Only recently have organometallic compounds begun to receive attention for use in nonlinear optical applications.

Organometallic compounds have a number of advantages over organic compounds. The metal adds a number of optical transitions that do not occur in organic compounds.[63] If the metal is a transition metal, electronic transitions can occur between the d orbitals. These metal centered transitions are known as d-d electronic transitions. Electronic transitions can also occur between the organic portions (ligands) and the metal. These transitions are known as metal to ligand charge transfer (MLCT) transitions when the electron is donated from the metal and ligand to metal charge transfer (LMCT) transitions when the ligand donates to the metal. Charge transfer transitions involve a separation of charge and, hence, couple extremely well to an applied optical electric field to yield very high extinction coefficients (1000-300,000 $M^{-1}cm^{-1}$). In addition, organometallic compounds can undergo transitions associated with organic compounds when the absorption is confined to the ligand; these transitions are known as intraligand (IL) transitions.

Two classes of organometallic compounds which have been extensively investigated are metal macrocycles and metal cluster compounds. Although RSA has been shown in both classes of compounds, the approaches have been slightly different. Van Stryland, et al., in collaboration with Perry and co-workers have concentrated on metal phthalocyanines and naphthalocyanines for optical limiting.[64] Most of these compounds are extremely photostable and often sublimable allowing easy thin film growth. These metal macrocycles typically have two intense absorptions bands, a Soret band in the ultraviolet and a Q band in the red to IR region. The visible absorption is relatively small and spectrally flat, ideal for the ground state absorption in the RSA process.

These researchers have shown that chloroaluminum phthalocyanine (CAP) has significant singlet-singlet excited state absorption for subnanosecond pulses, but for longer pulses, triplet-triplet dynamics begin to dominate. Limiting efficiencies change both as a function of optical pulse lengths and as a function of frequency. This is due to absorption changes between the singlet and triplet excited state absorptions. It is probable that most RSA materials have these dependencies. The excited state absorptions were estimated to be 10-

50 times as large as the ground state at 532 nm. One of the major disadvantages with CAP is the Soret band is located in the visible at 670 nm. At this wavelength the compound acts as a saturable absorber.[65] This limits the broad band capability to the blue green region of the spectrum. Fortunately, if the red region is not required, the compound in this spectral range will act as a simple filter up to quite large intensities and still give good RSA for the rest of the visible spectrum.

Perry, et al.[66], have recently reported a more promising material, silicon naphthalocyanine (SINC), for broadband limiting which exhibits a substantially lower limiting level. This compound was previously shown[67] to have a high third order susceptibility at 1907 nm. The Q band in this macrocycle is shifted outside the visible spectrum to 778 nm. This suggests that spectral coverage may cross the full visible spectrum.

Other groups have also reported limiting properties for metal macrocycles. Blau et al.[68] have shown RSA properties in free tetraphenyl porphyrins (H2TPP) and the metallated complexes (ZnTPP and CoTPP). They observed that the dynamics were sensitive to the nature of the metal. The Zinc TPP compound was believed to give RSA through excited singlet state absorption and the cobalt complex through triplet state absorption for 80 ps pulses. Fei and coworkers[69] recently showed that FeTPP was also an RSA material and further showed a large $\chi^{(3)}$ by a degenerate four wave mixing experiment. It is certain that many more organometallic macrocycles possess RSA properties which will be useful for limiting applications.

We have taken a different approach and concentrated on metal cluster compounds for optical limiting applications. Metal clusters are compounds containing two or more metals multiply interbonded. The ligands complete the metal valence and stabilize the structure. The lowest transition is typically a transition originating in a bonding d orbital of the metal cluster core and ending in an antibonding orbital also centered on the cluster core. This is a d-d transition which weakens the core but, through delocalization, the structure remains stable. Absorptions in the visible which are due to these transitions typically have extinction coefficients of 10 - 10,000 $M^{-1}cm^{-1}$. If the excited state absorption in these compounds was due to a charge transfer transition, which typically have extinction coefficients of 1000-300,000 $M^{-1}cm^{-1}$, then the molecule would likely possess RSA properties. Our approach to achieving optical limiting with such compounds was to start with a class of compounds with a well defined ground state transition and investigate the influence of molecular modifications on the optical limiting dynamics.

We have shown limiting action from a number of iron-tricobalt cluster compounds,[70,71] and have demonstrated that the limiting action depends on the nature of the ligand. The effect of ligands on RSA properties in a metal cluster compound would be expected to correlate most highly with an excited state which directly involves the ligand, i.e., a charge transfer transition. We observed virtually no change in the ground state absorption upon replacement of triethylphosphine with triphenylphosphine in μ-hydrido iron tricobalt decacarbonyl bistriethylphosphine, but a large change in the optical limiting properties was observed. This is consistent with a ground state transition which involves the metal core orbitals and is only slightly perturbed by the ethyl to phenyl substitution. If the excited state transition involved the ligand (i.e., charge transfer transition) then the excited state, and thus the limiting properties, would be heavily effected. A large change in the optical limiting properties was observed consistent with this hypothesis. These compounds are interesting from a scientific aspect, but their air sensitivity and the nonzero absorption cross section for CO replacement, leading to photodecomposition, reduce their attractiveness for device applications.

Recently, we investigated the class of highly stable tetrairon compounds whose parent complex is $[Fe(CO)_4Cyclopentadienyl]_4$, known as King's complex, after R. B. King, the noted chemist who first synthesized it.[72] The compound is extremely stable to light, oxygen, and heat (decomposing at temperatures above 160 C). We observed optical limiting using nanosecond optical pulses from solutions of King's complex in toluene and methylene chloride (Fig. 14).[40]

We further investigated the picosecond response of King's complex and its analogues to discover the underlying photodynamics.[73,74]. The optical response of a toluene solution of King's complex to picosecond pulses is also shown in Fig. 14. The pulses are of such short duration that little triplet state contributions will occur. Monitoring the transmission as a function of time, we were able to determine cross sections of 4.1×10^{-18} and 8×10^{-18} cm^2, for the ground (σ_1) and excited state (σ_2), respectively, and lifetimes of <1 ps, 120 ps, and 2.8 ns corresponding to τ_3, τ_2, and τ_{24}, respectively (see Fig. 4). It is of note that, from a detailed study of the fluence dependence of the RSA, we were able to provide a limit to the lifetime of the second excited state; a rarely accomplished result.

Using the previous parameters, an attempt was made to fit a five level model to the nanosecond response. It was found that the observed response could not be accounted for

by the five level model and, therefore, some other mechanism must also contribute to the nanosecond response in solution. By monitoring, as a function of incident optical intensity, the off-axis scatter of 532 nm, 7 ns pulses from a cell containing a solution of King's complex, we observed significant nonlinear scattering. The scattering is radially nonuniform and the relative spatial shape changes with incident intensity. A quantitative measurement of the scattering contribution was therefore not directly obtainable.

By incorporating King's compound into the solid host polymethylmethacryiate (PMMA), the induced scattering was eliminated. Measurement of the optical limiting response for this solid sample gave much weaker limiting. If one assumes the singlet dynamics are essentially unchanged upon incorporation into a solid, the three level model can very accurately describe the nanosecond limiting response. Little if any contribution from triplet state transitions are necessary. This suggests the majority of the optical limiting observed for nanosecond excitation of solutions of King's complex is due to induced scattering with only a small amount of RSA from excited singlet absorption.[75]

The nature of the excited singlet state transition was investigated[76,77] by comparison of King's complex with the ligand-substituted analogues [Fe(CO)Methylcyclopentadienyl]4 and [Fe(COAl(Ethyl)3)cyclopentadienyl]4. If the excited state transition was due to a charge transfer transition, the optical limiting response would be different for replacement of a ligand involved in the transition. The results revealed no change in the excited state transition and, therefore, indicates the transition is another more strongly absorbing d-d metal centered transition.

To provide a direct comparison of the optical limiting performance of a number of compounds to nanosecond pulses of 532 nm radiation, optical limiting measurements on each compound were performed under identical experimental conditions (Fig. 15). For these measurements, RSA and scattering can both provide important contributions to the limiting, and but they are not distinguishable. Hence, these measurements provide an upper limit for the RSA properties of the compounds. One notes the range of the limiting thresholds is not much larger than a factor of 20 from the best to the worst compound.

Because of their widely varying optical properties and the potential for molecular engineering to allow tailoring of a molecule to a specific application, organometallic compounds are very attractive for optical limiting, and it is likely that improved nonlinear responses will result from the increased attention that these materials are receiving. Future

improvements are certain to reduce the thresholds for optical limiting, but it is unlikely that the 5 orders of magnitude reduction in threshold necessary for direct eye protection will ever be achieved.

C. Fullerenes

The class of compounds now known as Buckminster fullerenes, was originally proposed and observed by Smalley and co-workers[78] in 1985 in the laser ablation products from graphite. The compounds received little attention, however, until the discovery and publication by Kratchmer et. al.[79] in 1990 of a simple synthesis for macroscopic quantities of fullerenes. The availability of this new form of carbon, coupled with the cage structure, high symmetry, and simplicity of the molecule, has intrigued both scientists and the public alike. Very rapidly, many new and unusual properties associated with this compound were discovered. Relatively high temperature superconductivity[80], the ability to nucleate diamond growth[81], the ability to reversibly accept at least 6 electrons[82], high stability to deformation[83], and the ability to trap atoms inside the cage[84,85,86] are among a few of the more unusual properties. Many large companies have obtained samples from the numerous commercial sources for fullerenes, indicating the commercial interest in actively pursuing research on fullerenes.[87]

The optical properties of fullerenes have been examined by numerous investigators. These studies have largely centered on the numerical evaluation of the dynamics of optical transitions. Early literature reports revealed[88] that C_{60} had a higher excited state absorption cross section than ground state absorption cross section over the complete visible spectrum. This information implied that the fullerenes are RSA materials and may have application to optical limiting for sensor protection. As part of an ongoing investigation of compounds which possess RSA properties and demonstrate potential for applications to eye and sensor protection, scientists at the Hughes Research Laboratories (HRL) initiated an investigation into the optical limiting properties of C_{60}.

The absorption spectra for C_{60} in toluene solution is shown in Fig. 16. The absorption cross section for C_{60} is relatively constant across the visible spectrum (400-700 nm), not varying by more than a factor of 2 from 425 to 625nm. The absorbance has a peak at 550 nm and a local minimum at 440 nm, which gives rise to the magenta color of the solutions. C_{70} on the other hand has a shoulder at 590 nm in the absorbance spectrum,

but the absorbance continues to increase to shorter wavelengths giving rise to the distinctive orange-red color of solutions containing even small quantities of C_{70}. The absorption cross section for C_{70} is significantly greater than for C_{60} in the blue region of the spectra.

The excited state absorption spectrum measured by Sension et. al.[89] is shown in the inset in Fig. 16. The results of other workers are in agreement.[88,90,91,92] The spectrum has the same general shape as the ground state absorption, which implies the induced absorption will not vary widely over the visible spectrum. This is ideal for a broadband optical limiter. These data and the data from the references 82,84, and 85 allow one to construct the five level electronic transition diagram as discussed in the section concerning RSA. The five level diagram for the wavelength of 532 nm is given in Fig. 17.

To test the optical limiting properties of solutions of fullerenes, investigators at HRL used a collimated beam testing geometry. The optical excitation source was a frequency-doubled, injection-seeded Nd:YAG laser, which generates 8 ns 532 nm optical pulses. The optical pulse from the laser was split and the incident intensity recorded for each pulse on a fast silicon diode. The other portion of the pulse was collimated by imaging the end of a saturated amplifier rod onto the sample with large f-number optics, so that the Rayleigh length at the sample was long compared to the sample thickness. The sample of pure fullerene in a toluene or methylene chloride solution was contained in a thin sample cell. The transmitted pulse was collected and measured with a fast silicon detector. This particular setup has the advantage that the pulse spatial profile at the sample is approximately a "top hat" profile(constant spatially) and the beam neither diverges nor converges as it propagates through the sample. This arrangement minimizes the effects of nonlinear refraction and is primarily sensitive to nonlinear absorption and scattering.

The transmitted intensity versus incident intensity for 70% transmitting toluene samples of C_{60} and C_{70} are shown in Fig. 18.[93] As one might expect, the optical limiting level of C_{70} is not as low as C_{60} at 532 nm. The higher ground state optical absorption of C_{70} with respect to C_{60} would require a much higher excited state absorption to give the same relative response. This is not observed.

To model the limiting behavior, the five level model and parameters of figure 17 were used. The predicted limiting levels were about twice the experimentally determined values. This indicated that either significant amounts of another nonlinear mechanism, such as scattering, are contributing or that the five level diagram for C_{60} was insufficient to predict

the optical response. The off-axis scattering was measured as a function of incident intensity and found to vary nonlinearly, indicating that this process is likely to influence the limiter response. The absolute magnitude of the nonlinear scattering component is difficult to measure as it tends to be very nonuniform in direction, but to a first approximation the nonlinear scatter observed could account for the discrepancy between the measured limiter response and theory. The angular distribution of the scattered intensity was approximately symmetric for forward versus back scatter, indicating the scattering may be Rayleigh and the centers smaller than the wavelength of light (<0.5 microns).

To further elucidate the mechanism for optical limiting in fullerenes, measurements were conducted on C_{60} embedded in a solid host, polymethylmethacrylate[94]. Samples were made that had a concentration similar to the toluene solutions. Unlike solid C_{60} thin films, which are yellow, the polymer samples were magenta and had an absorption spectrum that was nearly identical to the solution. This indicates there were no major perturbations of the electronic states due to the host change.

Measurement of the scatter from the samples versus intensity indicate the scatter was linear until breakdown of the polymer host (~1200 mJ/cm^2). The breakdown was easily observed, as scatter immediately increased and was not reversible when the damage threshold was exceeded. The measurement of the transmitted intensity with respect to incident intensity gave a threshold that was significantly higher than the liquid samples. Using the parameters in Fig. 17 and the equations for RSA dynamics, with no free parameters, theoretical responses that were very close to the observed responses for three different concentrations were obtained.

These results indicate the optical limiting response of pure C_{60} in a solid host can be completely described by nonlinear absorption. The liquid limiter response is a combination of nonlinear absorption and nonlinear scattering with similar relative contributions for this optical geometry.

Independently, Brandelik and coworkers at Science Applications International Corporation (SAIC) investigated the optical limiting properties of fullerenes.[95] Their research was prompted by their previous work on CBS. Since CBS is a good optical limiter for many applications, it was reasonable to compare the performance that this new type of carbon (i.e., the fullerenes) gave under similar conditions. Their work compared the performance of C_{60}/C_{70} mixtures to CBS in a converging beam configuration.

The measurement apparatus and conditions used were significantly different than those employed in the HRL studies, the major difference being the use of a focusing lens to provide a very small focal region of high intensity. The advantage of this experimental arrangement is three fold. First, the laser need not be a very high energy device to achieve the necessary fluences to observe the limiting action, due to the gain provided by the lenses. Second, nonlinear refraction processes can be readily observed and exploited. Lastly, this configuration lends itself naturally to conducting Z-scan measurements whereby nonlinear refraction can be separated from nonlinear absorption and scattering. The disadvantages are that the focal region is a small fraction of the sample and beam overlap region, and therefore, nonlinear absorption processes will not be nearly as evident.

The limiting threshold for C_{60}/C_{70} in toluene using the configuration of Brandilik, et al., was 330 mJ/cm^2 for a 66% transmitting sample dropping to 19 mJ/cm^2 at 34% transmittance. A measurement of the intensity distribution as a function of transmitted angle showed there was significant spreading into the paraxial region, which was subsequently shown to be consistent with a thermal defocusing mechanism. CBS was compared and found to give, in contrast, nonlinear scatter into wide angles. They also conducted a Z-scan of toluene solutions C_{60}/C_{70} solutions and observed strong nonlinear refraction, consistent with a thermal lensing mechanism. The Z-scans also clearly indicated a nonlinear absorption or scattering component at high fluences, consistent with observations at HRL.

The observation of a thermal nonlinearity can easily be explained by the high efficiency for radiationless intersystem crossing to the triplet state. When energy is absorbed by C_{60} or C_{70} the molecules are excited to the first excited state. Intersystem crossing to the triplet state level, which is 1.6 eV above the ground state, is rapid with a loss of ~30% of the energy of the 532 nm radiation. This energy is released by thermal dissipation and leads to thermal lensing during the pulse. At high repetition rates, multiple pulses can be expected to encounter higher thermal nonlinearities as the triplet state decays nonradiatively.

In summary, C_{60} shows nonlinear absorption properties in a solid host which may be useful for optical limiting. In solution, the nonlinear absorption is supplemented by nonlinear scattering and refraction. The dominant mechanism will depend on the device configuration. Maximum optical limiting performance can be expected to occur when the multiple nonlinear mechanisms are used in concert.

D. Semiconductors

Semiconductors exhibit a broad range of diverse nonlinearities that can be applied to passive optical limiting. Although the largest nonlinearities occur for optical excitation at the band edge of direct-gap semiconductors, these nonlinearities are narrow band and tend to saturate with high excitation. Hence, they have not been widely used in optical limiting applications. Nonlinearities in semiconductors that have been extensively studied for this purpose are TPA, free-carrier absorption, the electronic Kerr effect and nonlinear refraction associated with free carrier generation. Optical limiting based on nonlinear absorption in semiconductors was proposed and demonstrated[96,97,98] in the late 1960's. Although an optical limiter that combined spatial filtering with self-induced lensing in a liquid nonlinear medium was demonstrated[23] as early as 1967, it was not until 1984 that this process was applied, together with nonlinear absorption, in a semiconductor to construct an optical limiter[19]. This result demonstrated that, when an aperture was used prior to detection, the optical limiting in Si at 1.06 μm was, in fact, dominated by nonlinear refraction. Subsequently it was shown[99] that, for picosecond excitation at 1.06 μm, GaAs produced similar results, even though the mechanisms responsible for the limiting action in this semiconductor are considerably different from those in the Si limiter. The Si and GaAs optical limiters can serve as models for most of the semiconductor optical limiters that have since been demonstrated, and we discuss these examples in some detail below.

Si is an indirect bandgap semiconductor with a bandgap of 1.1 eV at room temperature. Excitation at 1.06 μm (1.17 eV) couples the valence band with the conduction band near the minima of the X-valleys. The Si optical limiter thus relies on linear indirect absorption ($\alpha \sim 10$ cm^{-1}) of the 1.06 μm light to generate free carriers. These carriers, once generated, are free to absorb additional photons (free-carrier absorption), thereby decreasing the transmission of the limiter. In addition, and more importantly, these carriers provide a negative contribution to the refractive index, which is found to be well described[100] by a simple Drude model (Eq. (31) with ω_g taken to infinity). The interband contribution to the index change is unimportant because of the large value of the direct gap energy (~3.5 eV). The electronic Kerr effect is also negligible relative to the free carrier contribution for this resonant excitation condition. The index change, together with the nonuniform beam profile in the Si, produces a negative lens that defocuses the beam, further reducing the limiter transmission.

For pulses that are long enough such that TPA is unimportant (> 10 ps) but short enough such that diffusion and recombination are negligible, the Si limiter is completely described by the linear absorption coefficient, α, the free carrier cross section, σ, and the index change per carrier pair, n_{eh}. Using 25 ps pulses at 1.06 μm, Boggess, et al.[101], demonstrated that values of $\sigma = 5\times10^{-18}$ cm^2 and $n_{eh} = -10^{-21}$ cm^3, very accurately describe the limiting action in Si. Since carriers are linearly generated in Si at 1.06 μm and the nonlinear absorption and refraction depends only on the number density of carriers generated, these nonlinearities are strictly fluence dependent. That is, the response of a Si limiter is independent of pulse duration under these circumstances. Again, this is a desirable feature, since one would prefer a limiter to function over a broad range of pulse durations. The recombination time in an indirect bandgap material such as Si can be many hundreds of nanoseconds. The ambipolar diffusion coefficient[100] in Si is ~10 cm^2/s , indicating that for spot sizes ~ 10 μm, the characteristic diffusion time is on the order of 100 ns. These factors indicate that the response of a Si optical limiter will be essentially independent of pulse width from picoseconds to a tenth of a microsecond.

In addition, the large effective masses of the X-valleys ($m^* = 0.98\ m_0$) and the heavy-hole valence band ($m^* = 0.49\ m_0$) result in a large density of states in both bands, allowing very high carrier densities to be generated without saturation. For example, a carrier density of 10^{19} cm^{-3} is readily generated at a fluence of ~ 200 mJ/cm^2 without saturating the absorption or damaging the Si surface. Such large carrier densities lead to very large index changes ($\Delta n = n_{eh}N \sim 0.01$) and, hence, very effective optical limiting.

On the other hand, the resonant nature of the carrier generation in a Si limiter severely restricts the bandwidth of this device. The frequency dependence of the linear absorption coefficient dictates that the limiter can be optimized for both linear transmission and limiting level over only a very narrow region of wavelengths.

In contrast with Si, GaAs is a direct gap semiconductor with a room temperature bandgap of 1.42 eV. As such, 1.06 μm light cannot induce single-photon transitions from the valence band to the conduction band. On the other hand, for sufficiently high intensities, significant TPA can occur. Hence, for short pulses at 1.06 μm, TPA reduces the GaAs limiter transmission. In addition, and again more importantly, this optical excitation results in nonlinear refraction associated with both the instantaneous electronic Kerr effect and with the generation of free carriers. The former is described by Eq. (26), while the latter is

well described by Eq. (32). It is important to note that the interband contribution in Eq. (32) must be included to accurately account for the accumulative refractive index change, due to the relatively small separation between the direct gap energy and the excitation photon energy.

At 1.06 μm, the TPA coefficient of GaAs[99,102] is ~ 25 cm/GW, the free carrier cross section is[99] ~ 3×10^{-18} cm^2, the nonlinear coefficient associated with the electronic Kerr effect is[17] $\gamma = -3.3\times10^{-4}$ cm^2/GW (-2.7×10^{-10} esu), and the index change per photogenerated carrier pair is[17] $n_{eh} = -8\times10^{-21}$ cm^3. These parameters essentially completely describe the optical limiting of short near infrared pulses in GaAs.

It must be emphasized that the nonlinearities that control the performance of a GaAs optical limiter at 1.06 μm are intensity dependent rather than fluence dependent. TPA and the electronic Kerr effect depend directly on intensity, while the free-carrier nonlinearities depend on TPA for generation of carriers. The values of the nonlinear coefficients dictate that the GaAs optical limiter, in contrast with the Si limiter, will operate effectively only for subnanosecond pulses. This situation is exacerbated in semiconductors with wider band gaps which may be considered for optical limiting at visible wavelengths, since the TPA coefficient is even smaller in these materials[14]. On the other hand, over a relatively broad spectral range, the frequency dependence of the TPA coefficient[15] is significantly weaker than the frequency dependence of the linear absorption coefficient in either direct or indirect gap semiconductors. Hence, optical limiters based on TPA and resultant nonlinearities have the potential to operate over a much broader bandwidth than limiters that rely on single photon absorption.

The optical limiting[103] of 25 ps 1.06 μm pulses in Si and GaAs is illustrated in Fig. 19. These data were obtained using a large f-number configuration with the materials placed near the intermediate focal plane. The Si sample is 1-mm thick and the GaAs sample is 3-mm thick. The limiter response for the two materials is remarkably similar. It must be emphasized, however, that the Si response would be unchanged for nanosecond excitation, while the GaAs response would be severely degraded.

While Si and GaAs serve as excellent examples of semiconductor optical limiters that operate using widely different nonlinear optical mechanisms, the bandgap energies of these materials clearly make them inappropriate for optical limiting at visible wavelengths. There

are, however, a broad range of semiconductors to choose from, and many of these are potentially suitable for limiting in the visible.

Van Stryland and co-workers have studied both refractive and absorptive nonlinearities in a wide variety of semiconductors[14,16,104,105,106] and have extensively examined optical nonlinearities in ZnSe for application to TPA-based optical limiting[17,25,26,107]. ZnSe is a direct-gap semiconductor with a bandgap at room temperature of 2.67 eV and pure material is, therefore, essentially transparent at low intensities over most of the visible spectrum. The mechanisms giving rise to limiting in this material at 532 nm are identical to those that govern the response of GaAs at 1.06 μm. This material is characterized by[17] a TPA coefficient $\beta = 5.5$ cm/GW, a nonlinear refractive coefficient (Kerr nonlinearity) of $n_2 = -4\times10^{-11}$ esu, and an index change per carrier pair of $n_{eh} = -8\times10^{-20}$ cm^3. As with TPA-based optical limiting in GaAs, the ZnSe limiter has the potential for broad band operation, but the small TPA coefficient requires short pulses for effective limiting.

Just as there exist TPA materials that are the visible bandgap equivalents of GaAs, there are also visible bandgap semiconductors analogous with Si. An excellent example is GaP. This is an indirect bandgap semiconductor with a room-temperature bandgap of 2.27 eV. Optical excitation of this material near the band edge (e.g., at 532 nm or 2.34 eV) results in linear indirect absorption and the promotion of electrons from the valence band to the conduction band minima near the X-points. The generation of these carriers provides a refractive nonlinearity described by Eq. (32), as well as free-carrier absorption, though the former has been shown to dominate the GaP optical limiter response. The optical nonlinearities in GaP at 532 nm are essentially the same as those in Si at 1.06 μm. In contrast with Si, which has a direct bandgap near 3.5 eV, the direct bandgap of GaP is only 0.51 eV above the indirect band edge. Thus, whereas the interband contribution to the index change per photogenerated carrier pair is negligible in Si at 1.06 μm, it makes a significant contribution in GaP at 532 nm. Again the indirect bandgap leads to long recombination times, and the high densities of states in the conduction and valence bands allows the generation of large carrier densities and, hence, large index changes. Optical limiting at eye-safe levels (0.2 μJ/cm^2) has been reported in this material[108] for 25 ps excitation. While this limiter should exhibit a similar response for nanosecond excitation, since the nonlinearities are fluence dependent, it suffers from the same bandwidth problem associated with the Si limiter.

While semiconductors exhibit large and varied optical nonlinearities, these materials have yet to exhibit all of the desired features that one would seek in an ideal optical limiter. Materials and mechanisms capable of exhibiting broad band operation typically require short pulses for activation. On the other hand, materials and nonlinear processes that exhibit a fluence dependent response are typically narrow band. Hence, there is a great deal of interest in either enhancing the TPA coefficients in materials for TPA-based limiting or enhancing the bandwidth associated with fluence dependent mechanisms for limiting.

E. Liquid Crystals

The last class of materials for optical limiting that we will discuss are the liquid crystals. Liquid crystals are best known for their use in active devices where an electric field can align the molecules to generate the ubiquitous displays on watches, calculators and numerous other electronic devices. While it is true that active liquid crystal limiting devices can and have been made for protection of sensors, they suffer the aforementioned activation speed problem. Some researchers have shown that liquid crystals can also be used for passive optical limiting.

Liquid crystals are molecules that are anisotropic in geometry and usually have conjugated p orbitals along their length to support charge separation. The delocalized p structure has been identified as a potential source of fast and large optical nonlinearities.[109] They can become orientationally ordered in response to fields giving rise to many of their interesting properties. Liquid crystals have received much interest by industrial companies for their application to imaging devices. It is only natural that applications in optical limiting should also be investigated.

Numerous researchers[110,111,112,113,114] have conducted studies of optical limiting with liquid crystals. Of the various mesophases of liquid crystals (nematic, smectic, cholesteric, and isotropic), the nematic phase has been found to be one of the most useful phases for optical limiting due to exhibition of various unique physical properties.[115,116,117] In particular, the nematic phase exhibits large, different interactions of the optical field with each of the refractive indices (ordinary and extraordinary ray) giving rise to large birefringence while still transparent. Khoo, et al.,[118] have investigated the temporal response of nematic liquid crystals to picosecond through millisecond pulses. In general they observed two distinct features in the nonlinear refractive index: a fast component

which builds up in about 100 ns and a slow component which rises to a maximum in 10 ms. They attribute these changes to density and temperature effects which had previously been reported.[119,120] A very fast component was also observed that manifested itself in a self diffraction of the incident beam. This was attributed to individual molecular responses and was also observed in smectic and isotropic phases.

Although nematic is one of the most promising phases of liquid crystals, Soileau, et. al.[121], have shown that isotropic phases of linear crystals can have large two photon absorption (~0.6 cm/GW). The liquid crystals they studied had nonlinear refractive indices an order of magnitude smaller than CS_2 and, hence, were not as effective at self lensing applications as nematic liquid crystals. When the two effects were used in concert, they showed optical limiting of 30 ps, 532 nm pulses at energies as low as 0.15 microjoules.

The continued investigation of liquid crystals is certain to yield further improvements in optical limiting performance. It is likely that many practical optical limiters will incorporate not only a passive device for protection against short pulses, but also an active device to protect against long duration pulses and CW threats. With liquid crystals, it is possible to incorporate active feedback to provide limiting of long pulses in situations where passive devices are ineffective. Hence, these materials offer the potential for both dynamic and passive control in one device.

5. Summary and Conclusions

In this review, we have attempted to provide a broad overview of the present state of optical limiting primarily for eye and sensor protection. We have discussed a variety of nonlinear mechanisms, including reverse saturable absorption, two-photon absorption, free-carrier absorption, nonlinear refraction, and optically-induced scattering, which have been and continue to be applied to optical limiting devices. We have outlined some of the problems associated with designing a practical optical limiter, with a particular emphasis on devices designed for eye protection. Finally we have discussed a number of materials, including carbon black suspensions, organometallic compounds, fullerenes, semiconductors, and liquid crystals, which have been implemented in optical limiting devices.

In spite of the variety of nonlinearities, materials, and device configurations that have been used to implement passive optical limiters, no single device or combination of devices has

yet been identified that will protect any given sensor from all potential optical threats. This is largely a consequence of the requirement that any practical optical limiter must not significantly reduce the performance of the sensor that it is meant to protect, but it also stems from the ready availability and wide variety of high-power optical sources currently in use. Progress in the development of high power optical sources has continued unabated since the invention of the laser. Advances have reduced the size, weight and complexity and increased the efficiency of lasers. Frequency tunable lasers have existed since the invention of the dye laser, but new advances in solid state laser materials, such as Ti:Sapphire, and efficient frequency conversion techniques have extended the utility of tunable lasers. Semiconductor lasers have recently been built which operate in the blue[122] and the output power of red semiconductor lasers continue to increase. It is expected that advances in laser development will continue, and therefore the need for protection from malicious and inadverdent damaging optical exposure will increase.

The research on optical limiting devices is still in its infancy; the devices that we have discussed are relatively new compared to the sensors they are designed to protect. Nevertheless, a growing number of companies are investigating their potential. To date we are unaware of any nongovernment devices on the market which operate in the sub 10 microsecond regime, but that will almost certainly change in the future. Due to the fact that many of the studies of optical limiting are aimed at protecting government sensors, it is likely that some research has been classified, and the results have not been published. In general though, the U. S. government has been very cooperative with researchers publishing their results in this area.

In the future, it is likely that many of the optical limiters will be designed for a specific optical sensor in a specific optical configuration. "Drop-in" optical limiters in general give poorer performance than devices that are optimized for a specific application. The major trade-offs are the dynamic range over which protection can be afforded, the field of view of the sensor, the physical dimensions of the limiter, threshold energy for activation, wavelength and pulse regimes for protection, and whether the device is fail-safe or fail-catastrophic. Further material research is clearly required to enable expanded sensor protection as well as new applications for these devices.

6. Acknowledgments

One of the authors (TFB) gratefully acknowledges support from the Defense Advanced Research Projects Agency and the U. S. Army Night Vision and Electro-Optics Directorate. The authors are also pleased to acknowledge contributions to this work made by G. R. Allan, M. B. Klein, Alan Kost, D. Labergerie, S. W. McCahon, S. J. Rychnovsky, A. L Smirl, and C. H. Venzke.

Figures

Figure 1 a) The optical response of an optical limiter to incident fluence. b) The optical response of an ideal optical switch to incident fluence. c) The "realistic" optical response of an optical switch.

Figure 2. Some optical limiters based on different mechanisms a) an induced absorption limiter, b) self defocusing limiter, c) self focusing limiter, d) induced scattering limiter, e) beam fanning limiter. f) photorefractive excisor device

Figure 3. a) three level model for RSA, b) five level model for RSA.

Figure 4. Plot of the incident intensity versus the transmitted intensity of a typical three level RSA material.

Figure 5. Theoretical results for the transmitted fluence as a function of input fluence for a TPA material for three input pulse durations. A TPA coefficient of 10 cm/GW and a material length of 1 mm were used to generate these curves.

Figure 6. Theoretical results for the transmitted fluence versus input fluence in the presence of free-carrier absorption for three values of the free carrier cross section. A linear transmission of 70% and a wavelength of 532 nm were assumed in generating these results.

Figure 7. a) Typical optical configuration for a self defocusing limiter. b) Typical optical configuration of a self focusing limiter,

Figure 8. Schematic representation of z-scan results for a negative refractive nonlinearity (dashed curve) and a positive refractive nonlinearity (dotted curve). Both curves have been corrected for absorption. The solid curve shows the result of removing the aperature from the measurement apparatus and collecting all the transmitted light, thus isolating the nonlinear absorption.

Figure 9. a) Scattering intensity versus angle from a Rayleigh scatterer. b) Scattering intensity versus angle from a Mie type scatterer with a size on the order of the wavelength of the incident light.

Figure 10. The ANSI standard for eye protection for different incident optical pulse widths with wavelengths between 400 and 700 nm.

Figure 11. Fluence as a function of position for optical pulses of various initial fluences propagating through a uniformly active, 2mm thick, RSA medium and example parameters of $\sigma_1=7.5\times10^{-18}$ cm^2, $\sigma_2=0$, $\sigma_3=1.2\times10^{-15}$ cm^2, $\tau_2=\tau_5=10$ ps, $\tau_3=120$ ns, $\tau_{24}=2.8$ ns and a gain of 100.

Figure 12. (Left) RSA concentration profile inside a 2 mm sample host. (Right) Fluence as a function of position for optical pulses of various initial fluences propagating through media with the RSA concentration profile on the left and the RSA parameters used in figure 11.

Figure 13. Relative contributions of scattering and absorptions to the transmittance of a CBS sample as a function of the incident intensity (from Ref.58).

Figure 14. Optical limiting response of a methylene chloride solution of King's complex to 7 nanosecond and 25 picosecond optical pulses of 532 nm radiation.

Figure 15. Optical limiting response of a variety of RSA active materials to 532 nm pulses.

Figure 16. Absorption spectrum of a toluene solution of C_{60}. Inset triplet excited state absorption of C_{60} (from ref 92).

Figure 17. Five level diagram for C_{60} optical dynamics.

Figure 18. Incident intensity versus transmitted intensity measured for C_{60} and C_{70}.

Figure 19. Optical limiting in Si (filled squares) and GaAs (open circles) for 25 ps, 1.06 μm pulses using an f/250 optical system.

8. References

1. D. J. Harter and Y. B. Band, *Springer Series in Chem. Phys.*, **38**, 102 (1984).

2. D. J. Harter, M. L. Shand, and Y. B. Band, *J. Appl. Phys.*, **56**, 865 (1984).

3. Y. B. Band, D. J. Harter, and R. Bavli, *Chem. Phys. Lett.*, **126**, 280 (1986)

4. S. E. Bialkowski, *Opt. Lett.*, **14**, 1020 (1989)

5. G. L. Wood,A. A. Said, D. J. Hagan, M. J. Soileau, and E. W. Van Stryland, *Proc. of the SPIE* , **1105**, 154 (1989).

6. R. C. Powell, R. J. Reeves, M. G. Jani, M. S. Petrovic, A. Suchoski, and E. G. Behrens, *Proc. of the SPIE* , **1105**, 136 (1989)

7. G. L. Wood,W. W. Clark III, and E. J. Sharp, *Proc. of the SPIE* , **1307**, 376 (1990).

8. G. L. Wood, A. G. Mott, E. J. Sharp, *Proc. of the SPIE* , **1692**, 2 (1992)

9. Y. R. Shen, *The Principles of Nonlinear Optics*, John Wiley and Sons, New York, (1984)

10. C. R. Guiliano and L. D. Hess, *IEEE J. Quantum Electron.* QE-3,358 (1967)
11. Thomas F. Boggess, K. Bohnert, K. Mansour, S. C. Moss, I. W. Boyd, A. L. Smirl, *IEEE J. Quantum Electron.*, QE-22, 360 (1986).
12. A. C. Walker, A. K. Kar, Ji Wei, U. Keller, S. D. Smith, *Appl. Phys. Lett.*, 48, 683 (1986).
13. Yia Chung Chang, A. E. Chiou, M. Khoshnevissan, *J. Appl. Phys.*, 71, 1349 (1992).
14. E. W. Van Stryland, H. Vanherzeele, M. A. Woodall, M. J. Soileau, A. L. Smirl, S. Guha, T. F. Boggess, *Opt. Engineering*, 24, 613 (1985).
15. B. S. Wherrett, *J. Opt. Soc. Am. B*, 1, 67 (1984).
16. D. C. Hutchings and E. W. Van Stryland, *J. Opt. Soc. Am. B*, 9, 2065 (1992).
17. see, e.g., A. A. Said, M. Sheik-bahae, D. J. Hagan, E. J. Canto-Said, Y.Y. Wu, J. Young, T. H. Wei, and E. W. Van Stryland, *Proc. of the SPIE* , 1307, 294 (1990).
18. see, e.g., C. M. Wolfe, N. Holonyak, and G. E. Stillman, Prentice Hall, New Jersey, 1989.
19. T. F. Boggess, S. C. Moss, I. W. Boyd, A. L. Smirl, *Opt. Lett.*, 9, 291 (1984).
20. S. J. Rychnovsky, G. R. Allan, C. H. Venzke, A. L. Smirl, and T. F. Boggess, *Proc. of the SPIE*, 1692, 191 (1992)
21. J. A. Hermann, *Optica Acta*, 32, 541 (1985)
22. J. A. Hermann and P. B. Chapple, *Proc. of the SPIE*, 1307, 401 (1990)
23. R. C. C. Leite, S. P. S. Porto, and T. C. Damen, *Appl. Phys. Lett.*, 10, 100 (1967).
24. A. E. Kaplan, Radiophys. Quantum Electron., 12, 692 (1969).
25. E. W. Van Stryland, Y. Y. Wu, D. J. Hagan, M. J. Soileau, and K. Mansour, *J. Opt. Soc. Am. B*, 5, 1980 (1988).
26. D. J. Hagan, E. W. Van Stryland, Y. Y. Wu, T. H. Wei, M. Sheik-Bahae, A. Said, K. Mansour, J. Young, and M. J. Soileau, *Proc. of the SPIE*, 1105, 103 (1989).
27. M. Sheik-Bahae, D. J. Hagan, A. A. Said, J. Young, T. H. Wei, and E. W. Van Stryland, Proceedings of the SPIE, 1307, 395 (1990).
28. M. Sheik-Bahae, D. J. Hagan, and E. W. Van Stryland, Phys. Rev. Lett., 65, 96 (1990).
29. D. C. Hutchings, M. Sheik-Bahae, D. J. Hagan, and E. W. Van Stryland, Optical and Quantum Electronics, 24, 1 (1992).
30. M. Sheik-Bahae, D. C. Hutchings, D. J. Hagan, E. W. Van Stryland, IEEE J Quantum Electron., 27, 1296 (1991).

31. D. H. Auston, S. McAfee, C. V. Shank, E. P. Ippen, and O. Teshke, *Solid-State Electron.*, **21**, 147 (1978)

32. M. Sheik-bahae, A. A. Said, D. J. Hagan, M. J. Soileau, and E. W. Van Stryland, *Proc. of the SPIE*, **1105**, 146 (1989)

33. M. Sheik-bahae, A. A. Said, D. J. Hagan, M. J. Soileau, and E. W. Van Stryland, Optical Engineering, **30**, 1228 (1991).

34. M. Sheik-Bahae, A. A. Said, and E. W. Van Stryland, *Opt. Lett.*, **14**, 955 (1989)

35. M. Sheik-Bahae, A. A. Said, T. H. Wei, D. J. Hagan, and E. W. Van Stryland, *IEEE J. Quantum Electron.*, **QE-26**, 760 (1990)

36. D. Sinclair, and Lamer, Chem. Rev., **44**, 245 (1949)

37. G. Mie, *Ann. d Phys.*, **25**, 377 (1908)

38. Van de Hulst, H.C., *Light Scattering by Small Particles*, Dover Publications, Inc., New York, 1981

39. R. R. Michael, C. M. Lawson, G. W. Euliss, and M. Mohebi, *Proc. of the SPIE*, **1626**, 205 (1992)

40. L.W.Tutt, S. W. McCahon, A. Kost, M. Klein, T. F. Boggess, G. R. Allan, S. J. Rychnovsky, D. R. Labergerie, and A. L. Smirl, *Proc of the First Int. Conf on Intell. Mat.*, Konogawa Japan (1992)

41. S. A. Asher , P. L. Flaugh, and G. Washinger, *Spectroscopy* , **1**,26 (1986)

42. S. A. Asher, R. Kesavanoorthy, S. Jagannathan, P. Rundquist, *Proc. of the SPIE*, **1626**, 238 (1992)

43. L. M. Peterson, 1986, *Optical Engineering* , **25**, 103 year?

44. D. F. Eaton, *Science*, **253**, 281 (1991)

45. J. Feinberg, *J. Opt. Soc. Am.*, 72, 46 (1982)

46. M. Cronin-Golomb, and A. Yariv, *J. Appl. Phys.*, **57**, 4906 (1985)

47. S. W. McCahon, and M. B. Klein, *Proc. of the SPIE*, **1105**, 119 (1989)

48. M. B. Klein, and G. J. Dunning, *Proc. of the SPIE*, **1692**, 73 (1992)

49. J. L. Shultz, G. J. Salamo, E. J. Sharp, G. L. Wood, R. J. Anderson, and R. R. Neurgaonkar, *Proc. of the SPIE*, **1692**, 78 (1992)

50. D. Sliney, *Proc. of the SPIE* , **1207**,2 (1990)

51. F. Bartoli, L. Esterowitz, M. Kruer, and R. Allen, *Appl. Opt.*, **16**, 2934 (1977)

52. S. W. McCahon and L. W. Tutt, *Optical Limiter Including Optical Convergence and Absorbing Body with Inhomogeneous Distribution of Reverse Saturable Absorption*, US patent #5,080,469, January 14 (1992)

53.D. J. Hagan, E. W. Van Stryland, M. J. Soileau, Y. Y. Wu, and S. Guha, *Opt. Lett.*, **13**, 315 (1988)

54. A. A. Said, T. H. Wei, R. De Salvo, Z. Wang, M. Sheik-Bahae, D. J. Hagan, E.W. Van Stryland, and J. W. Perry, *Proc. of the SPIE*, **1692**, 37 (1992)

55. K. M. Nashold, R. A. Brown, R. C. Honey, D. P. Walter, paper presented at First DoD Workshop on Liquid Cell Power Limiters, February 27-28 (1991), NRL, Washington , D. C. (unclassified)

56. K. M. Nashold, R. A. Brown, D. P. Walter, and R. C. Honey, *Proc. of the SPIE*, **1105**, 78 (1989)

57. R. R. Michael, C. M. Lawson, G. W. Euliss, and M. Mohebi, *Proc. of the SPIE*, **1626**, 205 (1992)

58. K. Mansour, *Characterization of Optical Nonlinearities in Carbon Black Suspension in Liquids*, University Microfilms International, University of North Texas (1990), order #9114124

59. K. Mansour, M. J. Soileau, and E. W. Van Stryland, *J. Opt. Soc. Am. B*, **9**, 1100, (1992)

60. R. C. Hoffman, K. A. Stetyick, R. S. Potember, and D. G. McLean, *J. Opt. Soc. Am. B*, **6**, 772 (1989)

61. G. H. Brown, ed. "Photochromism", Techniques of Chemistry, Vol. 3, ed. by A. Weissberger, Wiley Interscience, New York, (1971)

62. H. E. Lessing and A. Von Jena, *Chem Phys. Lett.*, **59**, 249 (1978)

63. G. L. Geoffroy and M. S. Wrighton, *Organometallic Photochemistry*, Academic Press, New York (1979)

64. D. R. Coulter, V. M. Miskowski, J. W. Perry, T.-H. Wei, E. W. Van Stryland, and D. J. Hagan, *Proc. of the SPIE*, **1105**, 42 (1989)

65. D. J. Lund, P. Edsall, and J. D. Masso, *Proc. of the SPIE*, **1207**,193 (1990)

66. J. W. Perry, L. R. Khundar, D. R. Coulter, D. Alvarez, Jr., S. R. Marder, T. H. Wei, M. J. Sence, E. W. Van Stryland, and D. J. Hagan, J. Messier et al. eds. *Nato ASI Series E* , **194**, 369 (1991)

67. N. Q. Wang, Y. M. Cai, J. R. Heflin, and A. F. Garito, *Mol Cryst. Liq. Cryst.*, **189**, 39 (1990)

68. W. Blau, H. Byrne, W. M. Dennis, and J. M. Kelly, *Optics Comm.*, **56**, 25 (1985)

69. H. Fei, L. Han, X. AI, R. Yin, and J. Shen, *Chin. Sci. Bull.*, **37**, 298 (1992).

70. L. W. Tutt, and S. W. McCahon, *Optics Lett.*, **15**, 700 (1990)

71. L. W. Tutt, S. W. McCahon and M. B. Klein, *Proc. of the SPIE*, **1307**, 327 (1990)

72. R. B. King, *Inorg. Chem.*, **5**, 2227 (1966)

73. G. R. Allan, D. Labergerie, S. J. Rychnovsky, T. F. Boggess, A. L. Smirl, L. W. Tutt, S. W. McCahon, and M. B. Klein, *Conf. on Lasers and Electr-Optics, Tech. Dig. Ser.* **10**, 172 (1991)

74. G. R. Allan, D. R. Labergerie, S. J. Rychnovsky, A. L. Smirl, T. F. Boggess, and L. W. Tutt, *J. of Phys. Chem.*, **96**, 6313 (1992)

75. T. F. Boggess, G. R. Allan, S. J. Rychnovsky, D. R. Labergerie, C. H. Venzke, A. L. Smirl, L. W. Tutt, A. Kost, S. W. McCahon, and M. B. Klein, to be published, Opt. Engineer., May 1993.

76. G. R. Allan, S. J. Rychnovsky, A. L. Smirl, T. F. Boggess, L. W. Tutt, A. Kost, and M. B. Klein, *Proc of the SPIE*, **1692**, 170(1992)

77. G.R. Allan, S. J. Rychnovsky, C. H. Venzke, T. F. Boggess, L. W. Tutt, submitted *J. Phys. Chem.*.

78. H. W. Kroto, J. R. Heath, S. C. O'Brien, R. F. Curl, and R. D. Smalley, *Nature*, **318**, 162 (1985)

79. W. Krätschmer, L. D. Lamb, K. Fostiropoulos, and D. R. Huffman, *Nature*, **347**, 354 (1990)

80. A. F. Hebard, M. J. Rosseinsky,, R. C. Haddon, D. W. Murphy, S. H. Glarum, T. T. M. Palstra, A. P. Ramirez, and A. R. Kortan, *Nature*, **350**, 600 (1990)

81. R. J. Meilunas, R. P. H. Chang, S. Liu, and M. M. Kappes, *Appl. Phys. Lett.* , **59**, 3461 (1991)

82. Q. Xie, E. Pérez-Cordero, and L. Echegoyen, *J. Am. Chem. Soc.*, **114**, 3978 (1992)

83. R. D. Beck, P. St. John,M. M. Alvarez, F. Diederich, R. L. Whetten, *J. Phys. Chem.*, **95**, 8402 (1991)

84. J. R. Heath, S. C. O'Brien, Q. Zhang, Y. Liu, R. F. Curl, H. W. Kroto, F. K. Tittel, and R. E. Smalley, *J. Am. Chem Soc.*, **352**, 7779 (1985)

85. M. M. Ross and J. H. Callahan, *J. Phys. Chem.*, **95**, 5720 (1991)

86. R. D. Johnson, M. S. de Vries, J. Salem, D. S. Bethune, and C. S. Yannoni, *Nature*, **355**, 239 (1992)

87. Private communication with the MER corporation, Tuscon AZ.

88. J. W. Arbogast, A. P. Darmanyan, C. S. Foote, Y. Rubin, F. N. Diederich, M. M. Alverez, S. J. Anz, and R. L. Whetten, *J. Phys. Chem.*, **95**, 11 (1991)

89. R. J. Sension, C. M. Phillips, A. Z. Szarka, W. J. Romanow, A. R. McGhie, J. P. McCauley, Jr., A. B. Smith III, and R. M. Hochstrasser, *J. Phys. Chem.*, **95**, 6075 (1991)

90. T. W. Ebbersen, K. Tanigaki, and S. Kuroshima, *Chem. Phys. Lett.*, **181**, 501 (1991)

91. Y. Kajii, T. Nakagawa, S. Suzuki, Y. Achiba, K. Obi, and K. Shibuya, *Chem. Phys. Lett.*, **181**, 100 (1991)

92. N. M. Dimitrijevic and P. V. Kamat, *J. Phys. Chem.*, **96**, 4811 (1992)

93. L. W. Tutt and A. Kost, *Nature*, **356**, 225 (1992)

94. A. Kost, L. Tutt, M. B. Klein, T. K. Dougherty, and W. E. Elias, *Opt. Lett.*, **18**, 334 (1993).

95. D. Brandelik, D. Mclean, M. Schmitt, B. Epling, C. Colclasure, V. Tondiglia, R. Pachter, K. Obermeier, and R. Crane, *Proc. of the Mat. Res. Soc.*, **247**, 361 (1991)

96. J. E. Geusic, S. Singh, D. W. Tipping, and T. C. Rich, *Phys. Rev. Lett.*, **19**, 1126 (1969).

97. J. M. Ralston and K. R. Chang, *Appl. Phys. Lett.*, **15**, 164 (1969).

98. V. V. Arsen'ev, V. S. Dneprovskii, D. N. Klyshke, and A. N. Penin, *Sov. Phys. JETP*, **29**, 413 (1969).

99. T. F. Boggess, A. L. Smirl, S. C. Moss, I. W. Boyd, and E. W. Van Stryland, *IEEE J. Quantum Electron.*, **QE-21**, 488 (1985).

100. J. P. Woerdman, *Philps Res. Rep. Supp.*, **7**, 1 (1971).

101. T. F. Boggess, K. Bohnert, D. P. Norwood, C. D. Mire, and A. L. Smirl, *Opt. Commun.*, **64**, 387 (1987).

102. J. H. Bechtel and W. L. Smith, *Phys. Rev. B*, **13**, 3515 (1976).

103. T. F. Boggess, A. L. Smirl, J. Dubard, A. G. Cui, S. R. Skinner, *Optical Eng.*, **30**, 629 (1991).

104. M. Sheik-Bahae, D. J. Hagan, A. A. Said, J. Young, T. H. Wei, and E. W. Van Stryland, *Proc. of the SPIE*, **1307**, 395 (1990).

105. M. Sheik-Bahae, D. J. Hagan, and E. W. Van Stryland, *Phys. Rev. Lett.*, **65**, 96 (1990).

106. M. Sheik Bahae, D. C. Hutchings, D. J. Hagan, E. W. Van Stryland, *IEEE J. Quantum Electron.*, **27**, 1296 (1991).

107. E. J. Canto, D. J. Hagan, J. Young, E. W. Van Stryland, *IEEE J. Quantum Electron.* **27**, 2274 (1991).

108. S. J. Rychnovsky, G. R. Allan, C. H. Venzke, A. L. Smirl, and T. F. Boggess, *Proc. of the SPIE*, **1692**, 191 (1992).

109. M. Lee, et. al. Proc. of the Int. Conf., "Optics of Liquid Crystals", Naples, Italy, July 15-18, (1986)

110. R. N. DeMartino, G. Khanarian, T. M. Leslie, M. J. Sansone, J. B. Stamatoff, H.N. Yoon, and R. L. Mitchell, *Proc. of the SPIE*, **1105**, 2 (1989)
111. M. Ozaki, A. Tagawa, T. Hatai, Y. Sadohara, Y. Ohmori, and K. Yoshino, *Mol. Cryst. Liq. Cryst.*, **199**, 213 (1991)
112. I. C. Khoo, Ping Zhou, R. R. Michael, R. G. Lindquist, and R. Mansfield, *IEEE J. of Quant. Elect.*, **25**, 1755 (1989)
113. I. C. Khoo, R. R. Michael, and G. M. Finn, *Appl. Phys. Lett.*, **52**, 2108 (1988)
114. H. J. Yuan, L. Li, and P. Palffy-Muhoray, *Proc. of the SPIE*, **1307**, 363 (1990)
115. I. C. Khoo, and Y. R. Shen, *Opt. Engineering*, **24**, 579 (1985)
116. I. C. Khoo, "Nonlinear Optics of Liquid Crystals" in "Progress in Optics", Vol. XXVI, ed. E. Wolf (North Holland, Amsterdam 1988)
117 N. V. Tabiryan and B. Y. Zeldovich, *Mol. Cryst. Liq. Cryst.*, **62**,637
118. I. C. Khoo, R. G. Lindquist, R. R. Michael, R. J. Mansfield, P. Zhou, and P Lopresti, *Proc of the SPIE*, **1307**, 336 (1990)
119. I. C. Khoo and R. Normandin, *Opt. Lett.*, **9**, 285 (1984)
120. I. C. Khoo and R. Normandin, *IEEE J. Quant. Electron.*, **QE-23**, 267 (1987)
121. M. J. Soileau, E. W. Van Stryland, S. Guha, E. J. Sharp, G. L. Wood, and J. L. W. Pohlman, *Mol Cryst. Liq. Cryst.*, **143**, 139 (1987)
122. M. A. Haase, J. Qui, J. M. DePuydt, and H. Cheng, *Appl. Phys. Lett.*, **59**, 1272 (1991)

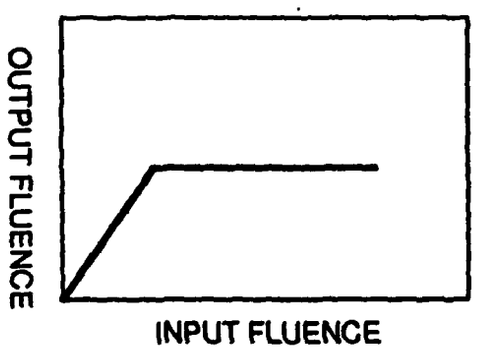
OUTPUT FLUENCE
INPUT FLUENCE

(A)

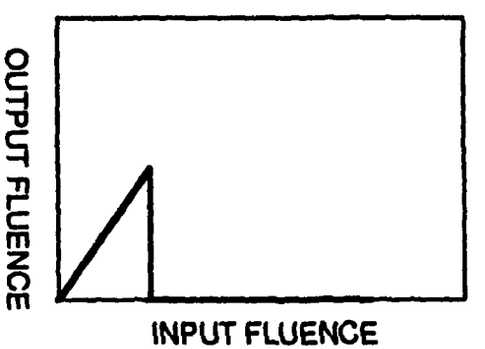
OUTPUT FLUENCE
INPUT FLUENCE

(B)

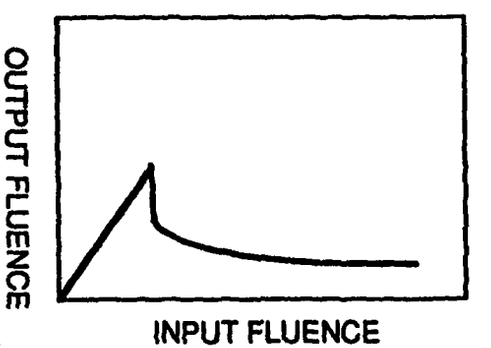
OUTPUT FLUENCE
INPUT FLUENCE

(C)

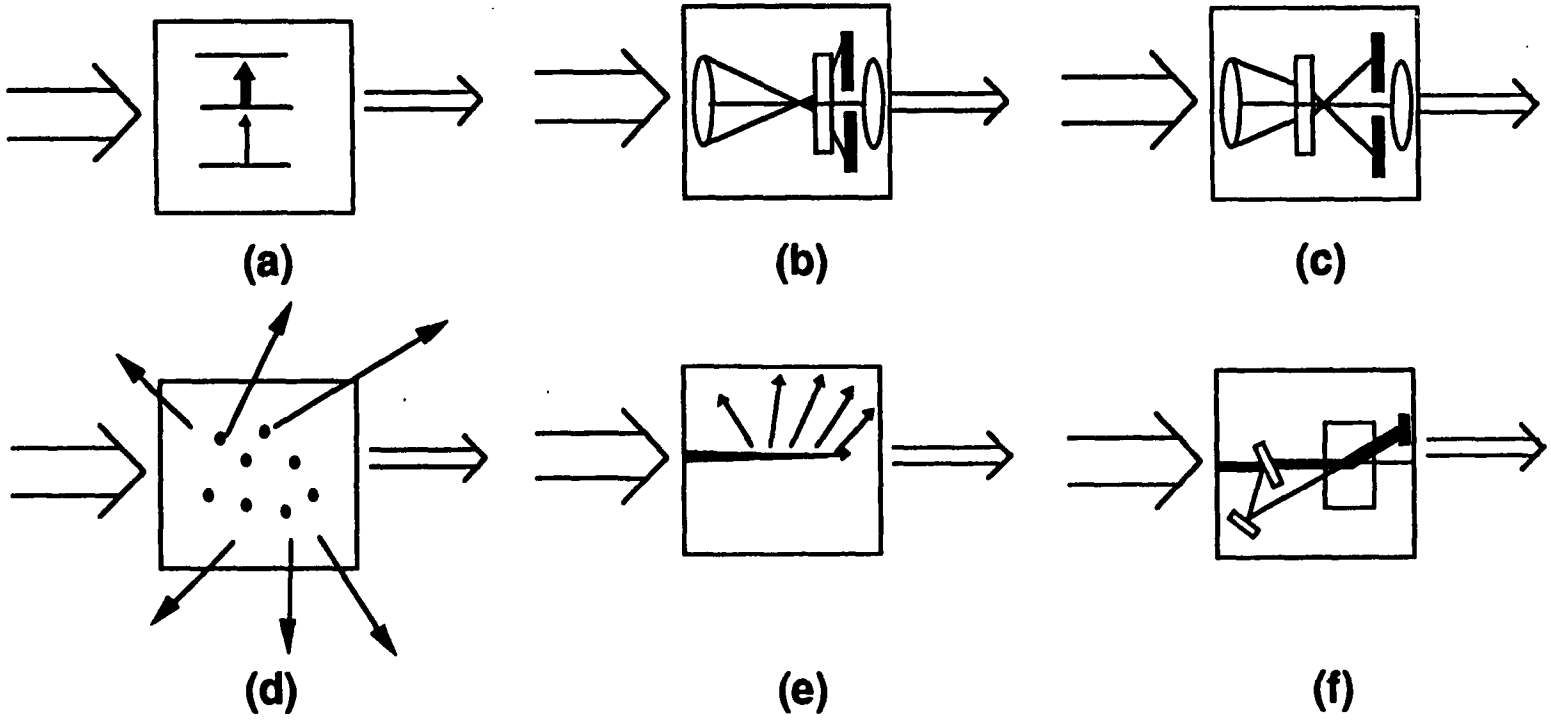
(a)
(b)
(c)
(d)
(e)
(f)

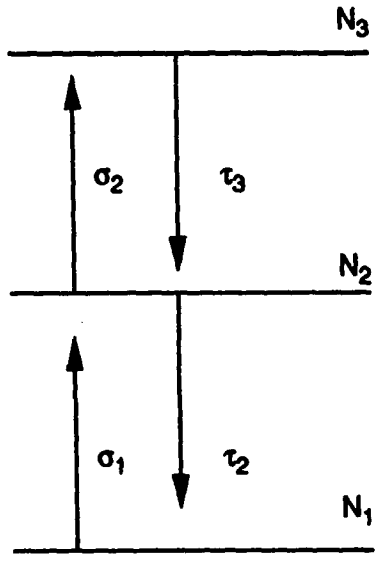

(A)

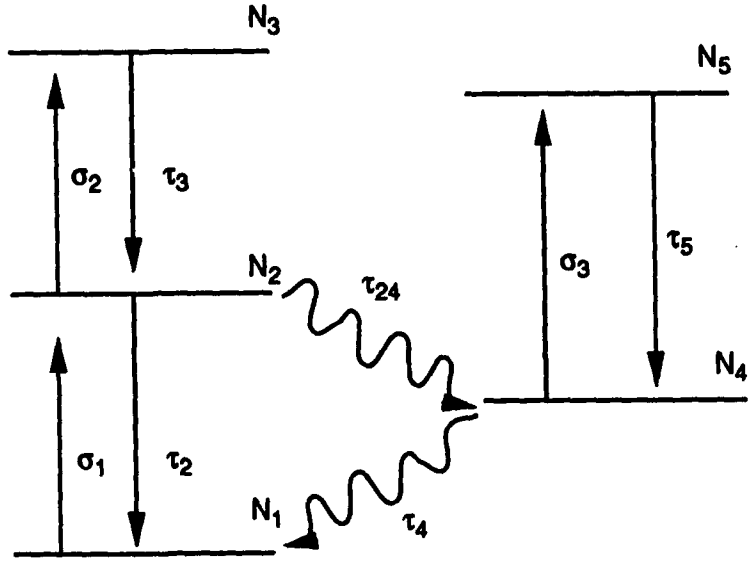

(B)

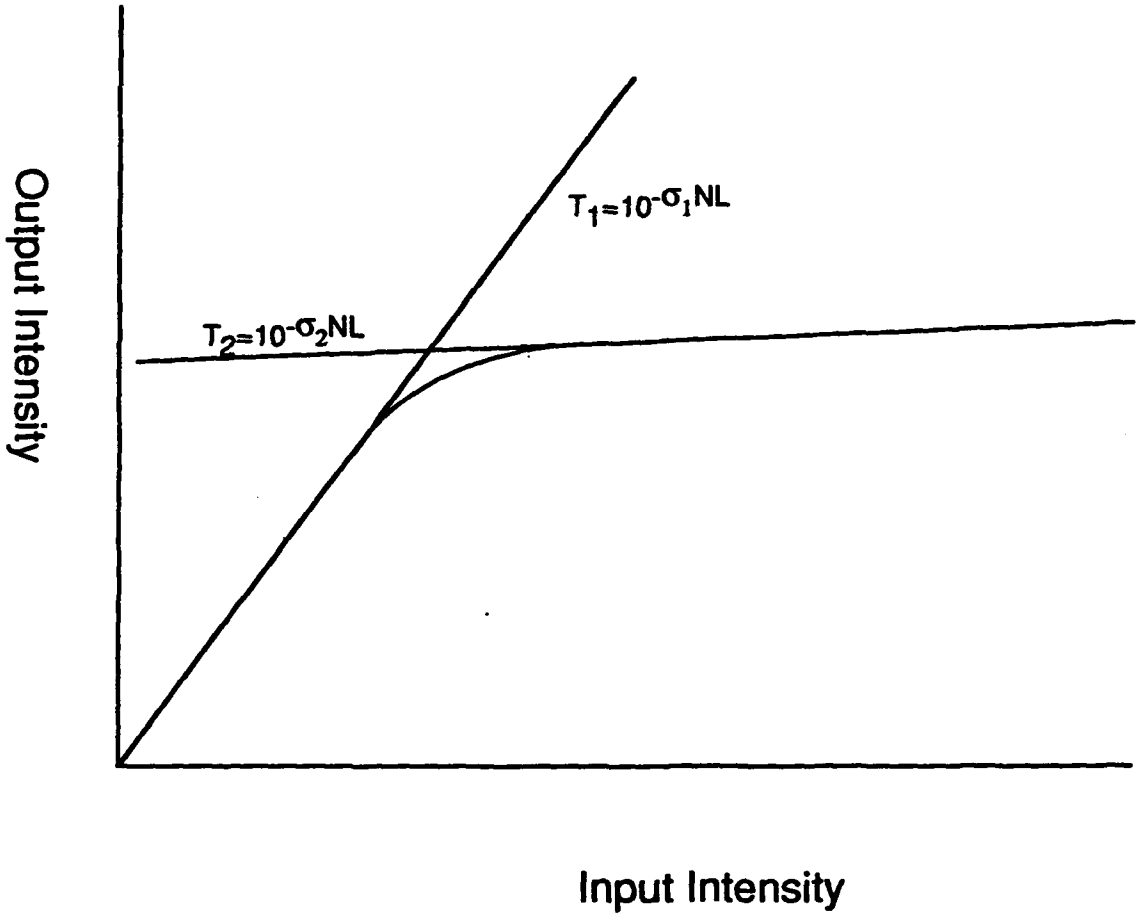
Output Intensity
$T_1=10^{-\sigma_1 NL}$
$T_2=10^{-\sigma_2 NL}$
Input Intensity

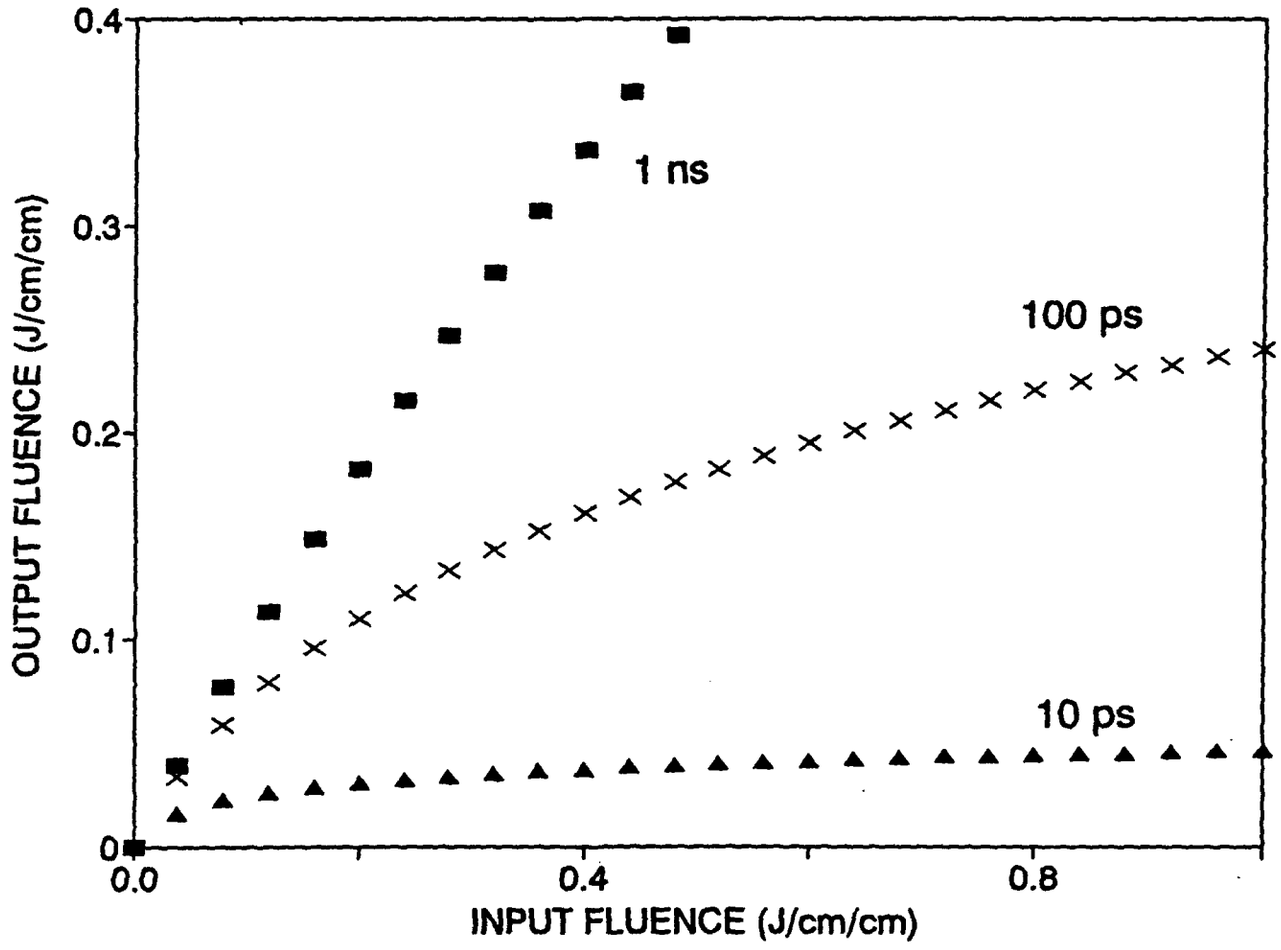
0.4
0.3
0.2
0.1
0
OUTPUT FLUENCE (J/cm/cm)
1 ns
100 ps
10 ps
0.0
0.4
0.8
INPUT FLUENCE (J/cm/cm)

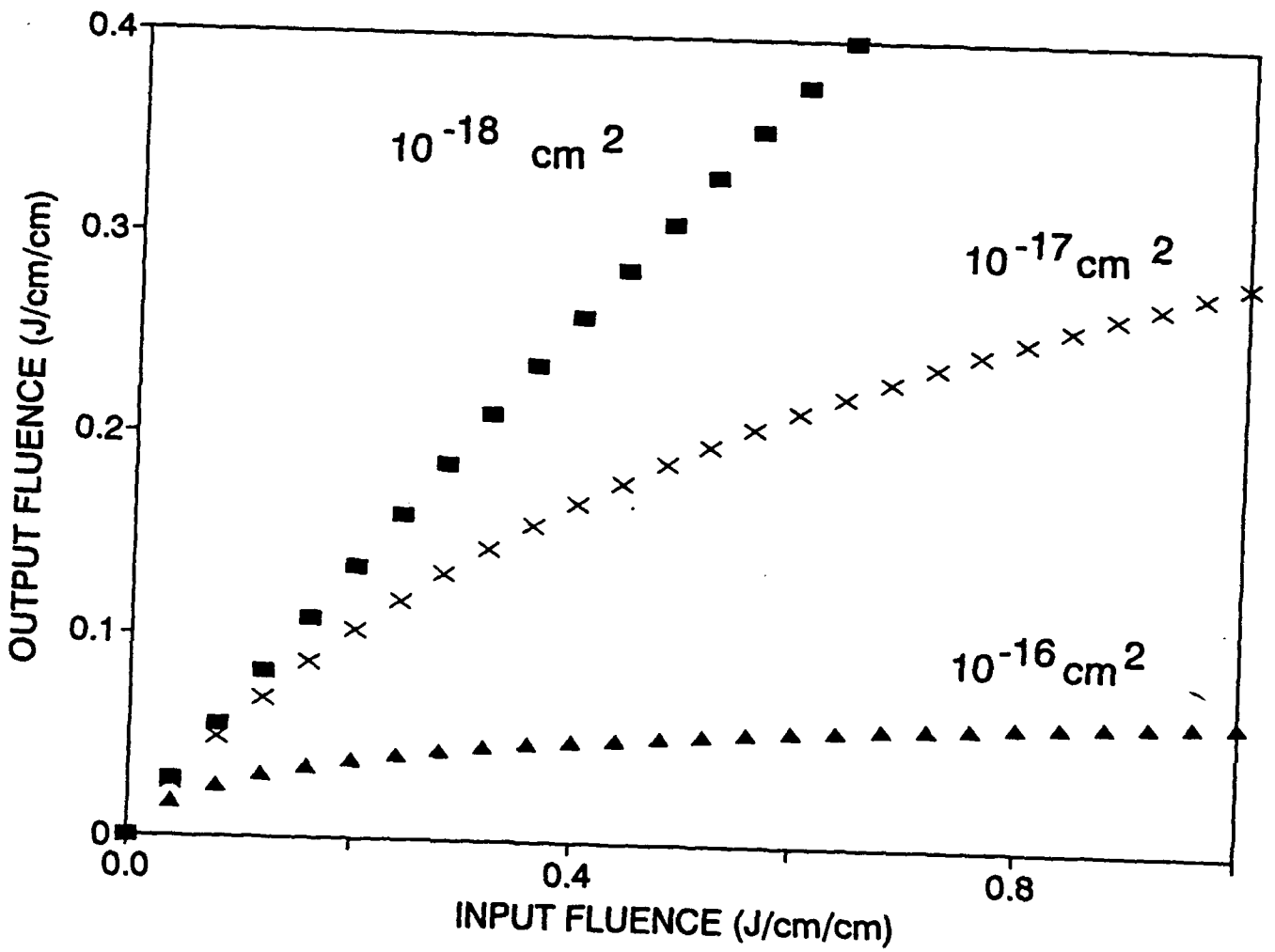
0.4
0.3
0.2
0.1
0
0.0
0.4
0.8
OUTPUT FLUENCE (J/cm/cm)
INPUT FLUENCE (J/cm/cm)
10 -18 cm 2
10 -17 cm 2
10 -16 cm 2

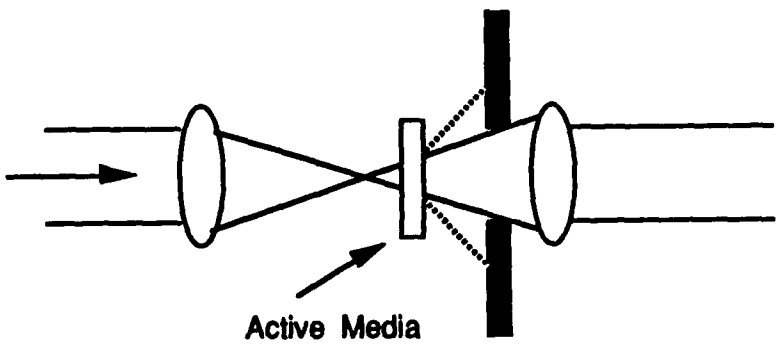

(a)

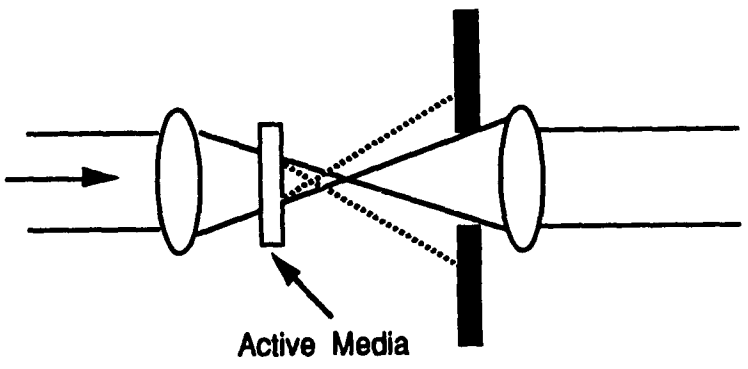

(b)

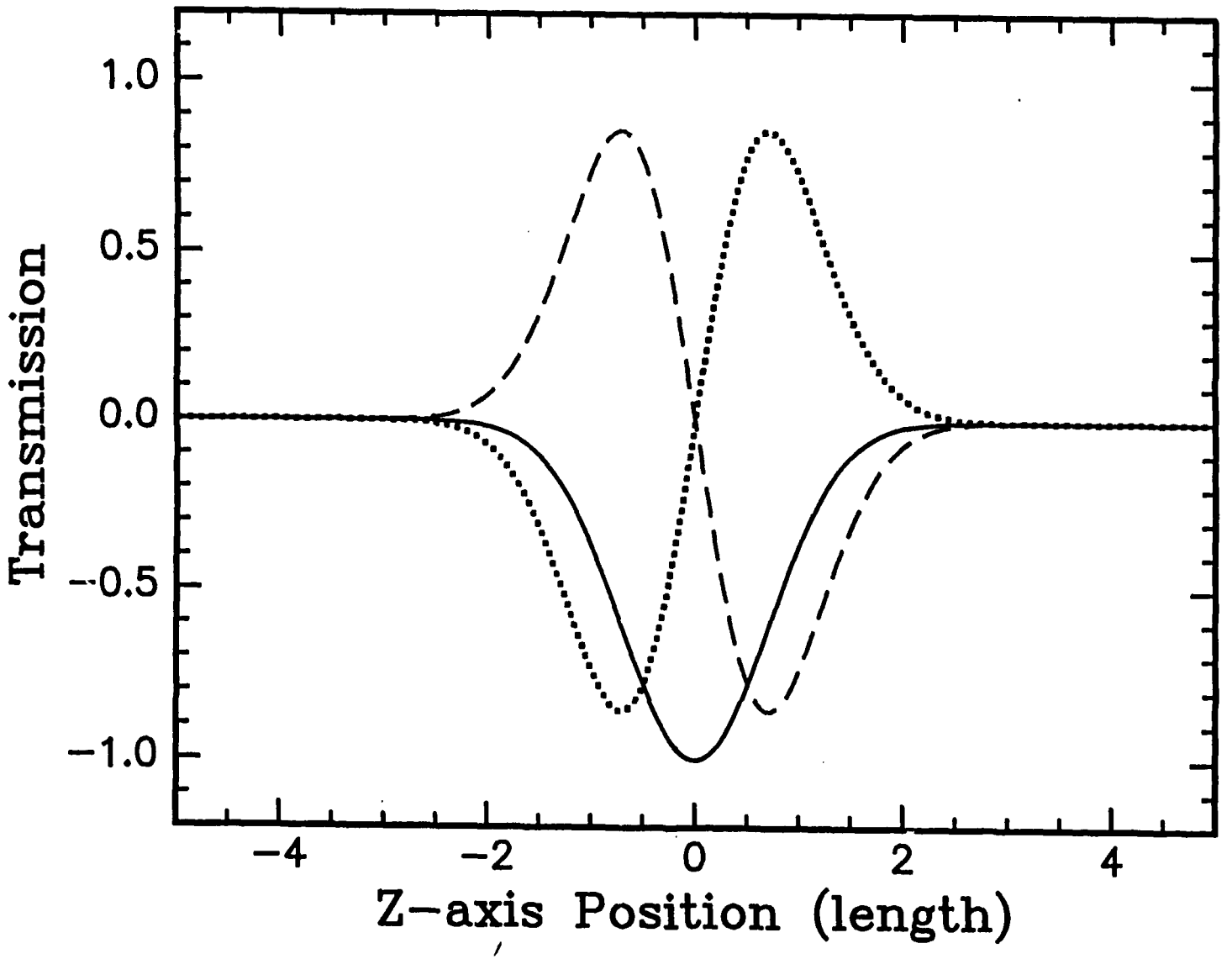
1.0
0.5
0.0
-0.5
-1.0
Transmission
-4
-2
0
2
4
Z-axis Position (length)

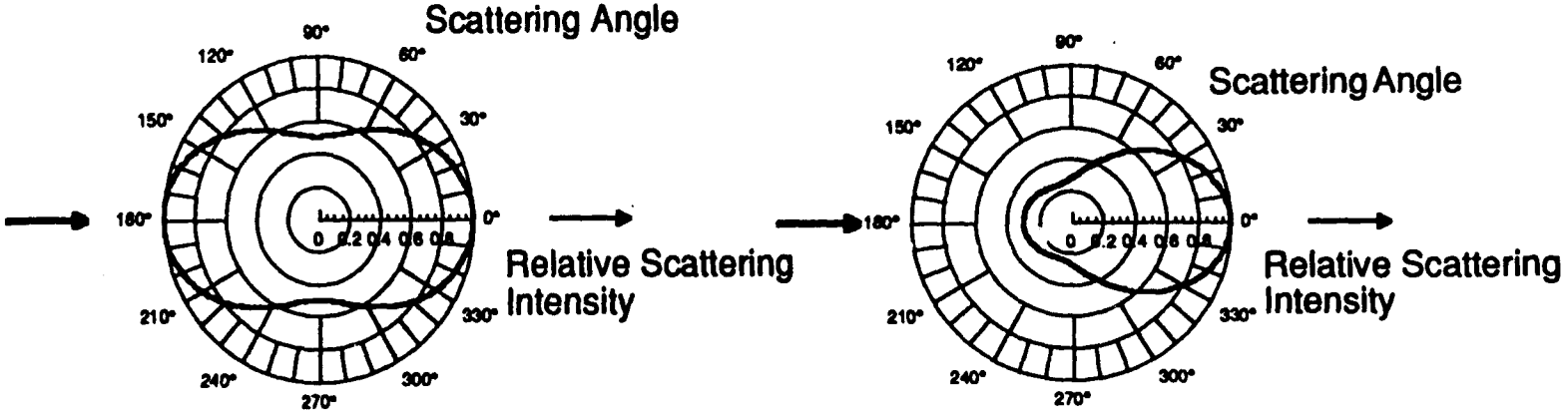
Scattering Angle
90°
120°
60°
150°
30°
180°
0°
210°
330°
240°
300°
270°
0 0.2 0.4 0.6 0.8
Relative Scattering Intensity
Scattering Angle
90°
120°
60°
150°
30°
180°
0°
210°
330°
240°
300°
270°
0 0.2 0.4 0.6 0.8
Relative Scattering Intensity

(a)

(b)

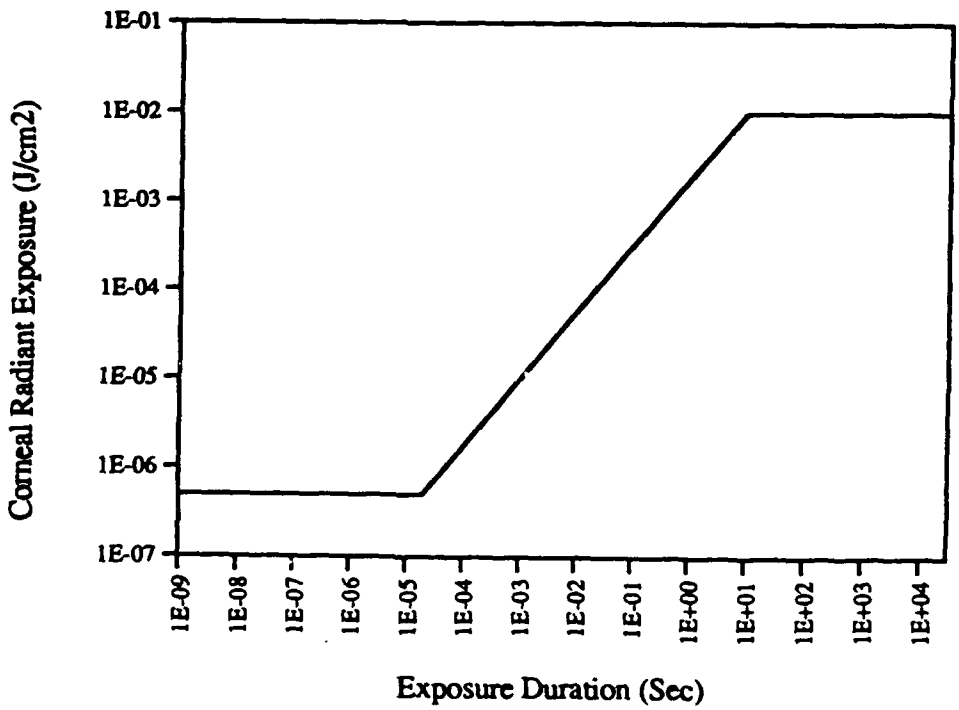
Corneal Radiant Exposure (J/cm2)
1E-01
1E-02
1E-03
1E-04
1E-05
1E-06
1E-07
1E-09
1E-08
1E-07
1E-06
1E-05
1E-04
1E-03
1E-02
1E-01
1E+00
1E+01
1E+02
1E+03
1E+04
Exposure Duration (Sec)

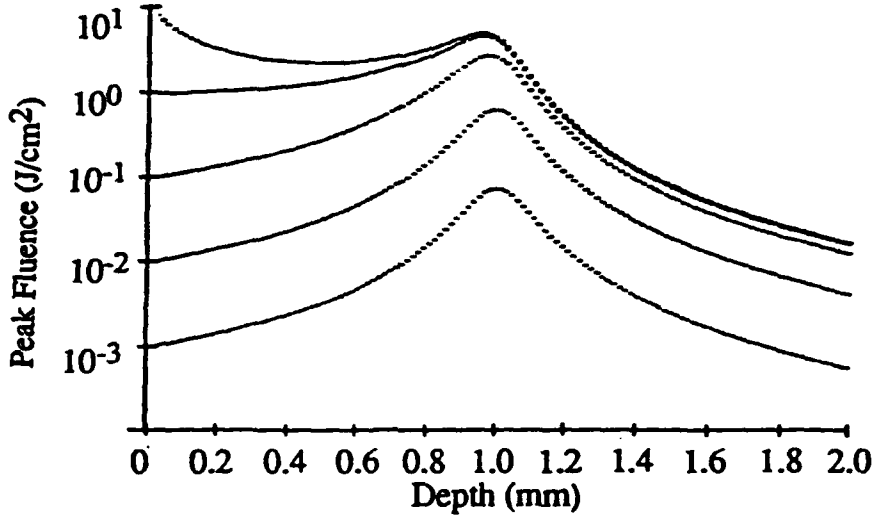
Peak Fluence (J/cm2)
10^1
10^0
10^-1
10^-2
10^-3
0
0.2
0.4
0.6
0.8
1.0
1.2
1.4
1.6
1.8
2.0
Depth (mm)

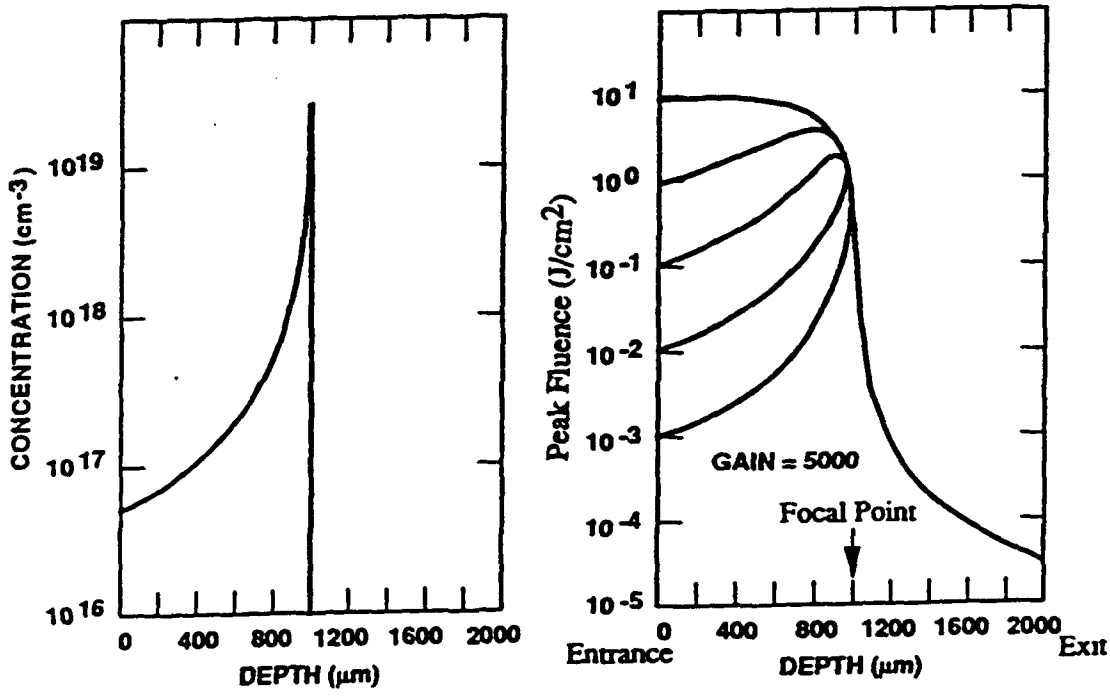
CONCENTRATION (cm-3)
10^19
10^18
10^17
10^16
0
400
800
1200
1600
2000
DEPTH (μm)
Peak Fluence (J/cm2)
10^1
10^0
10^-1
10^-2
10^-3
10^-4
10^-5
GAIN = 5000
Focal Point
Entrance
Exit
DEPTH (μm)

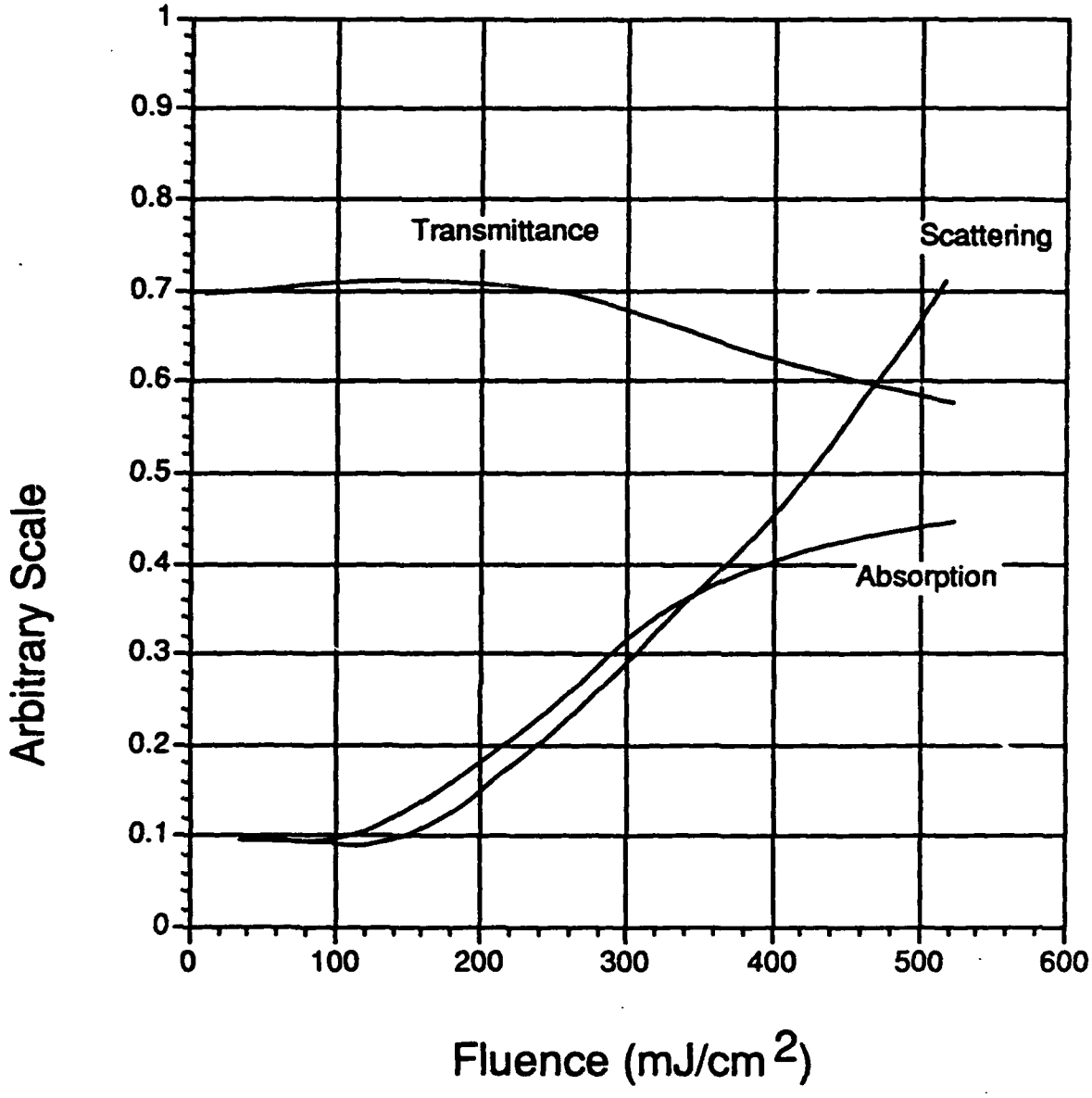
Arbitrary Scale
1
0.9
0.8
0.7
0.6
0.5
0.4
0.3
0.2
0.1
0
0
100
200
300
400
500
600
Transmittance
Scattering
Absorption
Fluence (mJ/cm 2)

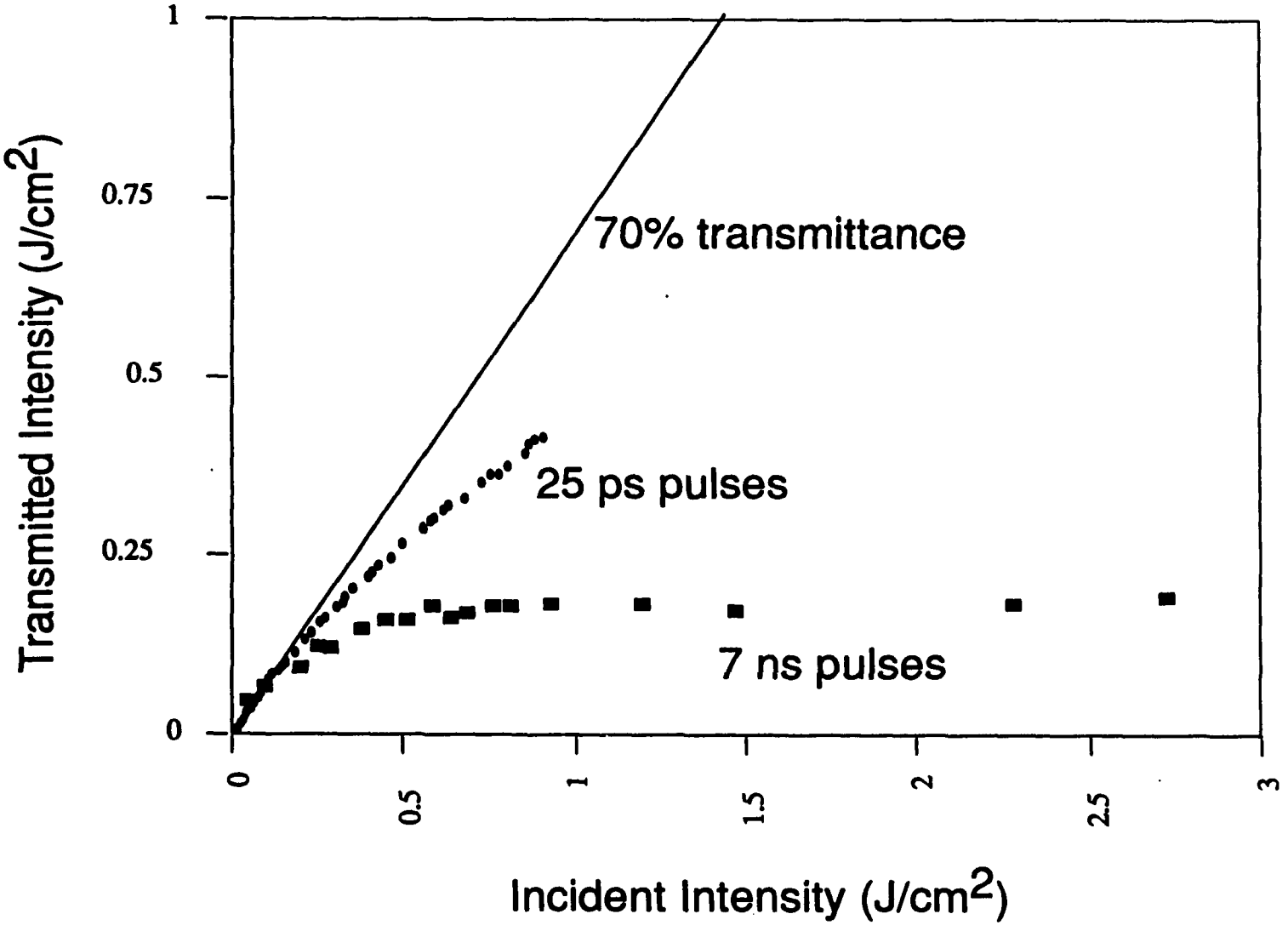
Transmitted Intensity (J/cm2)
1
0.75
0.5
0.25
0
70% transmittance
25 ps pulses
7 ns pulses
0
0.5
1
1.5
2
2.5
3
Incident Intensity (J/cm2)

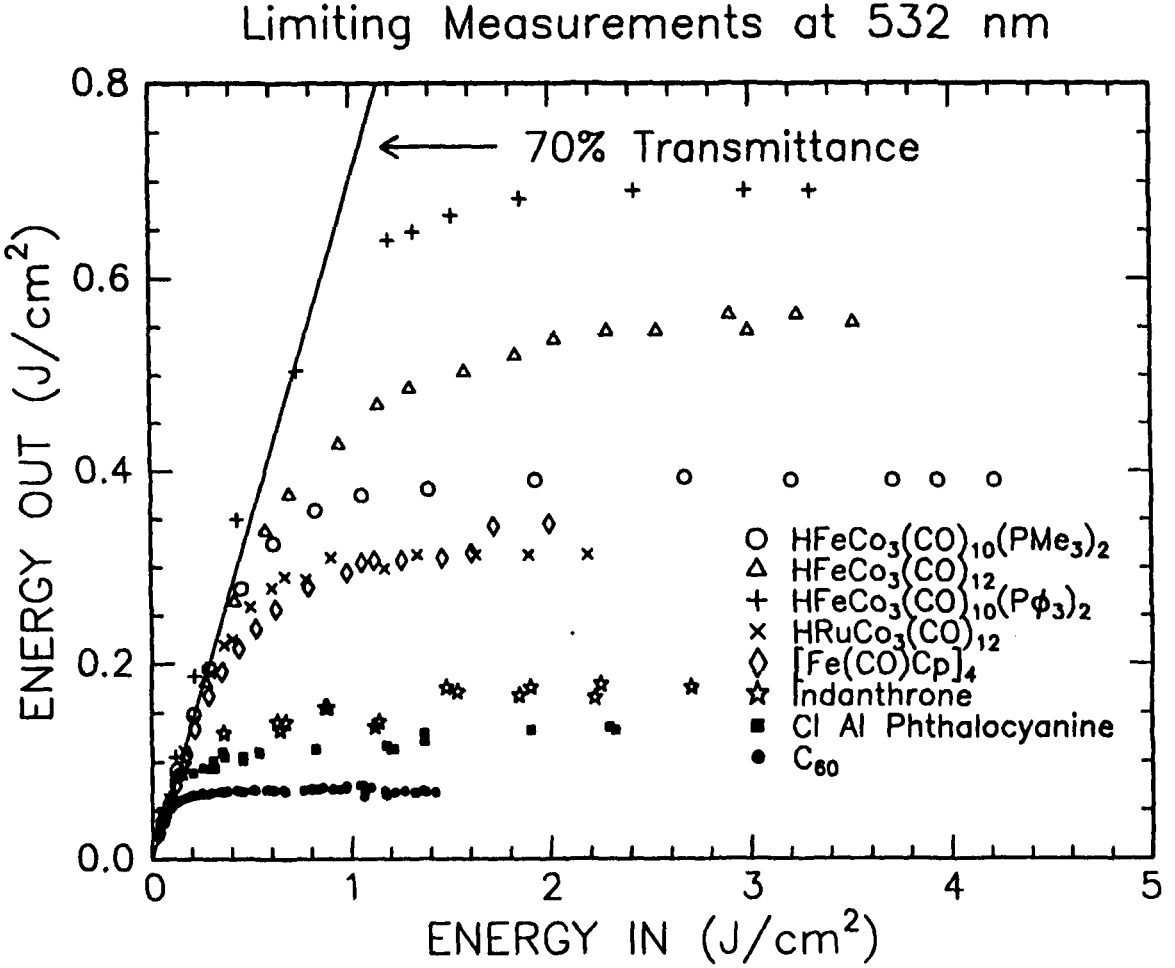
Limiting Measurements at 532 nm
70% Transmittance
ENERGY OUT (J/cm²)
ENERGY IN (J/cm²)
0.0
0.2
0.4
0.6
0.8
0
1
2
3
4
5
HFeCo₃(CO)₁₀(PMe₃)₂
HFeCo₃(CO)₁₂
HFeCo₃(CO)₁₀(Pϕ₃)₂
HRuCo₃(CO)₁₂
[Fe(CO)Cp]₄
Indanthrone
Cl Al Phthalocyanine
C₆₀

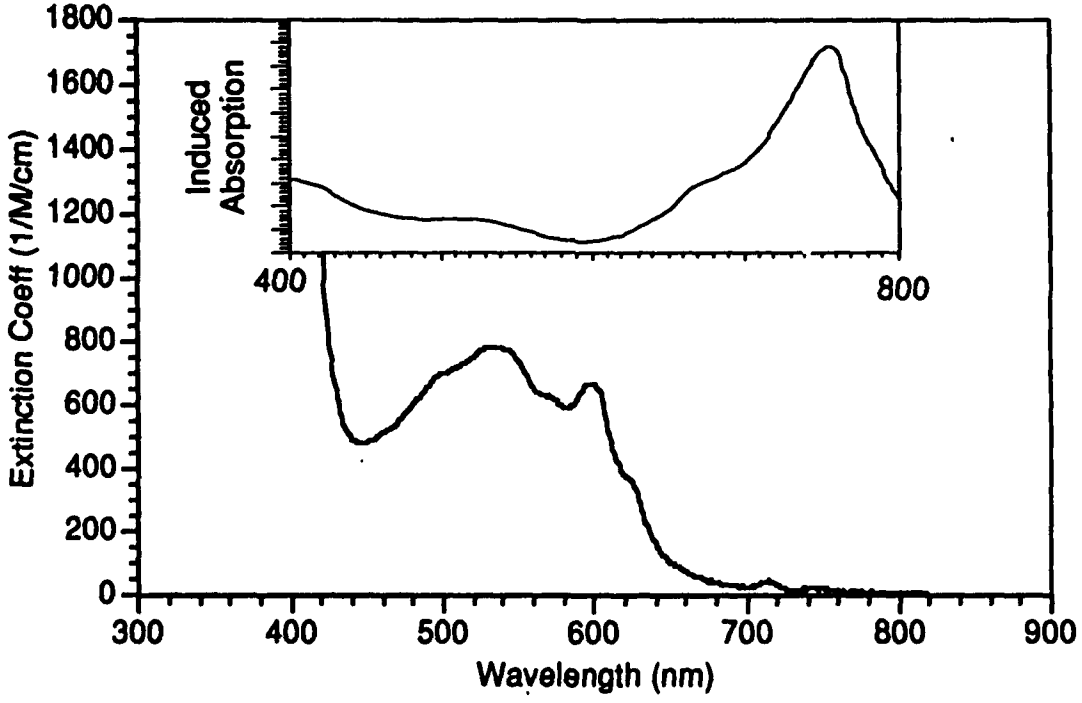
Extinction Coeff (1/M/cm)
1800
1600
1400
1200
1000
800
600
400
200
0
300
400
500
600
700
800
900
Wavelength (nm)
Induced Absorption
400
800

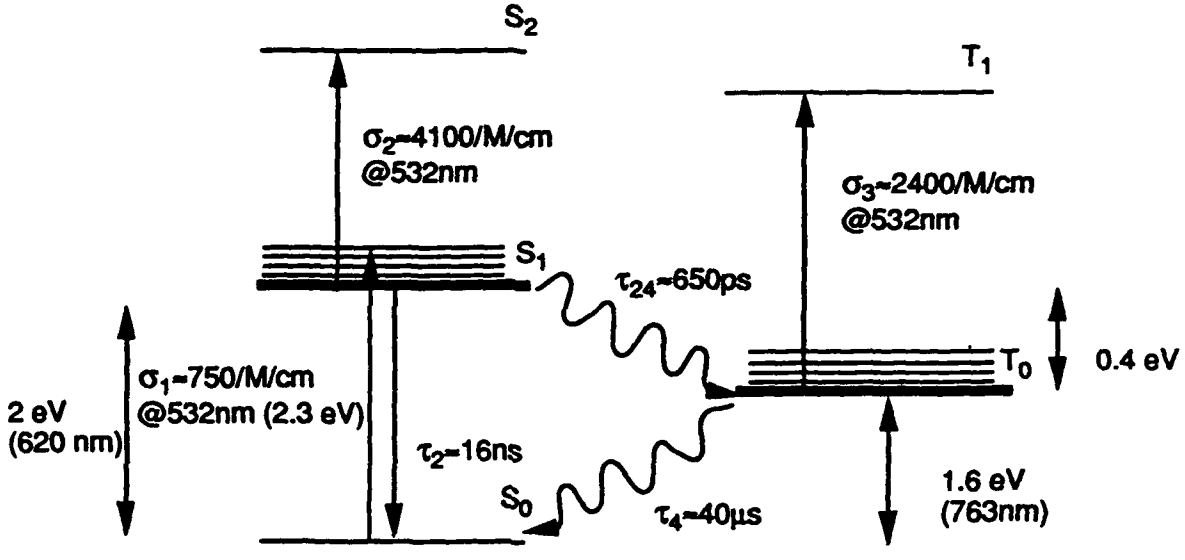
S_2
T_1
σ_2=4100/M/cm
@532nm
σ_3=2400/M/cm
@532nm
S_1
τ_{24}=650ps
T_0
0.4 eV
2 eV
(620 nm)
σ_1=750/M/cm
@532nm (2.3 eV)
τ_2=16ns
S_0
τ_4=40µs
1.6 eV
(763nm)

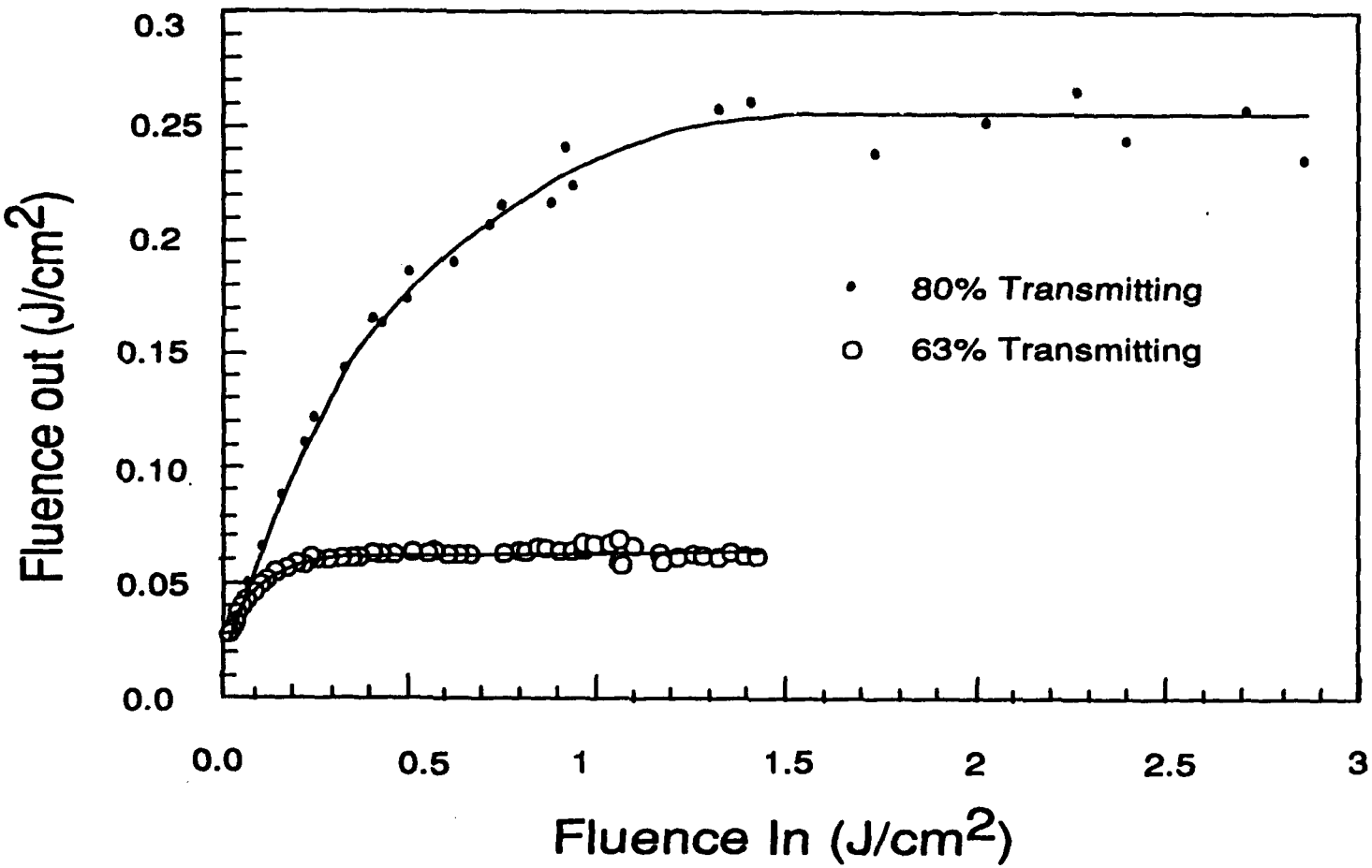
0.3
0.25
0.2
0.15
0.10
0.05
0.0
Fluence out (J/cm2)
80% Transmitting
63% Transmitting
0.0
0.5
1
1.5
2
2.5
3
Fluence In (J/cm2)

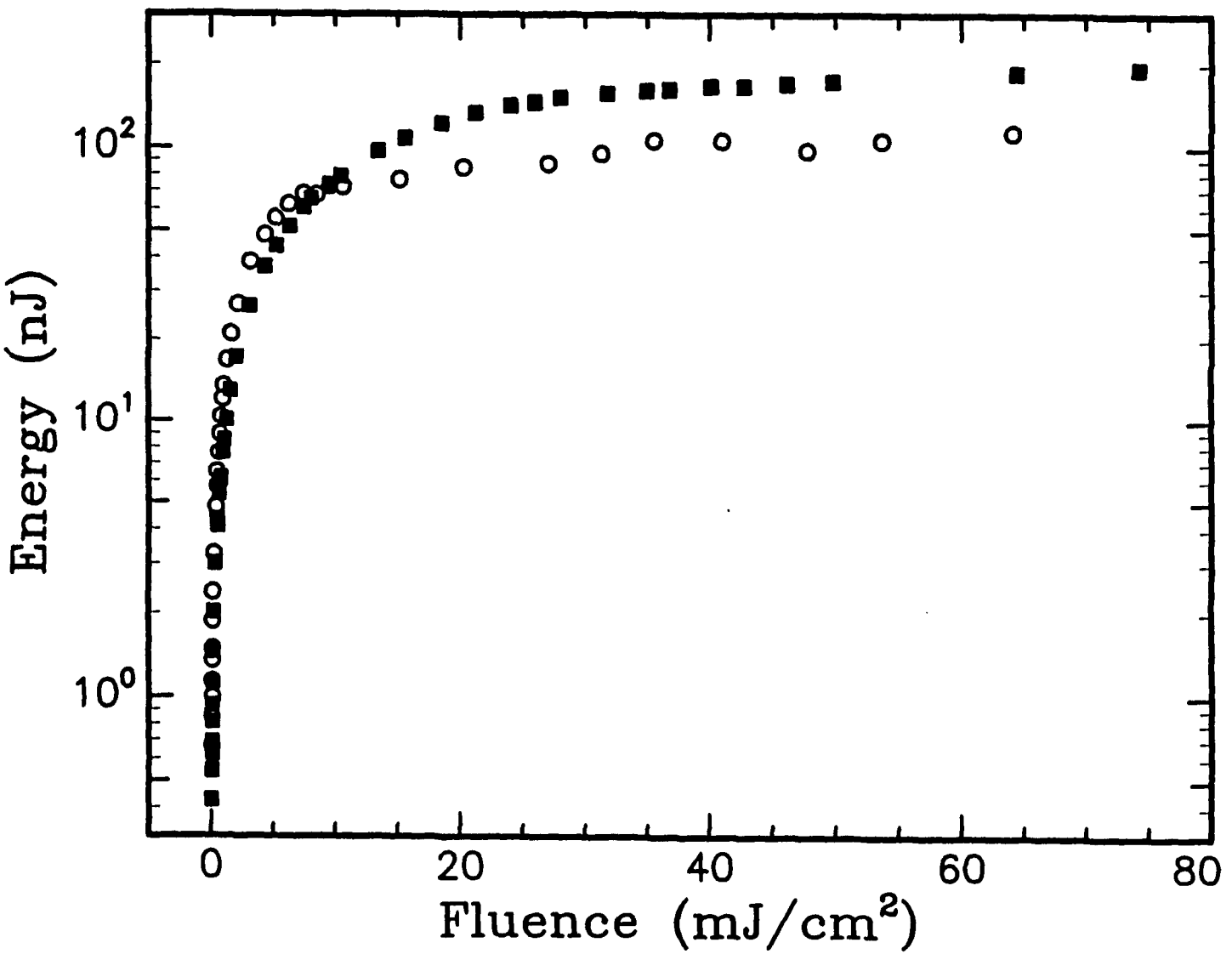
Energy (nJ)
10^2
10^1
10^0
0
20
40
60
80
Fluence (mJ/cm^2)

Appendix B

Fluence Dependent Optical Limiting for Eye Protection Using GaP

An Internal Report

FLUENCE DEPENDENT OPTICAL LIMITING FOR EYE PROTECTION USING GaP

Steve Rychnovsky, G.R. Allan, T.F. Boggess, C.H. Venzke, and A.L. Smirl

Center for Laser Science and Engineering, University of Iowa

ABSTRACT

We demonstrate an optical limiter at 532 nm using GaP in a low f/# configuration which achieves eye-safe limiting levels and a response which is fluence dependent on picosecond time scales. Picosecond techniques are used to measure the free carrier absorption, the index change per free carrier pair, and the two photon absorption coefficient. These results are used in a computer model to demonstrate that refraction associated with linearly generated free carriers acts as the dominant limiting mechanism. Therefore, for pulsewidths longer than picosecond duration these results indicate that this device will provide a fluence dependent response until recombination or diffusion begin to significantly affect the free carrier density.

With continuing advances in the development of broadly-tunable, high-power lasers, there is a need for a fast, passive, broadband optical limiter to protect optical sensors such as the human eye from exposure to damaging optical radiation. An ideal limiter would operate over the entire visible spectrum, have a large dynamic range and wide field of view (low f/#), and provide protection at any pulsewidth, i.e., possess a fluence dependent response. In principle these requirements could be satisfied by a device which utilizes a broadband, fluence dependent, nonlinear optical material which causes the system transmission to decrease as the input fluence increases. Consequently, optical nonlinearities have been investigated in a range of materials including organics, organometallics, liquid crystals, ferroelectrics, and semiconductors, with each showing potential for meeting at least some of the above requirements. However, in practice it has proven difficult to demonstrate optical limiting in these materials which satisfies all the above requirements simultaneously.

One promising approach of intereset here relies on nonlinear absorption and refraction in semiconductors to achieve optical limiting. Most of this work has focused on materials whose bandgap exceeds the photon energy so as to provide high linear transmission at low light levels, while at high inputs the transmission decreases with the onset of the Kerr nonlinearity, two photon absorption (TPA), and defocusing resulting from the free carriers created in the TPA process[1,2]. These devices show excellent limiting for picosecond pulses and are expected to be broadband due to the inherently broadband nature of these nonlinear mechanisms. However, both the TPA and Kerr nonlinearities are intensity, as opposed to fluence, dependent so that the switching energy increases with pulsewidth[3]. Consequently, the response of such an optical limiter may not provide adequate protection against a wide range of pulsewidths.

In order to insure a limiting response which is insensitive to pulse duration, we are investigating the use of inherently fluence dependent nonlinearities in semiconductors. Specifically, we generate optical nonlinearities by exciting free carriers via linear absorption, which unlike the TPA and Kerr nonlinearities, should result in a fluence dependent response. This mechanism has been used previously to demonstrate optical limiting in the indirect bandgap semiconductor, Si excited just above the band edge at 1.06 microns[4]. Although this limiting was at infrared wavelengths and only a single pulsewidth was

used, this same approach should be useful for fluence dependent, visible wavelength eye protection by another choice of semiconductor.

In order to determine the feasibility of this concept we are investigating optical limiting in GaP, an indirect gap semiconductor with a band edge located at 550 nm. An optically thin piece of this material should provide high transmission at low input fluences so as not to impair vision, yet provide a reduced throughput at higher inputs with the onset of free carrier nonlinearities. Specifically, excitation near the band edge will result in the linear generation of free carriers, and the subsequent changes in absorption and refraction are expected to result in fluence-dependent optical limiting for time scales shorter than the characteristic recombination and diffusion times in this material. Indirect gap materials are advantageous for this application since they typically have a large joint density of states which helps to prevent saturation of the free carrier generation mechanism and long free carrier recombination times which helps to insure a fluence dependent response.

Here we demonstrate that eye-safe optical limiting can be achieved in GaP at 532 nm using near plane wave illumination in an f/15 system and we show that the limiting is dominated by fluence dependent refractive nonlinearities associated with linear carrier generation. This is determined by first performing absorptive experiments to quantify both the free-carrier absorption (FCA) cross section, σ_{fc}, and TPA coefficient, β. We note here that although the single photon energy is above the band gap, this TPA is readily observed and is in fact stronger than expected, although it plays only a minor role in the optical limiting at these pulsewidths. Experiments are then performed at different pulsewidths to determine the source of the refractive nonlinearity. These results indicate that free carrier refraction completely dominates the Kerr contribution, which allows us to extract a value for the index change per free carrier pair, n_{eh}. This dominance is primarily due to the fact that excitation at 532 nm is above the indirect bandgap, resulting in the generation of large free carrier densities.

The sample used for these studies is a wafer of undoped, single crystal GaP, 135 μm thick. The wafer was polished and antireflection coated on both surfaces, resulting in a linear transmission of 26% at 532 nm, the wavelength at which all measurements were performed. To quantify the free-carrier absorption in this sample, we used a standard two-beam, pump-probe measurement, where an intense

pump pulse excites the sample, while a much weaker cross-polarized probe pulse provides a time resolved measurement of the pump-induced changes in transmission. Typical results are shown in Fig. 1 for 25 ps FWHM pulses and various fluences. Two distinct features are observed in the data: an induced absorption that is essentially constant on a nanosecond time scale and an induced absorption that occurs only near zero delay. The long-lived signal, which persists until the carriers recombine, is found to directly depend on the photogenerated carrier density, and we attribute it to FCA. The induced absorption observed near zero delay scales with intensity, is symmetric about zero delay, and occurs only when both pulses are present, i.e. it follows the cross-correlation of the pump and probe pulses. All of these factors are consistent with this feature being associated with an instantaneous (relative to 25 ps) induced absorption, and we attribute it to TPA. We emphasize that, since the photon energy used here is ~500 meV below the direct band edge, this induced absorption is not likely to be the result of near resonance effects such as the AC Stark effect. Also, since the signal corresponds to a loss in the weak, cross-polarized probe, it is not likely that it is the result of a coherent artifact. The observation of TPA under these experimental conditions is somewhat unusual in that it is observed in the presence of strong linear absorption, since the single photon energy is above the indirect band edge. Similar results have been observed for optical excitation above the band edge in both Si[5,6] and diamond[7]. Including both TPA and FCA in a rate equation model allows us to fit the data in Fig. 1 for all fluences with a single set of parameters: $\beta_{\perp}$=7 cm/GW and σ_{fc}=0.8x10^{-18} cm^2. To confirm this measurement, the experiment was repeated using a 45 ps pulsewidth and the results were found to be consistent with those predicted using the measured parameters given above. This scaling with pulse width supports our conclusion that the induced absorption at zero delay is indeed due to TPA.

It is important to note that $\beta_{\perp}$ is the cross-polarized TPA coefficient, which is distinct from the single beam (co-polarized) TPA coefficient, $\beta_{||}$, needed for modeling the optical limiting response. In general these two parameters are not simply related[8]. On the other hand, for the zinc-blende structure of GaP, if one assumes the carriers thermalize within the bands before FCA takes place, the FCA coefficient measured in this cross-polarized experiment will be the same as that measured in a single beam co-polarized experiment. For our excitation rates and carrier densities, this is a valid assumption,

and we may safely assume that the σ_{fc} value measured here can be used to model the optical limiting behavior.

The nonlinear refractive parameters and $\beta_{||}$ are measured using the arrangement illustrated in the inset of Fig. 2. This experiment is identical in form to a z-scan[9] except that instead of a Gaussian beam, a severely-clipped Gaussian beam is used as the input. This configuration allows us to quickly change the input and output f/# to mimic more realistic optical limiter geometries. However, since no closed form solutions exist for the z-scan response for this configuration, the results must be analized numerically. To verify the anticipated propagation behavior, we performed beam scans near focus to verify that these agree with the beam profiles predicted by our computer code.

The first experiment performed is an open aperture z-scan, which is sensitive only to nonlinear absorption. By modeling these results, we determine a value of 19 cm/GW for the co-polarized TPA coefficient, $\beta_{||}$ and a value of 1.1×10^{-18} cm^2 for the free-carrier cross section, a value that is in reasonable agreement with that obtained from the pump-probe measurements. As before this experiment repeated at a longer pulsewidth verifies our measured values of $\beta_{||}$ and σ_{fc}. The magnitude of this coefficient is surprisingly large. Application of the well-known scaling law[10] for TPA to GaP gives a value of only 2.4 cm/GW. While we recognize that this scaling law is arrived at using a two-band parabolic model for direct-gap materials, we note that here the TPA transition is in fact direct and that this model has been shown to apply quite well to a range of semiconductors and insulators where a simple two band assumption is not justified[10]. Examination of the band structure[11] of GaP indicates that the anomalously large TPA coefficient may be due either to near resonance effects associated with a higher lying conduction band or with the existence of an optical critical point at this wavelength located along the X direction in k space.

The refractive nonlinearity is determined by repeating the z-scans using a restricted output aperture. The input aperture is kept at a diameter of 3.6 mm and the output aperture is set to a diameter of 1.6 mm. The results for pulsewidths of 25 and 95 ps are given in Figure 2 along with theoretical fits which use an n_{eh} value of -3.1×10^{-22} cm^3. The data are nearly identical for the two pulsewidths, indicating that even for picosecond pulses the response is dominated by the fluence dependent

nonlinearities associated with linearly generated free carriers. Furthermore, since the response is nearly antisymmetric about focus, it is clear that nonlinear absorption is also dominated by the refractive nonlinearity. The implication of these results is that the response of a GaP optical limiter will be dominated by the nonlinear refraction associated with linearly generated free carriers, a fluence dependent process.

For optical limiting measurements we again use the experimental configuration shown in the inset of Fig. 2, but in this case we set the input and output apertures to diameters of 7.8 mm and 6.6 mm respectively, which for our focal lengths corresponds to an f/15 system. This value was chosen since it is the smallest f/# for which we may still assume a thin limiter configuration[3], thus allowing us to compare actual performance with that which we predict using our measured parameters. We note that such an f/# also approaches that used in many practical optical systems. The results for two different pulsewidths are given in Fig. 3, along with a reference curve giving the linear transmission. Theoretical fits using the parameters extracted above are given by the solid lines and are seen to agree very well with the data. For both pulsewidths the response is consistent with the model, and the two sets of data are nearly indistinguishable, again indicating the dominance of the fluence-dependent nonlinear processes. In each case, a switching level (i.e., the input energy at which the output clearly deviates from that expected for a linear response) of <30 nJ is observed, and above this level excellent limiting is achieved even above the damage threshold of approximately 100 nJ. For input energies up to 400 nJ, the output energy remains below 10 nJ, which is two orders of magnitude below the 0.2 μJ maximum permissible exposure limit for the human eye for short, visible pulses.

A measure of the dynamic range of the device is defined as the ratio of the input energy at which measurable damage to the GaP occurs to the input switching energy. In the present configuration this corresponds to ~ 5 dB. This range is limited by the relatively low GaP damage threshold of ~100 mJ/cm^2. We emphasize, however, that the limiter continues to operate at input fluences far above the GaP damage threshold, i.e., the device may be considered to "fail-safe". If we define an effective dynamic range for fail-safe operation as the ratio of the input energy at which the output exceeds the maximum possible exposure to the input energy required for switching, we expect this value to be many tens of dB.

In summary, we have demonstrated eye-safe optical limiting at 532 nm using GaP in a low f/# configuration. In addition, we have used picosecond optical techniques to measure the FCA cross section, the index change per photogenerated carrier pair, and the TPA coefficient. This TPA process is anomalously large, and is in fact strong enough to be observed in the presence of significant linear absorption. While, intensity dependent processes are clearly present and measurable for our experimental conditions, we have demonstrated that it is the fluence dependent refraction associated with linearly-generated carriers that dominates the limiter response. The implication of this is that the device should function similarly for longer pulse durations, provided these durations do not approach the carrier recombination time nor does diffusion out of the illuminated spot become significant during the pulse. Finally, we note that, while the GaP limiter exhibits an eye-safe response over a broad effective dynamic range, this device suffers from a narrow bandwidth of operation dictated by the frequency dependence of the linear absorption coefficient. We are currently exploring approaches that might extend this bandwidth in GaP, as well as investigating other materials and mechanisms that offer broader operating bandwidths while maintaining a fluence dependent response.

We gratefully acknowledge the support of the Advanced Research Projects Agency and the U. S. Army Night Vision and Electro-Optics Directorate.

References

1. Thomas F. Boggess, Jr., Arthur L. Smirl, Steven C. Moss, Ian W. Boyd and Eric W. Van Stryland, IEEE J. Quantum Electron., QE-21, 488 (1985)

2. A. A. Said, M. Sheik-bahae, D. J. Hagan, E. J. Canto-Said, Y.Y. Wu, J. Young, T.H. Wei, and E. W. Van Stryland, SPIE Vol. 1307, 294 (1990)

3. E.W. Van Stryland, Y.Y. Wu, D.J. Hagan, M.J. Soileau, and Kamjou Mansour, J. Opt. Soc. Am. B, 5, 1980 (1988)

4. Thomas F. Boggess, Steven C. Moss, Ian W. Boyd, and Arthur L. Smirl, Opt. Lett. 9, 291 (1984)

5. Thomas F. Boggess, Jr., Klaus M. Bohnert, Kamjou Mansour, Steven C. Moss, Ian W. Boyd, and Arthur L. Smirl, IEEE J. Quantum Electron., QE-22, 360 (1986)

6. D. H. Reitze, T.R. Zhang, Wm. M. Wood, and M.C. Downer, J. Opt. Soc. Am. B, 7, 84 (1989)

7. J. I. Dadap, G. B. Focht, D.H. Reitze, and M.C. Downer, Opt. Lett., 16, 499 (1991)

8. M.D.Dvorak, W.A.Schroeder, D.R. Andersen, and A.L. Smirl, IEEE J. Quantum Electron., in press

9. M. Sheik-bahae, A.A. Said, and E.W. Van Stryland, Opt. Lett., 14, 955 (1989)

10. E.W. Van Stryland, H. Vanherzelle, M.A. Woodall, M.J. Soileau, A.L. Smirl, S. Guha, and T.F. Boggess, Opt. Eng. 24, 613 (1985)

11. "Data in Science and Technology: Semiconductors-Group IV Elements and III-V Compounds", editor O. Madelung, Springer-Verlag, New York (1991)

Figure 1 Pump probe experiments at (+)17, (▪) 28, and (o) 38 mJ/cm^2 using 25 ps pulses indicate both a long lived free carrier absorption and a two photon absorption process.

Figure 2 A modified z-scan experiment using (o) 95 and (+) 25 ps pulses illustrates a nonlinear refraction which is fluence dependent. Furthermore, the nearly antisymmetric nature of this data indicate that free carrier nonlinearities dominant absorptive processes in this experiment.

Figure 3 F/15 experiments using (o) 95 and (+) 25 ps pulses demonstrate an limiting response which is predominantly fluence dependent. The levels achieved are eye safe even above the damage threshold of the material. Solid and dashed lines are numerical predictions based on the measured values for the nonlinear parameters and are seen to agree very well with the measured response.

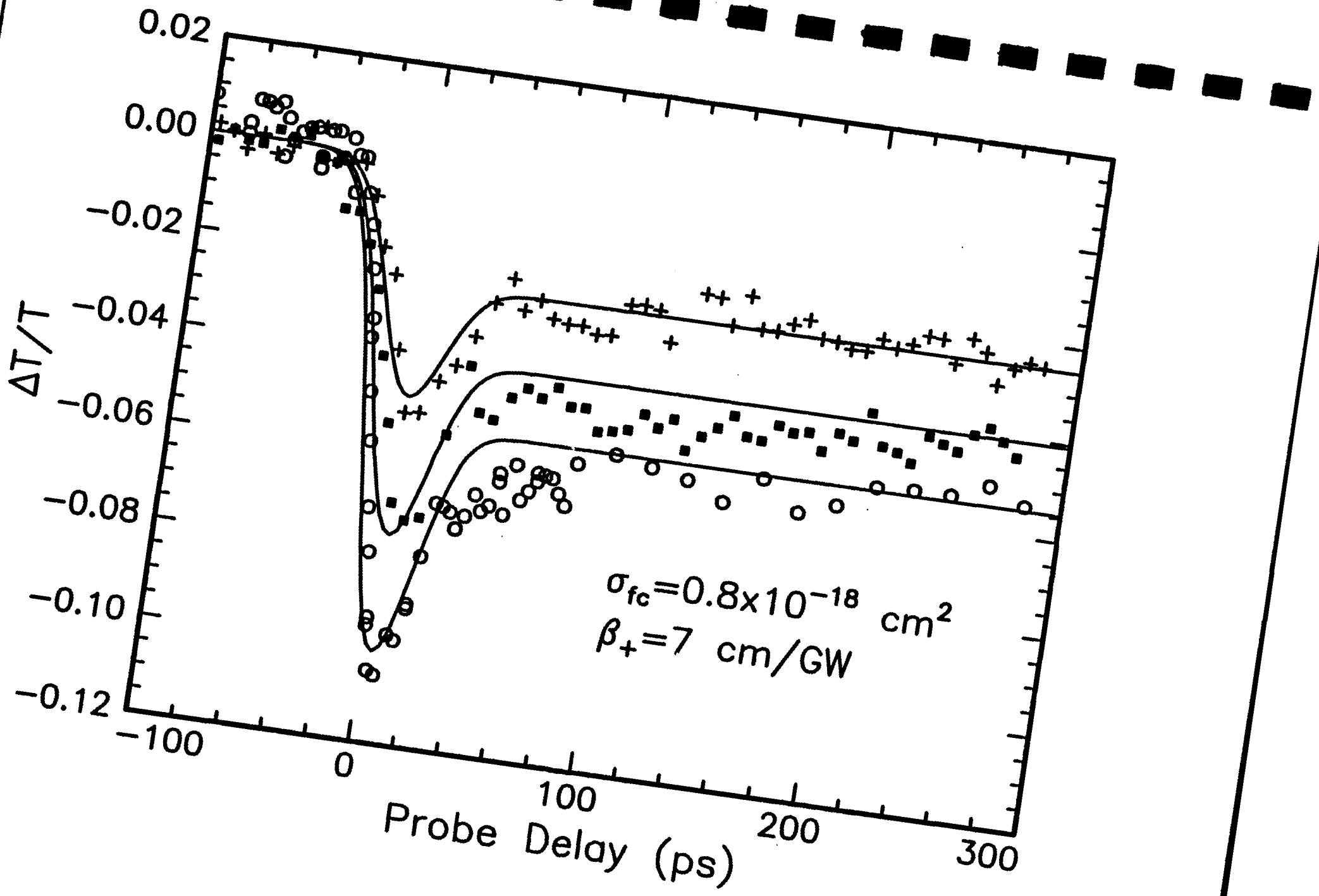
0.02
0.00
−0.02
−0.04
−0.06
−0.08
−0.10
−0.12
ΔT/T
−100
0
100
200
300
Probe Delay (ps)
σ_{fc}=0.8x10^{-18} cm^2
β_+=7 cm/GW

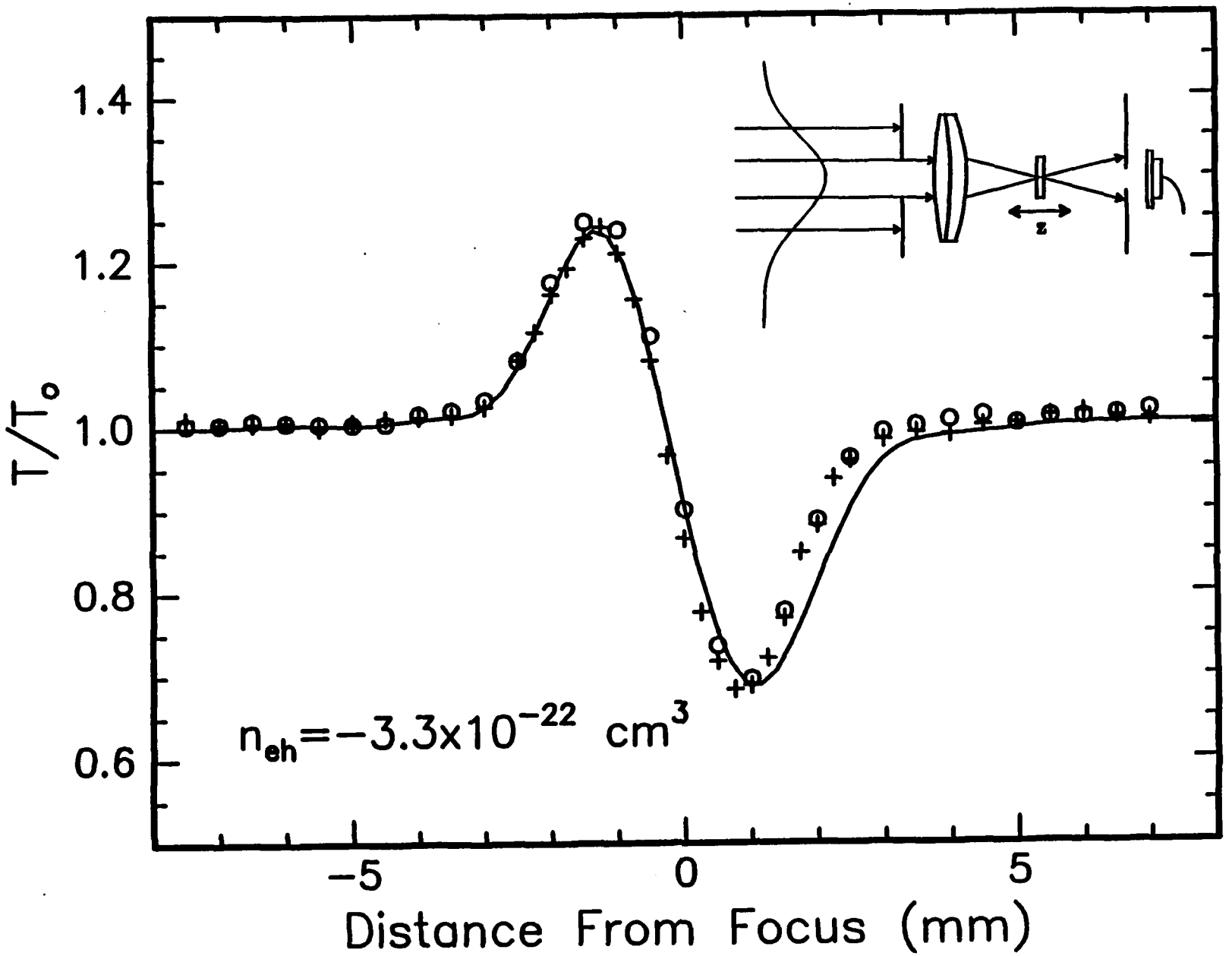
1.4
1.2
1.0
0.8
0.6
T/T$_o$
n_{eh}=−3.3x10^{-22} cm^3
−5
0
5
Distance From Focus (mm)
z

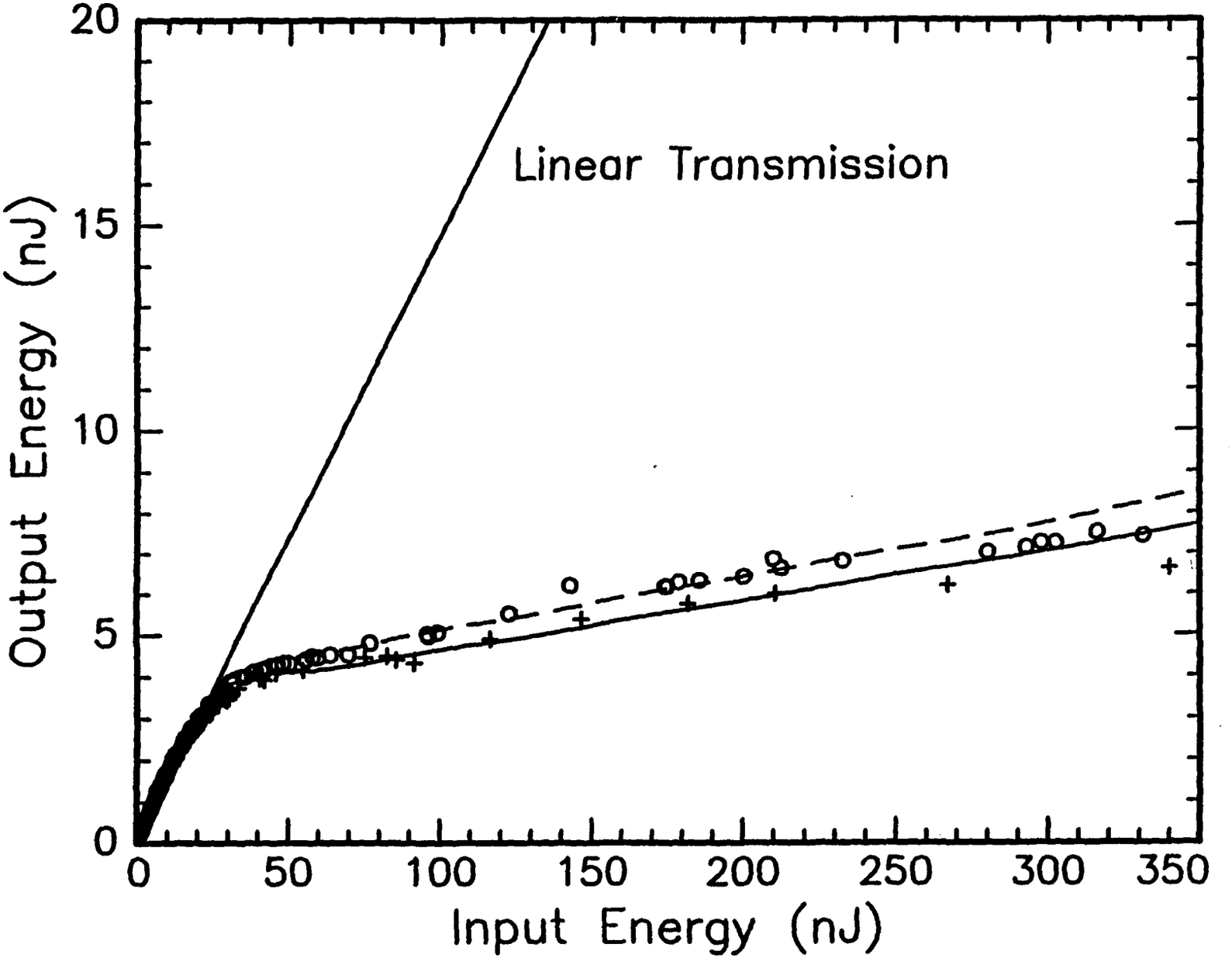
Linear Transmission
Output Energy (nJ)
Input Energy (nJ)
0
5
10
15
20
0
50
100
150
200
250
300
350